LABORATÓRIO NACIONAL
DE ENGENHARIA CIVIL

EXPERIMENTAL STUDY OF RESERVOIR TURBIDITY CURRENTS

Development and application of data processing routines for velocity and bed profiles

Lisboa • Março de 2007

I&D HIDRÁULICA E AMBIENTE

RELATÓRIO 104/**2007 – NRE**

**Experimental study of reservoir turbidity currents.
Development and application of data processing routines for
velocity and bed profiles**

**Estudo experimental de correntes de turbidez em albufeiras.
Desenvolvimento e aplicação de rotinas para o processamento de
dados de perfis de velocidade e perfis do fundo**

**Estudio experimental de corrientes de turbidez en embalses.
Desarrollo y aplicación de rutinas para el procesamiento de datos
de velocidad y perfiles de fondo**

**Etude expérimentale des courants de turbidité dans retenues.
Développement et application des routines pour l'analyse des
donnés des profils de vitesse et du fond**

ABSTRACT

This work describes the activities performed to support the realization of experiments that simulate the occurrence of a turbidity current in a reservoir. These experiments involved the utilization of an Ultrasonic Velocity Profiler (UVP) to measure the velocity of the current in the form of instantaneous profiles and also a bed profiler to measure the thickness of the deposits. As a result a set of routines programmed in Fortran90 and MATLAB languages have been developed to facilitate the post processing and analysis of the data.

RESUMO

Este estudo descreve as actividades desenvolvidas para apoiar a realização de ensaios experimentais de simulação da ocorrência de correntes de turbidez em albufeiras. No estudo experimental foi utilizado o sistema UVP (Ultrasonic Velocity Profiler) na medição dos perfis de velocidade instantâneos das correntes de turbidez e um seguidor de fundos na medição da espessura dos depósitos. Nesse âmbito, foi desenvolvido um conjunto de rotinas programadas em Fortran90 e MATLAB para o pós-processamento e análise dos dados.

RESUMEN

En este trabajo se describen las actividades realizadas para apoyar el desarrollo de experimentos destinados a simular la ocurrencia de corrientes de turbidez en un embalse. En los experimentos se utilizó un dispositivo para medir perfiles de velocidad mediante ultrasonido (UVP) y un seguidor de fondo para medir la espesura de los depósitos. Como resultado, fueron desarrolladas una serie de rutinas programadas en leguajes Fortran90 y MATLAB con el fin de facilitar el post proceso y analisis de los datos.

TABLE OF CONTENTS

1. INTRODUCTION

This study is part of the research project POCTI/ECM/45778/2002 – *Sedimentation in reservoirs by turbidity curre*nts, funded by FCT (Portuguese Foundation for Science and Technology). The project involves the Laboratório Nacional de Engenharia Civil (LNEC) and Instituto Superior Técnico (IST).

The main objective of this research project is to ameliorate the physical understanding of turbidity currents phenomena in reservoirs, namely, the location of the plunge point, the velocity of the currents, the amount of sediment carried by the current, whether or not currents could reach the dam and where they will settle. This research project will be undertaken in two main axes, namely in an experimental front and in the development of mathematical models to simulate and predict reservoir sedimentation due to turbidity currents.

Within the project, a fellowship was assigned to the author to support the experimental component of the project. This document describes the work developed during his presence at LNEC, between June 2006 and March 2007.

This report is structured into seven main chapters. Chapter 1 corresponds to this introduction; Chapter 2 summarizes the literature review of the most important contributions for the experimental study of turbidity currents. Special emphasis is given to the experimental facilities, sediments properties and flow conditions considered by different authors. A summary of the main results and conclusions is also presented. Chapters 3 and 4 describe the experimental facility and measuring instrumentation used in the present study. The instrumentation includes the Ultrasonic Velocity Profiling (UVP) device used to measure velocity profiles. Chapter 5 describes the routines developed for data processing of the velocity and bed profiles. In Chapter 6 the velocity measurements taken at different experiments are processed using the routines depicted in the previous chapter. Finally Chapter 7 gives a brief summary of conclusions and recommendations.

2. LITERATURE REVIEW

2.1 General Considerations

In this section a literature review of several thesis works and publications related with sedimentation in reservoirs is presented. The review is focused on experimental facilities and flow conditions in order to study the range of values commonly used for independent variables in experimental simulations of turbidity currents. Also the review includes the principal characteristics of the sediments used to simulate the turbidity currents.

2.2 "Effects of Obstacles and Jets on Reservoir Sedimentation Due to Turbidity Currents"

This work was carried out by Christoph Oehy at the Laboratoire de Constructions Hydrauliques, École Poytechnique Fédérale de Lausanne. It consists in a study of the effects of obstacles, jets and a bubble curtains in the hydrodynamics of turbidity currents and consequently in the deposition of the fine sediment. The main goal was to investigate new control measures for reservoir sedimentation due to turbidity currents.

Using a 1D conceptual model of the turbidity current, Oehy (2003) compares the experimental results with numerical simulations.

2.2.1 *Experimental Facility*

The experiments were carried out in a flume with a total length of 8.55 m, 27.2 cm wide and 90 cm high. The slope was variable between 0 and 5%.

The flume was divided with a sliding gate, forming an initial section of 80 cm length which serves as a stilling box for the mixture of water and fine sediment. In this way, the portion of the flume over which the turbidity current runs has a length of 7.1 m starting at the sliding gate. The ending part of the flume was intended for the turbidity current drainage.

The mixture was prepared in a mixing tank separated of the flume but connected to the stilling box by means of a pipe circuit provided with a pump, an electromagnetic flowmeter and a valve. The capacity of the tank was 1500 l and it had a propeller-type mixer to create the mixture.

Turbidity current flow velocity measurements were taken using UVP (Ultrasonic Velocity Profiler), which allowed a complete instantaneous profile measurement. The velocity of the turbidity current front was measured making video recordings and measuring the time at

which the head passes different locations. Fine sediment concentration in the turbidity current was not measured. Instead, a new electrical system was developed to measure local bed thickness (deposits) through the electrical resistance of the sediment layer.

2.2.2 *Sediment Properties*

The material used to simulate the turbidity current was ground polymer with a density of 1135 kg/m^3. The grain-size distribution of the sediment had a characteristic diameter d_{50} of 90 μm, with a standard deviation, σ_g, of 1.6. The fall velocity of the sediment was calculated following the Stoke's law and considering a particle diameter such that the fall velocity associated to it, is equal to the averaged settling velocity of the sediment material. This diameter corresponded to 97 μm and the respective fall velocity was 0.522 mm/s.

2.2.3 *Conditions of the Experiments*

Seven series of experiments were carried out, each one corresponding to a different configurations of obstacles for the turbidity current flow. For all the experiments the initial depth of the turbidity current, h_o, was 4.5 cm, corresponding to the opening of the sliding gate. Two values for the bottom slope were used: 4.64% and 0%. The water depth at the sliding gate was near 52 cm with a variation of ±2% for the experiments with a slope of 4.64% and near 89 cm with a variation of ±1% for the experiments with horizontal bottom. The initial discharge varied between 0.0005 and 0.00137 m^3/s (0.5 l/s and 1.37 l/s), and the volumetric fine sediment concentration varied between 1.9% and 4.63%.

2.2.4 *Results and Conclusions*

Obstacles only provide effective blocking if the approaching flow is subcritical. For this case Oehy (2003) proposed as a criterion for a complete blocking of the turbidity current that the obstacle had a height at least twice of the turbidity current height.

The effect of permeable screens or geotextiles was strongly related to its porosity, not being very sensible to the characteristics of the approaching flow. The criteria for this case is that the screen must have a height equal to three times the height of the turbidity current, with a porosity of less than 30%.

Using jets inclined 45º a complete blocking can be achieved if the opposing momentum of the jets is 50% higher than the momentum of the turbidity current.

Finally, in the case of a bubble curtain, it was concluded that they can not be recommended to stop or control turbidity currents in reservoir.

2.3 "Depositing and Eroding Sediment-driven Flows: Turbidity Currents"

This is the PhD thesis work of Marcelo García, developed at the St. Anthony Falls Hydraulic Laboratory of the University of Minnesota. It consists in experiments conducted to observe the behavior of turbidity currents in the vicinity of the slope break between a submarine canyon and its associated depositional fan.

2.3.1 *Experimental Facility*

The experiments were conducted in a channel 30 cm wide, 78 cm height and 11.6 m length. The channel had a slope transition from an inclined bed 5 m long with a slope of 0.08 and a 6.6 m long horizontal bed. In the initial portion of the channel a submerged sluice gate serves as the control structure to release the current towards the simulated canyon-fan system.

The dense fluid was prepared in a mixing tank with a capacity of 2000 l. From this tank the dense fluid was pumped up to a constant head tank from where it was piped to the recipient defined by the submerged sluice gate. The pump system is provided with control valves and a flow meter.

At the end of the flume a tank, with its bottom below the channel bottom, served as a submerged free overfall drainage system and acts to avoid the reflection of the current into the flow domain. The drainage was made by means of a valve near the bottom of this tank. In the top part of this area clear water was supplied to make up for the water entrained by the turbidity current.

To measure turbidity current velocities García (1990) used a 3 mm diameter micropropeller, Shinoauka model SV-3, which had a measuring range of 2 cm/s to 100 cm/s with a reported accuracy of 10%. The device needed to be calibrated periodically and it was not originally designed for contaminated water. In spite of this, García (1990) reported a good behavior of the equipment and its adequacy to perform the measurements.

The concentration of fine sediment with uniform size was measured by a Kenek model PM-206 optical light probe. The working principle of this device is to measure the attenuation of light due the presence of suspended sediment. However, in the case of poorly sorted fine sediment the conventional system of siphons placed in a rake was used. All the measuring devices were placed in a trolley that could be moved over rails placed along the whole flume.

2.3.2 *Sediment Properties*

García (1990) made experiments with saline density currents and with turbidity currents. For the turbidity currents three grades of silica and two grades of glass were used. Also, two

grades of crushed coal were used for experiments with turbidity currents where sediment entrainment was to be studied. All the sediments were characterized by means of the geometric mean size, D_{sg}, described by García (1990) and its standard deviation σ_{sg}. The geometric mean size varied between 4 μm and 180 μm with a standard deviation between 0.47 and 1.00. The fall velocity of the particles, v_s, was comprised between 0.02 mm/s and 6.20 mm/s.

2.3.3   *Conditions of the Experiments*

Before each experiment, the mixing tank and the flume were filled with clear water. To produce a density different, salt or sediment were added to the mixing tank until the desire density was achieved, and started to be circulated through the constant head system. A few minutes before the beginning of the experiment, clear water was supplied to the damping tank by the surface manifold, at a rate about twice of that was set in the mixing tank. In the bottom of the damping tank, the valve was set to drain water. After this, the trolley with the measuring equipment was placed at a selected station.

A typical run was started by delivering the dense fluid to the flume, through the opening of the sluice gate accordingly to the desired flow rate. The emanating underflow was allowed to develop until it reached the end of the tank. After this, the operator of the trolley placed the instruments at a selected station and started to measure velocity and concentration in the vertical direction at different locations. At the end of the vertical measurements the computer connected to the trolley displayed in the monitor the velocity and excess fractional density profiles, allowing the operator to overcome possible errors.

There were made three kinds of runs: conservative saline currents, depositional turbidity currents and sediment-entraining turbidity currents. In all these experiments the initial depth of the turbidity current was 3 cm, the initial depth-averaged velocity varied between 8.3 and 14.3 cm/s and the initial depth-averaged volumetric concentration of fine sediment varied between 1.3 and 8.6. In the case of saline current the initial fractional density varied between 0.002 and 0.025.

2.3.4   *Results and Conclusions*

García (1990) concluded that the vertical velocity structure of the turbidity current depends on the flow regime. No significant differences were found in the vertical structure, before and after a hydraulic jump, when comparing saline density currents and turbidity currents with similar inlet conditions.

García (1990) stated that saline and turbid internal hydraulic jumps have similar characteristic, and in both cases, the entrainment of water from above is small. A marked

reduction in the bed shear stress downstream of the jump was also found, which lead to an increase in the thickness of the bed deposit.

Regarding the sediment deposits, it was observed that there exists a strong relation between the deposit characteristic and the grain size of the sediment driving the flow. Coarser grains lead to thicker deposits and a roughly exponential variation of this was observed in the downstream direction. The median grain size of the deposits showed vertical and longitudinal variations that depend on the local turbidity current flow regime. The break in the slope did not cause any effect on the deposition pattern, but the hydraulic jump induced by this break was indeed the responsible for the changes observed on it.

García (1990) proposed a new empirical sediment entrainment function using the similarity collapse of the data collected through his experiments.

2.4   "Reservoir Sedimentation by Turbidity Currents"

This work was carry out by Giovanni De Cesare at the Laboratoire de Constructions Hydrauliques of the École Polytechnique de Lausanne. The objective of the study was to understand the physical phenomena that contribute to reservoir sedimentation. Under the study, measurements of water and sediment motion on site were carried out, as well as physical and numerical modeling of turbidity currents. The physical model was intended to describe a 2-D turbidity current, including the spreading that occurs when it enters in the reservoir. The numerical model used was based on the commercial CFX-F3D code, to which sediment deposition and erosion modules were added.

2.4.1   *Experimental Facility*

The experimental facility was divided in three major tanks. The first was intended to prepare the sediment mixture, the second was a feeding control tank and the last one was projected for the development of the turbidity current.

The mixing tank had a capacity of 2000 l. It received the sediment and water inflows and was provided with a mixer to keep the particles in suspension and guarantee a constant concentration throughout the whole run.

The feeding tank had a capacity of 600 l and was provided with a sluice control gate of 0.5 m height, a recirculation pump and a weir oriented to the mixing tank. This weir had two main objectives: to ensure the interchange of the mixture with the mixing tank, and to control the level in the feeding tank.

The last tank, where the turbidity current was formed, had a rectangular geometry with a variable bottom slope between 0 and 6 % along a channel distance of 3 m, and between 0 and

3 % along a distance of 6 m. The width of this tank was 1.5 m and the height was 65 cm. In the downstream end there was a vertical wall and the water level was controlled by a free fall weir.

After the gate, but before entering the final tank, the mixture was forced to pass through a set of horizontal tubes of variable diameter and 20 cm long, disposed from the bottom of the channel, where the diameter was 8.8 mm, to the top of the gate, where the diameter was 23.5 mm. The tubes render a constant velocity for the current and ensure a directional discharge.

De Cesare (1998) used UVP instrumentation to measure the velocity of the turbidity current. The UVP transducer were placed accordingly with three different main configurations in order to allow for a three dimensional study of the velocity field.

2.4.2 *Sediment Properties*

The sediment used to generate the turbidity current was homogeneous clay called OPALIT, which has the following characteristic diameters: $D_{10} = 0.002$ mm, $D_{50} = 0.020$ mm, $D_{90} = 0.140$ mm. The fall velocity calculated using Stoke's law corresponding to the mean diameter was 0.4 mm/s. The density of this mixture was 2740 ± 10 Kg/m^3 and the apparent density was 900 ± 100 Kg/m^3.

2.4.3 *Conditions of the Experiments*

Three runs were used for numerical simulation and comparisons, namely runs 2, 5 and 7. In all of these experiments the opening of the gate was 5 cm and the concentration of the mixture was in the range 0.2% to 2%. Runs 2 and 5 were executed using a bottom slope of 4 % and run 7 was executed using 1 %. Each experiment was carried out using a different disposition of the UVP transducers. For run 2 the transducers were located over the current, in the run 5 transducers were located in front of the current and in run 7 the transducers were located in a square frontal formation. Four transducers were located in one side of the channel and the other four in the downstream part of the channel, all of them facing the current. This allowed to measure a two dimensional field of velocities.

In the run 2, 7 transducers were located over the current and one in the frontal direction to measure the initial exit velocity. The inclination angle with respect to the bottom plane of the transducers located over the current was about 60°. All transducers where oriented in the opposite direction of the turbidity current flow, resulting in negative velocity measurements. The mean exit velocity, after passing the tube set, was near 10 cm/s. It was observed that due to the lack of sediment particles in the zone above the current, the velocity measurements in this zone presented a significant deviation.

In the run 5, 6 transducers were located facing to the current flow direction and two where located over the current at the exit of the gate to make vertical profiles measures. The measurements of transducers located in front of the current were affected by the echo of pulses coming from the successive transducers. Therefore the time evolution of the front position had to be obtained by means of video recordings. The initial exit velocity from the tube set was near 5 cm/s.

In the run 7, the transducers were accordingly to a square 4 by 4, covering an area of 625 mm by 625 mm. This area was included on one half of the channel and extended from 125 mm to 750 mm from the exit of the current. In the side and the end part of the channel, the two transducers that were pointing to the region near the gate were separated 125 mm, the third and fourth transducer of each side were separated 250 mm.

2.4.4   *Results and Conclusions*

The velocity measurements obtained with the different dispositions of the transducers were used to validate a numerical model. This model was developed based on the CFX-F3D commercial code, using its module of multi-phase fluids, and adding modules programmed by the author. These modules were developed taking into account the interaction between the mixture and the bed in terms of entrainment and deposition of particles.

After validation the numerical model was used to study a real case of a flood in the Luzzone reservoir, which was made difficult by the lack of the occurrence of significant events and the absence of information in some periods of the available historical data. However, the author reports as satisfactory the results of the numerical simulation.

2.5   "Progradational Sand-mud Deltas in Lakes and Reservoirs. Part 2. Experimental and Numerical Simulation"

This work was published by Svetlana Kostic and Gary Parker in 2003. It was carried out at the St. Anthony Falls Hydraulic Laboratory of the University of Minnesota. Kostic and Parker (2003b) carried out two experiments of sand-mud transport and deposition in a flume in order to test a previously developed 1D conceptual and numerical model of deltaic sedimentation in lakes and reservoirs. The experiments showed the interaction of sand and mud deposits and the way that it evolves in time. They also allowed the study of the influence of significant parameters as friction coefficient, fall velocity and plunging mixing coefficient, in the evolution of the deposits.

2.5.1   Experimental Facility

The experimental facility used to perform the experiments consisted of a flume 12.8 m long, 0.304 m wide and 0.76 m deep, with glass walls to facilitate flow visualization. It had the same configuration of the flume used by García (1990) described in the section 2.3, with an initial inclined reach followed by a decrease in the slope and a damping tank at the downstream end to avoid the reflection of the turbidity current. In this case only 7 m of the downstream end of the flume were used to perform the experiments. The initial upstream end was steep and short and the remaining portion had a bottom slope of 0.012.

A mixing tank with a capacity of 2000 l and provided with a propeller was used to supply the mixture for the turbidity current. In addition, a bulk screw feeder was used to feed the sand. The mixing tank was used to initially supply only clear water, in order to allow for the progression of the fluvial sand delta. After this period the clear water was replaced with the mixture for the turbidity current simulation.

The clear water and the turbidity mixture were delivered to the flume at an indentation just upstream of the crest of the ski jump, which served as a stilling basin. The sand was delivered just downstream of this basin.

The delivery rate of the turbidity current mixture to the flume was controlled with a valve and set to specific values obtained by means of weighting of samples, while the delivery rate of sand was controlled by a dial on the screw feeder, and also set to specific values obtained by the same procedure.

A grid with 10 cm increments was drawn on the glass wall in order to facilitate the measurements of the bed profiles. This grid was extended over 5.3 m of the study reach.

2.5.2   Sediment Properties

Silica flour was chosen to be used in the mixture of the turbidity current. It was white in color and composed predominantly of silt sizes, by this reason was referred as white silt. Two grades of this white silt were used. In Experiment 1 material with a median size of 24.2 µm was used, while in Experiment 2 the median size was 40.8 µm.

The silica flour or white silt was an angular powder with a specific gravity of 2.65 g/cm^3. Its grain-size distribution was poorly sorted. 17% of the silt used in the Experiment 1 was coarser than 62.5 µm and thus in the sand range, and 6% was finer than 1 µm. 38% of the white silt used in Experiment 2 was coarser that 62.5 µm, and 5% was finer than 1 µm. It can be seen that although predominantly in the silt sizes, the white silt or silica flour included significant fractions of material in the sand and clay sizes.

The sand was represented by an angular black siliceous by-product of the burning of coal, and so referred as black sand. It had a specific gravity of 2.60 g/cm3 and a median size of 420 µm. The grain-size distribution of the sand was well sorted. However a small but noticeable fraction of the sand consisted of thin flakes and curls which were considerably more mobile than the rest of the sand.

2.5.3 *Conditions of the Experiments*

Each experiment was composed by an initial part were only clear water and sand were delivered to the flume, followed by successive runs in which the clear water was replaced by the white silt and water mixture while the sand continued to be delivered. The first part was intended to the development of the fluvial sand delta, and the following runs were intended to simulate turbidity currents events. The run with clear water was denominated Run 1 – T0 in the case of Experiment 1 and Run 2 – T0 in the case of Experiment 2. Before each experiment, the flume was filled with standing water to a depth of 0.41 m.

After the initial run, the experiments were recommenced but this time delivering the turbidity current mixture instead of clear water. The duration of these runs, 8 in Experiment 1 and 6 in Experiment 2, was about 13 to 15 min, during which about 1400 l of the mixture was supplied. At the end of this period the experiment was halted, the tank was filled again with the mixture and then the experiment was recommenced with the next run.

In both experiments and in all the runs the inflow discharge of water or mixture was set equal to 2.0 l/s, the design volume concentration of white silt was 0.0239 corresponding to a feed rate of 127.2 g/s. The design feed rate of black sand was 14.1 g/s in Experiment 1 and in Experiment 2 was 6.69 g/s. In this way the black sand constituted about 10% of the incoming sediment by weight in Experiment 1 and about 5% in Experiment 2.

During the experiment, inflow water discharge and sand income were monitored and adjusted continuously. Mixture samples were taken from time to time in order to determine the concentration of white silt. Water surface elevations were monitored from the grid on the flume wall. Profiles of bed deposition were obtained by drawing colored lines in the glass wall and extracting data from the grid, and at the end of each experiment the central line of the deposit was pointed with a gage. Video footage and photographs were also taken to document the progress of the experiment and the final state. From time to time coal powder was also added to the mixture to allow for the turbidity current visualization. Measurements of turbidity current velocities or suspended sediment concentrations were not taken.

2.5.4 *Results and Conclusions*

The numerical model developed in Kostic and Parker (2003a) was tested against the experimental data. For each experiment, the friction coefficient of the turbidity current and the

mixing coefficient for plunging were calibrated to obtain the best fit of the data with the numerical model.

Using the numerical model the influence of a change in the various coefficients and parameters in the final results for the bed deposit was studied. For example, for Experiment 1 it was obtained that a change in the friction coefficient for the turbidity current from 0.01 to 0.02 results in a very small displacement of the sediment deposit interface in the downstream direction, and a small depression of its elevation. On the other hand, an increase from 0.01 to 0.05 of the friction coefficient results in a negligible downstream displacement and a more noticeable depression of its elevation.

In the case of the initial mixing coefficient for plunging, it was obtained a more pronounced effect in the bottomset deposit near the toe of the delta. As lower is the value of the coefficient as higher is the concentration of fine sediment at the inflow boundary of the turbidity current, leading to a quicker built up of the bottomset deposit.

Regarding to fall velocity, it could be observed through numerical simulation that an increase in the median size, and consequently in the magnitude of fall velocity, leads to a decrease in the deposit interface streamwise velocity and to a much more pronounced increase in the bottomset thickness. As the bottomset deposits aggrades more rapidly, the height of the delta decreases and increases its rate of progradation.

2.6 "Depositional Turbidity Currents in Diapiric Minibasins on the Continental Slope: Experiments and Numerical Simulation."

This work was developed by Horacio Toniolo, Gary Parker and Vaughan Voller. Its main objective was to the study the morphodynamics of the turbidity currents and sediment deposition in diapiric minibasins.

The authors proposed that turbidity currents occurring in diapiric minibasins can be ponded. In this way the turbidity current is divided in two regions by an internal hydraulic jump. The upstream region is supercritical and fully turbulent and the downstream region is a ponded zone where the turbulence is low. If the surface area of this zone is sufficient, all the water may detrain across a settling interface so there is no overflow over the downstream end of the minibasin even with continuous inflow. The main purpose of this work was to implement the theory in a numerical model and verify it against experiments.

2.6.1 _Experimental Facility_

The experimental facility used to perform the experiments was the same flume used by Kostic and Parker described in section 2.5.1 with some minor modifications.

The general structure of the flume, with all its dimensions; the mixing tank; the whole water and turbidity current mixture supply system; and the drainage tank at the downstream end were kept equal to the facility used by Kostic and Parker (2003b).

The same 7 m of the downstream part of the flume were used for the experiments. The simplified minibasin model had a length of 4 m with and inclined upstream region of constant slope equal to 0.298 and a nearly horizontal region with a slope of 0.017. At the downstream end of this 4 m region, a nearly vertical wall was located.

To measure concentration profiles of the turbidity current, 17 siphons were staked vertically in three rakes. The first contained 5 siphons and the other two contained 6. In the rake with five siphons, these were separated by 1, 3, 4 and 12 cm in order from bottom to top. On the rakes with six siphons, a last one was place 12 cm above the previously highest siphon. The rakes were mounted on three carts and distributed over the model.

Another independent siphon was used to measure suspended sediment concentration of outflow over the vertical wall at the downstream end. It served to quantify the outflow of sediment from the model.

2.6.2 *Sediment Properties*

Glass beads (ballotini) were used in the mixture for the turbidity current simulation. The density of the glass beads was 2.5 g/cm^3, the median size was 45 μm, the geometric mean size was 46 μm and the standard deviation was 1.25.

Black sand was included only in one experiment performed to verify a numerical model of reservoir trap efficiency. This experiment was conducted in the same installation described above. The black sand had a specific gravity of 2.60, geometric mean size of 500 μm and a geometric standard deviation of 1.47. In this experiment the white silt used for the turbidity current mixture had a specific gravity of 2.50, a geometric mean size of 53 μm and a geometric standard deviation of 1.3.

2.6.3 *Conditions of the Experiments*

Initially three experiments were performed, but only two were comprised by the theory developed in the first part of the work, namely Experiment 1 and 3. In both experiments the turbidity current mixture had a volumetric concentration of 0.05 and the maximum water depth in the flume was 0.46 m.

The mixture was discharged to the minibasin slot in the upstream end of the flume, and a horizontal headgate restricted the flow to a depth of 2 cm. The delivery rate was controlled by a valve calibrated by weighting several samples.

The concentration measurement through the siphons were performed as closer in time as was possible, in order to get a snapshot of the suspended sediment profile in the model. The samples were analyzed to obtain sediment concentration and grain size distribution. The distributions were determined using an Elzone particle counter machine.

Fine coal was added after each period of concentration measures in order to mark the stratigraphy of the deposit. Also during Experiment 1 shots of Rhodamine dye were introduce to improve the hydraulic jump visualization.

Experiments 1 and 3 differ in its upstream inflow discharge. Experiment 1 was performed with a small discharge of 0.33 l/s and duration of 60 min in order to obtain a completely ponded turbidity current. Experiment 3 was performed with an inflow discharge of 1.9 l/s and duration of 11 minutes, and was intended to obtain an overflow at the downstream end vertical wall.

After the experiment the bed was profiled using a point gauge every 5.08 cm in the streamwise direction. The longitudinal variation in grain-size distribution of the bed deposit was characterized by means of 7 bed samples in Experiment 1 and 10 samples in Experiment 3.

In the experiment performed to verify the numerical model of reservoir trap efficiency the procedure was the same described for the experiments of Kostic and Parker. The value for the upstream discharge of water and mixture was 1 l/s, the volume concentration of white silt was 2.5%. The black sand feed rate was 9 g/s and the white silt feed rate was 12.6%.

In this experiment, only one rake of 5 siphons was used. The distance from the water surface to the siphons was 3.5, 8.5, 18.5, 28.5 and 37.5 cm. The cart was placed at a point located 170 cm upstream of the vertical wall. One independent siphon was located over the lip of the wall. Bed profiles were also obtained drawing colored lines on the glass wall.

2.6.4   *Results and Conclusions*

The experiment allowed the verification of the fact that it is possible for a turbidity current to reach a ponded state without outflow even under continuous inflow to the minibasin. This is the consequence of the water detrainment that takes place in the subcritical zone of a ponded turbidity current and which is directly related to the fall velocity and thus to the fine particle size.

The experiments confirmed several theoretical conclusions of the Toniolo (2003) work, including the nearly uniform thickness of the deposit in the ponded zone. This is a consequence of the fact that the fine sediment concentration, after the hydraulic jump, becomes almost uniform in both, streamwise and vertical directions.

In the experiment which included black sand, the same phenomena of mixture of sediments was observed: the presence of white silt in the topset and foreset deposits and black sand at the bottomset deposit. This was due to the presence of particles in the black sand which fall in the fine range and the presence of particles in the white silt that fall in the coarse range. For this reason, the white silt and black sand grain size distribution had to be corrected in order to represent correctly the coarse and fine fractions in the numerical model. The corrected feed rates for coarse and fine materials were 13.3 g/s and 58.14 g/s respectively and the corresponding corrected sizes were 295 μm and 49.7 μm.

2.7 "Weakly Depositing Turbidity Currents on Small Slopes"

This work was carried out by Mustafa Altinakar at the Laboratoire de Recherches Hydrauliques of the École Polythecnique Fédérale de Lausanne.

The main goal of the research was to investigate the influence of a small slope on the hydrodynamics of turbidity currents and the influence of weak sedimentation on the behavior of the current.

Several quantities and parameters of the body and the head of the current were studied. Some of them were measured directly. Among the coefficients studied for the turbidity current body, special attention was made on the entrainment coefficients for ambient water and bed sediment.

In order to evaluate the influence of the slope in the hydrodynamics of the current, experiments were carried out in a tilting channel considering several values for the slope and initial buoyancy flux. To determine the influence of fall velocity of particles, experiments using two different materials having different grain size distributions were performed. In addition, to investigate the case of zero fall velocity and no sediment interchange with the bed, a series of experiments using saline water to simulate the current was performed.

2.7.1 *Experimental Facility*

The experiments were performed in a tilting flume with 16.55 m length, 50 cm wide and 80 cm high. The base of the flume was mounted over a special steel structure designed to avoid deflection. The structure was supported at a central pivot point and at two jacking stations at each side of the pivot, both separated by a distance of 8.8 m. With this configuration the channel could take a slope between -1% and 3.6%. The slope was read with a surveyed

vernier on a long scale of 25 cm located near the upstream screw jacking station. The sides of the flume were constructed from 9.5 mm thick transparent plate glass supported at 1 m intervals by cantilever members.

The channel could be divided in three principal sections, starting with an upstream inlet tank where clear water supply was performed. Its length was 1.25 m ending with a sliding gate (SL1). After this section the second principal one started, being the flume itself. The flume section was divided into two subsections of unequal length by means of a second sliding gate (SL2) located at approximately 2 m downstream of the first gate. The first shorter section by the second gate, serves as a head tank and stilling box for the mixture of the turbidity current while the larger section constituted the working area where the turbidity current took place. The downstream end of this flume sections ended in a dismountable sharp crested weir used to control the water level. The final principal section was a discharge tank, 1.3 m long, which started after the sharp crested weir with a downward step in the bottom of the flume, intended to trap the turbidity current and for its drainage through a bottom opening.

Immediately upstream of the second gate, a baffle fabricated by filling a box of a large mesh screen with balls of 2 cm diameters served to dissipate the initial momentum of the current and reduced the scale of the initial turbulence. An inclined PVC plate was placed behind the second gate to guide the mixture to the exit baffle region.

Two tanks adjacent to the flume each one with a capacity of 5500 l served to prepare and store the mixture. The mixing tank was provided with a three blade propeller-type mixer which had a velocity of 2000 rpm. The mixture was pumped to the stilling box through a 150 mm diameter PVC pipe provided with orifice and electromagnetic meters. At the end of the supply pipe a special flow divider was used to delivery the correct amount of mixture to the stilling box. The position of flow divider was calibrated measuring the time required to fill a box of known volume against the position of the divider. In this way a constant discharge rate of 14.5 l/s could be used in the supply pipe to avoid sedimentation on it.

To measure the velocities a series of micro-propeller current-meters mounted on motorized gauges and controlled by a computer were used. The velocity measure range varied between 2 cm/s and 150 cm/s. Three of five available probes where located at 2, 4 and 8 m from the entrance gate.

Density of water and the mixture were measured before each experiment with a standard Casagrande type Hydrometer. Density profiles of the body were measured at three stations using three suction probe rakes, one of 20 tips and two of 16 tips. They were connected to a collector unit provided with bottles of 1 l capacity. At the end of the experiment the density of the samples were measured using the hydrometer.

Photography and video recording were also used to analyze the current height. The shadowgraph technique was also used to visualize saline currents.

2.7.2 *Sediment Properties*

In this work saline and turbidity currents were generated. For saline currents a common low quality salt was used. For turbidity currents two different quartz flours were selected. These materials, called K-06 and K-13, were not naturals and the particles were not perfect spheres but had angular shapes. Both flours had a density of 2.65 gr/cm^3.

The median diameters of K-06 and K-13 were 0.032 mm and 0.014 mm respectively. In the same order, their geometric mean diameters were 0.025 mm and 0.013 mm and the standard deviations for the log normal distribution, $\sqrt{d_{84}/d_{16}}$, were 0.86 and 2.81.

Altinakar (1993) choose the grain size with a settling velocity equal to the average value to be the representative particle size for the sediment material. The velocity of each size was calculated by means of the Stoke's law, since this was applicable for the range of sizes of the sediment material. The resulting diameters and fall velocities were 0.0467 mm and 1.96 mm/s for K-06 and 0.026 mm and 0.61 mm/s for the K-13.

2.7.3 *Conditions of the Experiments*

Several runs with different conditions were performed, all having a common procedure. Before the beginning of each experiment the mixing tank was filled with clear water and the mixer was activated. This clear water was started to be pumped in a closed circuit at 14.5 l/s, to obtain additional stirring. After this, the sediment or salt was added slowly taking care that it all particles were wetted and no flocks were formed.

In the flume, sliding gates 1 and 2 were opened and the clear water supply was started until the water level reached the crest of the downstream weir, after this both gates were closed again. The bottom valve at the stilling box formed between the gates was opened and clear water was drained. The plug of the incoming mixture pipe was then reinserted in the stilling box, as long as the level is next to the clear water level in the rest of the flume, the plug is slided slowly until the desired calibrated position for the target discharge. At this moment the sliding gate 2 was opened slowly and the turbidity or saline current started to flow.

With this procedure 7 series of experiments were carried out. Maximum and minimum values for the slope were 0.0321 and horizontal, the discharge varied between 6.4 l/s and 1.1 l/s, the opening of the gate varied between 5.5 cm and 3.5 cm, the density of the turbid or saline mixture from 1.001 to 1.05 gr/cm^3 and the maximum water depth between 30 cm and 70 cm.

After the experiments involving turbidity currents were terminated, bed samples at specified location were taken for grain-size analysis.

2.7.4 *Results and Conclusion*

Based on the experimental data several conclusions regarding the dynamics of the turbidity current head and body could be obtained. It was shown that small slopes diminished the head velocity and that the head growth rate was increased with sedimentation.

For the body of the current the value of the shape factors involved in the motion equations were calculated and confirmed to be close to the unity in a narrow range. However no definitive conclusion could be made on the dependency of these factors on the slope or rate of the fall velocity to depth-averaged velocity.

The similarity collapse for the velocity profiles was confirmed not only at different locations in the same turbidity current but also between different turbidity currents flowing in different slopes. These profiles were calculated using the Ellison and Turner (1959) integral scales.

The similarity of density profiles was confirmed for measurements taken at different locations in the same turbidity current, but not between profiles taken in different turbidity currents.

For the water entrainment coefficient the attempts to define a water entrainment coefficient in terms of a shear Richardson number were not successful.

Sediment entrainment coefficients were calculated using the experimental data. The result showed the depositional character of the developed turbidity currents. The ratio of the near bed sediment concentration to the depth averaged mean concentration showed a little tendency to decrease with decreasing of the ratio between fall velocity and depth averaged mean velocity, but the constant value of 2 proposed by García (1993) was still consistent with the data.

Regarding the bed-friction coefficient, Altinakar concluded that a better choice to represent the friction characteristics of the turbidity current is to define a friction coefficient in terms of a maximum velocity based on the Reynolds number.

The grain size analysis of the sediment concentration samples collected during experiments showed that not only longitudinal sorting is present in the turbidity current, but also vertical sorting.

As an important general conclusion, should be retained the fact that the length of the channel used by Altinakar did not allow for a good computation of sediment and water entrainment coefficients. It was pointed that a much longer flume would required and less intrusive and

indirect measure techniques for velocity and concentration should be used in future works to accomplish these objective.

2.8 Summary

Within the previous sections, the characteristics of the facilities and instrumentation used by different authors were reviewed. Also the properties of the sediment used and the type of measures performed in each work were described. In this section a brief summary is given with the aim of showing the range of values of the most important parameters.

2.8.1 *Experimental Facility Characteristics*

Table 2.1 resumes the principal geometric characteristics of the channels used by the different authors to simulate turbidity currents. Some of the channels had a variable slope and others were divided in two reaches defining two values for the slope in order to simulate a delta configuration. The capacity of the mixing tanks used to prepare the turbidity current mixture is also presented.

Table 2.1 Characteristics of the channels used in different experimental studies

Author	Oehy (2003)	García (1990)	De Cesare (1998)	Kostic and Parker (2003)	Toniolo (2003)	Altinakar (1993)
Length [m]	8.55	11.6	9	12.8	11.6	16.55
Width [cm]	27.2	30	150	30.4	30	50
Height [cm]	90	78	65	76	78	80
Slope [-]	0 – 0.05	0 – 0.08	0 – 0.06	0.012	0.017 – 0.298	0 – 0.032
Mixing tank capacity [l]	1500	2000	2000	2000	2000	5500

2.8.2 *Sediment Properties*

Table 2.2 resumes the principal characteristics of the sediment used by the authors to simulate the turbidity current. Some authors have described the sediment using the mean diameter and the standard deviation while others have used the geometric mean diameter and the associated geometric standard deviation. Altinakar (1993) used the standard deviation for the log-normal distribution $\sqrt{d_{84}/d_{16}}$.

Delta deposits were simulated only in the work of Kostic & Parker (2003b). The sand used to simulate the coarse sediment had a median size of 420 μm.

In some studies values for grain-size deviation and fall velocity of particles were not specified.

<p align="center">Table 2.2 Principal characteristics of the fine sediment used by different authors</p>

Author	Oehy (2003)	García (1990)	De Cesare (1998)	Kostic and Parker (2003)	Toniolo (2003)	Altinakar (1993)
Material	Ground Polymer	Silica, Glass and Crushed Coal	OPALIT	Silica Flour	Glass Beads (Ballotini)	Quartz Flour
Characteristic diameter [μm]	d_{50} 90	d_{sg} 4 - 180	d_{50} 20	d_{50} 24.2 - 40.8	d_{50} 45	d_{sg} 14 – 32
Standard deviation [-]	σ_g 1.6	σ_{sg} 0.47 – 1.0	-	-	σ_g 1.25	$(d_{84}/d_{16})^{1/2}$ 0.86 – 2.81
Fall velocity [mm/s]	0.522	0.002 – 0.620	0.4	-	-	0.026 – 0.61

2.8.3   *Conditions of the Experiments*

The values for the principal variables as flow discharge, inflow fine sediment concentration and turbidity current initial depth are resumed on the Table 2.3.

In the experiments of García (1993) the flow discharge value corresponds to the inlet turbidity current velocity multiplied by the inlet area defined by the sluice gate height and the wide of the flume. All the experiments presented in the table are of the same kind, where a turbidity current is developed in a flume with a 1D configuration.

The experiments conducted by De Cesare (1998) followed a more like 2D configuration. The volumetric concentration in the experiments of De Cesare (1998) was in the range 0.2% to 2%. In all the experiments the height at the gate was 5 cm. The velocity at the same place was 10 cm/s for two of the experiments and 5 cm/s for the remaining. The water depth in the tank in each experiment was not stated explicitly but can be inferred by the dimensions of the tanks and the operation. At the downstream end the tank was 65 cm height, the configuration of the tanks was such that the water overflows at the downstream end. Also in the Experiment 7 the depth of measure of UVP devices is 658 mm. This indicates that the depth of water could be well approximated by a value of 66 cm.

Table 2.3 Values for the principal flow variables through the experiments of different authors

Author	Oehy (2003)	García (1990)	Kostic and Parker (2003)	Toniolo (2003)	Altinakar (1993)
Flow discharge [l/s]	0.5 – 1.37	0.75 – 1.3	2	0.33 – 1.9	1.1 – 6.4
Volumetric fine sediment conc. [%]	1.9 -4.63	0.13 – 0.86	2.39	5	0.6 - 3
Initial depth for turbidity current [cm]	4.5	3	Plunging	2	3.5 – 5.5
Water depth [cm]	52	78	41	46	30 - 70

3. EXPERIMENTAL FACILITY

3.1 General Description

The experimental facility used in this study can be divided in four principal parts: the water supply tank, the channel, the coarse sediment feeder and the turbidity current mixture preparing tank.

3.1.1 *Water Supply Tank*

The water supply tank (Figure 3.1) is a reservoir intended for supply water to the channel at low accurate rates. It is composed of three subsections or mini tanks.

The first is a rectangular tank 6.3 m long with a rectangular cross section of 80 cm width by 88 cm high. At the upstream end a bomb, connected to the reservoir by means of a flexible pipe of 5 cm diameter, provide water at a constant rate of 15 l/s. The water is taken from the general underground reservoir of the laboratory. Near the location of the inflow flexible pipe, a large circular weir controls the overflow from the first subsection returning water to the underground reservoir. At the downstream wall a bottom plane circular valve connects this section with the next.

The next subsection is also a rectangular mini tank 48 cm width, 80 cm high and 2 m long. This tank is provided with a bottom control valve that also returns water to the general reservoir. A rectangular top opening of 30 cm width and 32 cm high located at the middle of the right wall connects this subsection with the third one.

Finally, the third subsection has 30 cm width, 30 cm high and 2.5 m long channel which is provided with a hydrostatic head meter. At the downstream end a triangular weir is used to control the inflow rate to the channel by means of the of the head meter measurements.

The water level at the triangular weir, and consequently the inflow discharge to the channel, is controlled by means of the bottom valve in the second mini tank. When the lower inflow rates are pursued, the water level in the tanks can decrease down of the circular weir culvert. This weir at the same time that prevents water overflowing from the whole system, acts to reduce water level variations due to bomb inflow rate oscillations. Thus, during the experiments where low inflow discharges are involved the circular plane valve that connects the first mini tank with the second one will be set to a smaller opening, in order to raise the water level until the circular weir starts the overflow. Figure 3.1 shows the water supply tank with the three main subsections.

Figure 3.1 Water supply tank

3.1.2 *Channel*

The channel, starting just downstream of the triangular weir, has a constant width of 30 cm and a total length of 17.1 m. It comprises three distinctive parts intended to simulate the configuration of a delta deposit: the first is a 4.75 m long reach with a slope of 0.026 that simulates the river entering to the reservoir. The second is a short reach 0.65 m long with an abrupt change in the slope to a value of 0.57 in order to simulate the foreset of the delta, and the last is the one that simulates the reservoir itself with a total length of 11.7 m and a bottom slope of 0.015.

The maximum height at the end of the channel is 79 cm, in this area a bottom valve serves for the drainage of the water and turbidity current mixture. Figure 3.2 shows the triangular weir and the delta foreset zone in the channel.
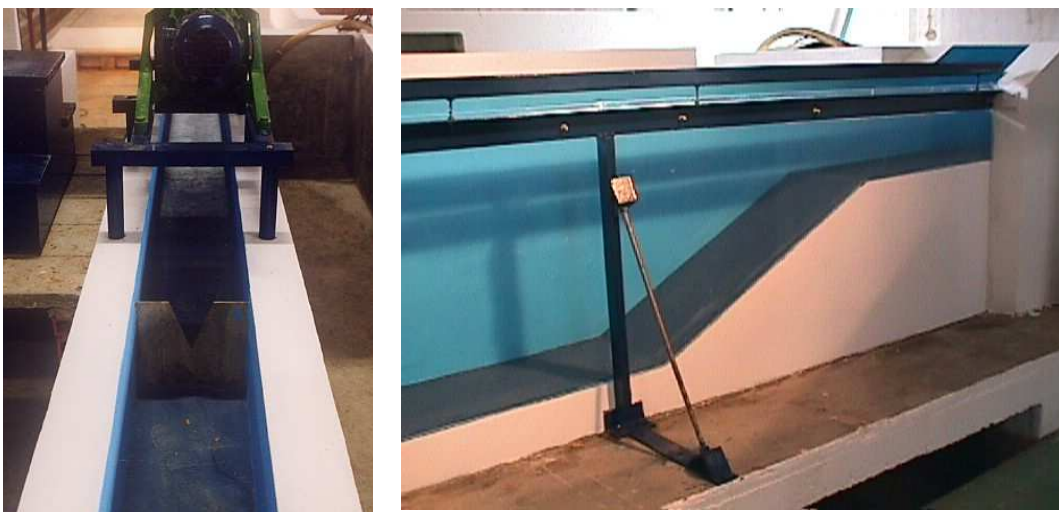
Figure 3.2 Triangular weir (left) and delta zone connecting the river and reservoir parts in the flume (right)

3.1.3 *Coarse Sediment Feeder*

The coarse sediment feeder is constituted by a pyramidal container and a constant velocity screw driver that introduces the sediment in the channel 1.5 m downstream of the triangular weir (See Figure 3.3). The pyramidal container ends with a cylinder where the sediment feed rate is established.

The sediment feed rate is controlled by two ways. In the case of low feed rates (<7.5 g/l) four orifices placed at the bottom of the container (cylinder) are opened sequentially such that the sequential opening of each one determines the feed rates. The diameter of each orifice has been selected to achieve predefined feed rates accordingly to the screw driver constant speed. The diameter of each orifice is: 3.5 mm for the first, 4 mm for the second and 4.5 mm for the last two of them.

Higher feed rates (>7.5 g/l) are achieved by the rotation of the cylinder bottom, which is attached to the pyramidal structure by means of a screw placed at the center of it. This rotation defines different lateral openings associated to different feed rates. A total of twelve marks are placed at the cylinder to measure how much the bottom has been rotated. The sand does not start to fall uniformly until the bottom of the cylinder has been rotated a complete turn plus the necessary fraction to place it at position 5.

Figure 3.3 Coarse sediment feeder

3.1.4 *Calibration Process of the Coarse Sediment Feeder*

Some measurements were conducted to complement previous data concerning the feed rate associated to each opening. The procedure used consisted of the weighting of sand samples collected during a specific amount of time. The total weight divided by the corresponding

time gives the feed rate. The measurements finally considered to establish the feed rate associated to each opening, after discarding all the ones with out of range values due to experimental errors, are presented in the tables 3.1 to 3.8.

Table 3.1 Measurements selected to establish the feed rate. Opening orifice of 3.5 mm

Date	Orifice opening [mm]	Simple number	Time [min]	Net weight [gr]	Feed rate [g/min]	Feed rate [g/s]
24-05-2005	3.5	1	15	1088.2	72.5	1.21
24-05-2005	3.5	2	15	1091.6	72.8	1.21
24-05-2005	3.5	3	15	1104.2	73.6	1.23
24-05-2005	3.5	4	15	1100.2	73.3	1.22
10-06-2006	3.5	5	15	1043.2	69.5	1.16
10-06-2006	3.5	6	15	1079.8	72.0	1.20
10-06-2006	3.5	7	15	1055.2	70.3	1.17
10-06-2006	3.5	8	15	1081.8	72.1	1.20
10-06-2006	3.5	9	20	1438.6	71.9	1.20
10-06-2006	3.5	10	15	1088.2	72.5	1.21
10-06-2006	3.5	11	20	1423.2	71.2	1.19
10-06-2006	3.5	12	15	1108.2	73.9	1.23
10-06-2006	3.5	13	20	1203.6	60.2	1.00
10-06-2006	3.5	14	15	1103.6	73.6	1.23
10-06-2006	3.5	15	25	1975.8	79.0	1.32
10-06-2006	3.5	16	15	1095.6	73.0	1.22
24-05-2005	3.5	1	15	1088.2	72.5	1.21
24-05-2005	3.5	2	15	1091.6	72.8	1.21
24-05-2005	3.5	3	15	1104.2	73.6	1.23
Characteristic Values						
Mean feed rate [g/min]		Standard deviation [g/min]		Maximum feed rate [g/min]		Minimum feed rate [g/min]
72.0		3.8		79.0		60.2

Table 3.2 Measurements selected to establish the feed rate. Opening orifices of 3.5 mm and 4 mm

Date	Orifice opening [mm]	Simple number	Time [min]	Net weight [gr]	Feed rate [g/min]	Feed rate [g/s]
24-05-2005	3.5+4	1	15	2699.0	179.9	3.00
24-05-2005	3.5+4	2	15	2713.0	180.9	3.01
24-05-2005	3.5+4	3	15	2696.8	179.8	3.00
24-05-2005	3.5+4	4	15	2664.6	177.6	2.96
11-06-2006	3.5+4	5	15	2081.6	138.8	2.31
11-06-2006	3.5+4	6	15	2609.2	173.9	2.90
11-06-2006	3.5+4	7	15	2606.2	173.7	2.90
11-06-2006	3.5+4	8	20	2972.2	148.6	2.48
11-06-2006	3.5+4	9	20	3496.8	174.8	2.91
11-06-2006	3.5+4	10	20	3287.0	164.4	2.74
24-05-2005	3.5+4	1	15	2699.0	179.9	3.00
Characteristic Values						
Mean feed rate [g/min]		Standard deviation [g/min]		Maximum feed rate [g/min]		Minimum feed rate [g/min]
169.2		14.5		180.9		138.8

Table 3.3 Measurements selected to establish the feed rate. Opening 3.5 mm, 4 mm and one of 4.5 mm

Date	Orifice opening [mm]	Simple number	Time [min]	Net weight [gr]	Feed rate [g/min]	Feed rate [g/s]
24-05-2005	3.5+4+4.5	1	15	4303.4	286.9	4.78
24-05-2005	3.5+4+4.5	2	15	4216.2	281.1	4.68
24-05-2005	3.5+4+4.5	3	15	4270.4	284.7	4.74
24-05-2005	3.5+4+4.5	4	15	4161.0	277.4	4.62
24-05-2005	3.5+4+4.5	5	15	4741.2	316.1	5.27
24-05-2005	3.5+4+4.5	6	15	4725.0	315.0	5.25
10-06-2006	3.5+4+4.5	7	15	4736.6	315.8	5.26
10-06-2006	3.5+4+4.5	8	15	4637.4	309.2	5.15
10-06-2006	3.5+4+4.5	9	15	4682.8	312.2	5.20
10-06-2006	3.5+4+4.5	10	15	4380.8	292.1	4.87
10-06-2006	3.5+4+4.5	11	15	4426.2	295.1	4.92
10-06-2006	3.5+4+4.5	12	15	4461.4	297.4	4.96
10-06-2006	3.5+4+4.5	13	15	4767.6	317.8	5.30
Characteristic Values						
Mean feed rate [g/min]		Standard deviation [g/min]		Maximum feed rate [g/min]		Minimum feed rate [g/min]
300.1		14.9		317.8		277.4

Table 3.4 Measurements selected to establish the feed rate of all orifices opened simultaneously.

Date	Orifice opening [mm]	Simple number	Time [min]	Net weight [gr]	Feed rate [g/min]	Feed rate [g/s]
24-05-2005	3.5+4+4.5+4.5	1	15	6785.0	452.3	7.54
24-05-2005	3.5+4+4.5+4.5	2	15	6791.4	452.8	7.55
24-05-2005	3.5+4+4.5+4.5	3	15	6864.4	457.6	7.63
24-05-2005	3.5+4+4.5+4.5	4	15.5	6929.6	447.1	7.45
24-05-2005	3.5+4+4.5+4.5	5	15	6747.6	449.8	7.50
12-06-2006	3.5+4+4.5+4.5	6	15	6969.6	464.6	7.74
12-06-2006	3.5+4+4.5+4.5	7	10	4520.4	452.0	7.53
12-06-2006	3.5+4+4.5+4.5	8	15	6544.8	436.3	7.27
12-06-2006	3.5+4+4.5+4.5	9	15	6237.6	415.8	6.93
12-06-2006	3.5+4+4.5+4.5	10	10	4398.6	439.9	7.33
12-06-2006	3.5+4+4.5+4.5	11	15	6660.2	444.0	7.40
12-06-2006	3.5+4+4.5+4.5	12	10	4484.8	448.5	7.47
Characteristic Values						
Mean feed rate [g/min]		Standard deviation [g/min]		Maximum feed rate [g/min]		Minimum feed rate [g/min]
446.7		12.3		464.6		415.8

Table 3.5 Measurements selected to establish the feed rate with bottom of the cylinder

at position 1 turn plus position 5

Date	Bottom position [turn + mark]	Simple number	Time [min]	Net weight [gr]	Feed rate [g/min]	Feed rate [g/s]
15-11-2006	1+ 5	1	10	5553.8	555.4	9.26
15-11-2006	1+ 5	2	10	5416.4	541.6	9.03
15-11-2006	1+ 5	3	10	5158.8	515.9	8.60
15-11-2006	1+ 5	4	10	5230.4	523.0	8.72
15-11-2006	1+ 5	5	10	5597.2	559.7	9.33
15-11-2006	1+ 5	6	10	5350.2	535.0	8.92
16-11-2006	1+ 5	7	10	5107.2	510.7	8.51
17-11-2006	1+ 5	8	10	5611.8	561.2	9.35
17-11-2006	1+ 5	9	14	8183.0	584.5	9.74
17-11-2006	1+ 5	10	10	5600.2	560.0	9.33
17-11-2006	1+ 5	11	10	5610.8	561.1	9.35
Characteristic Values						
Mean feed rate [g/min]		Standard deviation [g/min]		Maximum feed rate [g/min]		Minimum feed rate [g/min]
546.2		22.9		584.5		510.7

Table 3.6 Measurements selected to establish the feed rate with the bottom of the cylinder

at position 1 turn plus position 6

Date	Bottom position [turn + mark]	Simple number	Time [min]	Net weight [gr]	Feed rate [g/min]	Feed rate [g/s]
15-11-2006	1 + 6	1	10	7533.0	753.3	12.56
15-11-2006	1 + 6	2	10	7454.8	745.5	12.42
15-11-2006	1 + 6	3	10	7562.8	756.3	12.60
15-11-2006	1 + 6	4	10	7251.6	725.2	12.09
16-11-2006	1 + 6	5	10	7064.6	706.5	11.77
16-11-2006	1 + 6	6	10	7099.0	709.9	11.83
16-11-2006	1 + 6	7	10	7085.8	708.6	11.81
17-11-2006	1 + 6	8	11	8356.6	759.7	12.66
17-11-2006	1 + 6	9	10	7683.2	768.3	12.81
17-11-2006	1 + 6	10	10	7412.2	741.2	12.35
17-11-2006	1 + 6	11	10	7565.0	756.5	12.61
Characteristic Values						
Mean feed rate [g/min]		Standard deviation [g/min]		Maximum feed rate [g/min]		Minimum feed rate [g/min]
739.2		22.7		768.3		706.5

Table 3.7 Measurements selected to establish the feed rate with the bottom of the cylinder

at position 1 turn plus position 7

Date	Bottom position [turn + mark]	Simple number	Time [min]	Net weight [gr]	Feed rate [g/min]	Feed rate [g/s]
16-11-2006	1+7	1	10	9326.6	932.7	15.54
16-11-2006	1+7	2	10	9658.6	965.9	16.10
16-11-2006	1+7	3	10	9947.2	994.7	16.58
17-11-2006	1+7	4	10	9130.2	913.0	15.22
17-11-2006	1+7	5	10	9081.2	908.1	15.14
17-11-2006	1+7	6	10	9447.2	944.7	15.75
17-11-2006	1+7	7	10	9335.2	933.5	15.56
17-11-2006	1+7	8	5	4555.8	911.2	15.19
17-11-2006	1+7	9	15	13925.8	928.4	15.47
17-11-2006	1+7	10	10	9362.0	936.2	15.60
17-11-2006	1+7	11	10	9102.0	910.2	15.17
Characteristic Values						
Mean feed rate [g/min]		Standard deviation [g/min]		Maximum feed rate [g/min]		Minimum feed rate [g/min]
934.4		26.6		994.7		908.1

Table 3.8 Measurements selected to establish the feed rate with the bottom of the cylinder

at position 1 turn plus position 8

Date	Bottom position [turn + mark]	Simple number	Time [min]	Net weight [gr]	Feed rate [g/min]	Feed rate [g/s]
16-11-2006	1+8	1	7	8098.2	1156.9	19.28
16-11-2006	1+8	2	5	5623.2	1124.6	18.74
16-11-2006	1+8	3	5	5636.6	1127.3	18.79
Characteristic Values						
Mean feed rate [g/min]		Standard deviation [g/min]		Maximum feed rate [g/min]		Minimum feed rate [g/min]
1136.3		17.9		1156.9		1124.6

The measurements presented in tables 2.1 to 2.8 are resumed in Figure 3.4 and the mean feed rates values are presented in Figure 3.5.
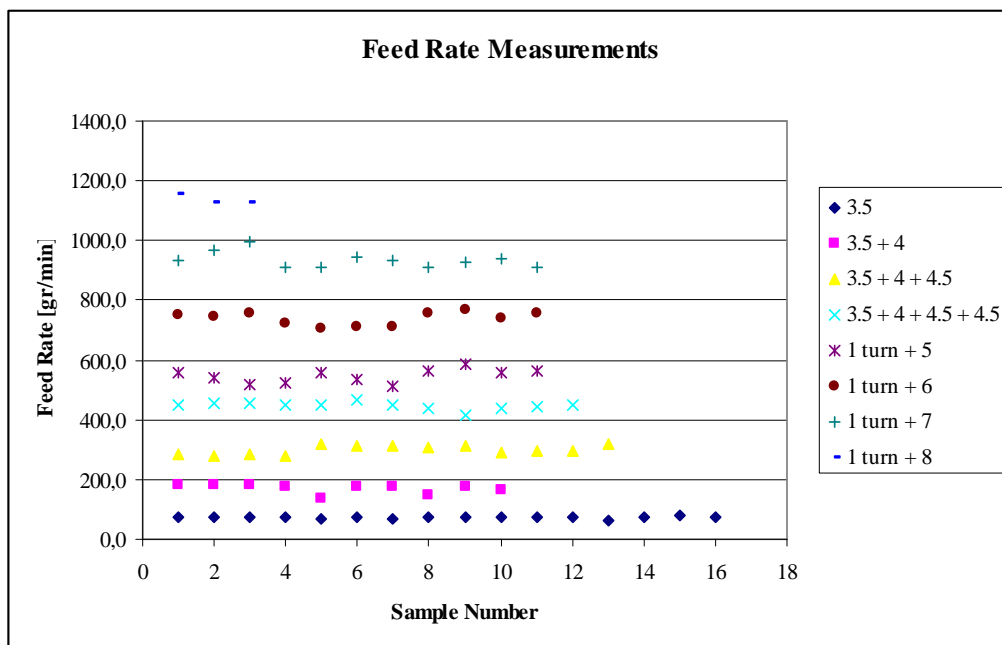

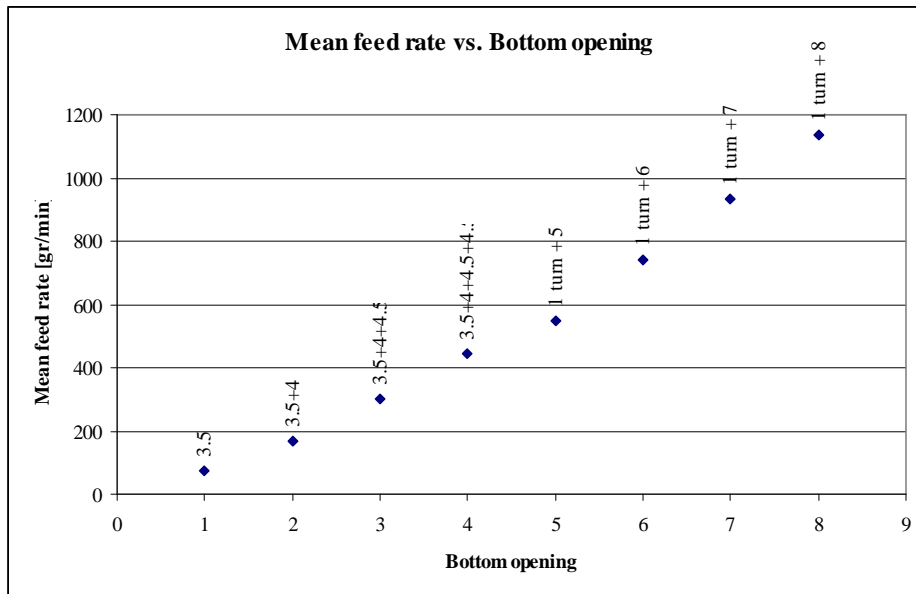**Figure 3.4 Resume of feed rate measurements**

Figure 3.5 Mean values of the feed rate versus the opening at the bottom of the cylinder

3.1.5 *Turbidity Current Mixture Preparing Tank*

The tank used to prepare the mixture of water and fine sediment which will originate the turbidity current in the flume, is formed by an almost cubic recipient with a capacity of 2947 l. In the middle of the tank, a circular metallic structure supporting several plastic plates is rotated by means of a motor to provide the turbulence required to keep the fine sediment suspended in the water column. The corners of the tank have been rounded to avoid zones with dead flow (See Figure 3.6).

The tank is connected to the flume through a pipe circuit. A pump installed in the tank sends the water to a principal pipe provided with a flow meter and a control valve used to set the desired flow rate, downstream of this valve the circuit is divided in two branches, each one with a check valve that are used to open or close the flow. One of the branches returns to the mixture tank and is used to re-circulate the mixture while the flow rate is being set. The other connects with the main flume and is used to inject the mixture to the model.

Figure 3.6 Turbidity current mixture preparing tank

4. MEASURING INSTRUMENTATION

4.1 Introduction

In this chapter the different methods and devices used to measure the variables of the turbidity current flow and the bed deposits are described.

Measurements of the turbidity current involve basically flow velocity and bed deposits thickness. Velocity measurements are carried out using a relatively new device which is based on ultrasound properties called UVP (Ultrasonic Velocity Profiler). The second type, involving the bed deposits are carried out using a special electric device developed at the Scientific Instrumentation Centre of the Laboratório Nacional de Engenharia Civil (LNEC).

4.2 Velocity Measurements

4.2.1 *General*

Velocity measurements are performed using the UVP (Ultrasonic Velocity Profiler) device, which measures an instantaneous velocity profile in the liquid column using the Doppler Effect to detect the frequency shift of an echoed signal. UVP has been used in the last decade in many experimental research works because it presents a lot of advantages over the traditional methods, among them, could be cited:

- Can be placed outside of the flow field thus avoiding any disturbance effect. Also due to its small size can be placed inside the flow generating a rather small disturbance.
- Can be used with opaque fluids.
- It can reduce the measuring time since it establishes a rather instantaneous and direct measure of the velocity.
- Since the Doppler shift frequency is directly related to the velocity value, the UVP does not require any calibration process besides the determination of sound velocity in the liquid of interest
- Since it can detect the sign of the flow, a true velocity vector can be measured. Also using additional transducers a multi-dimensional flow field can be mapped.

4.2.2 *UVP Basic Principle: Doppler Effect*

The Doppler Effect consists, basically, in the fact that when a source of waves and an observer are in relative movement, the frequency of the waves perceived by the observer does not match the original frequency emitted by the source.

To derive the relation between the velocity and the change in the frequency, the case when a static source is emitting a pulse and a particle that moves away from this at a constant velocity v_o is receiving it, will be considered. Let a static source emitting a signal with a period T_o and wavelength λ_o be considered in order to study the time instants when the observer particle receives two pulses of the signal emitted by the source. Then let $t_o = 0$ and $t_1 = T_o$ be the instants when the source emits the pulses and t_2 and t_3 those when the moving particle receive and echoes them. Figure 4.1 illustrates the situation, where a is the speed of propagation of the waves and λ_o is the original wavelength of the signal emitted by the source.
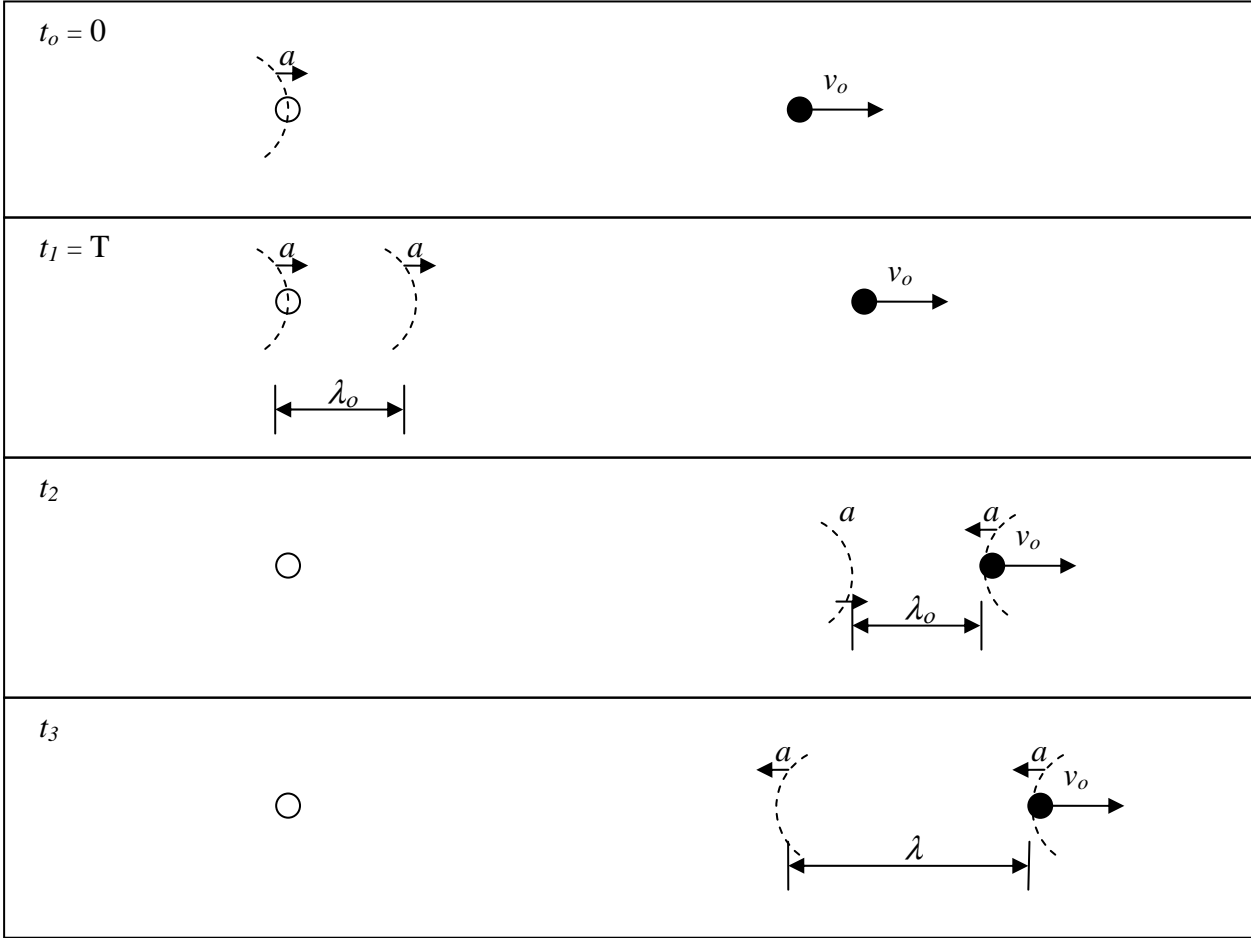

Figure 4.1 Sketch of the Doppler effect for a static source and a moving observer

Focusing the attention in time instants t_2 and t_3 and denoting d to the distance that the observer particle travels between instants t_2 and t_3, it is clear that the new wavelength is given by:

$$\lambda = \lambda_o + 2d \tag{4.1}$$

If a denotes the speed of propagation of the waves, then at the instant t_3 the following relations holds:

$$d = v_o(t_3 - t_2) \tag{4.2}$$

$$\lambda_o + d = a(t_3 - t_2) \tag{4.3}$$

From where it can be obtained:

$$t_3 - t_2 = T = \frac{\lambda_o}{a - v_o} \tag{4.4}$$

$$d = \frac{v_o \lambda_o}{a - v_o} \tag{4.5}$$

Using (4.5) in (4.1) results:

$$\frac{\lambda}{\lambda_o} = \frac{a + v_o}{a - v_o} \tag{4.6}$$

This relation can be written in terms of frequency as:

$$\frac{f}{f_o} = \frac{a - v_o}{a + v_o} \tag{4.7}$$

The relative change in frequency is then:

$$\frac{f - f_o}{f_o} = \frac{\Delta f}{f_o} = \frac{-2v_o}{a + v_o} \tag{4.8}$$

and assuming that the velocity of the observer is much lower that the speed of the waves,

$$\frac{f - f_o}{f_o} = \frac{\Delta f}{f_o} \approx \frac{-2v_o}{a} \tag{4.9}$$

This relations states that the frequency decreases when the observer is moving away from the source just like the sketch of Figure 4.1 shows.

4.2.3   *UVP Description*

The velocity measurement device has two mayor components. The first component corresponds to the transducers which are the responsible of emitting the ultrasonic signal and receiving the echo. The second component corresponds to the UVP-DUO unit which receives

the information from the transducers, transforms the analog echoed signal to digital and performs the measurement computations.

The velocity profiles are performed dividing the measurement axis in a series of individual cells called channels. These correspond to small cylindrical space volumes where the echo of ultrasonic burst will be monitored. This is illustrated in Figure 4.2 and Figure 4.3.
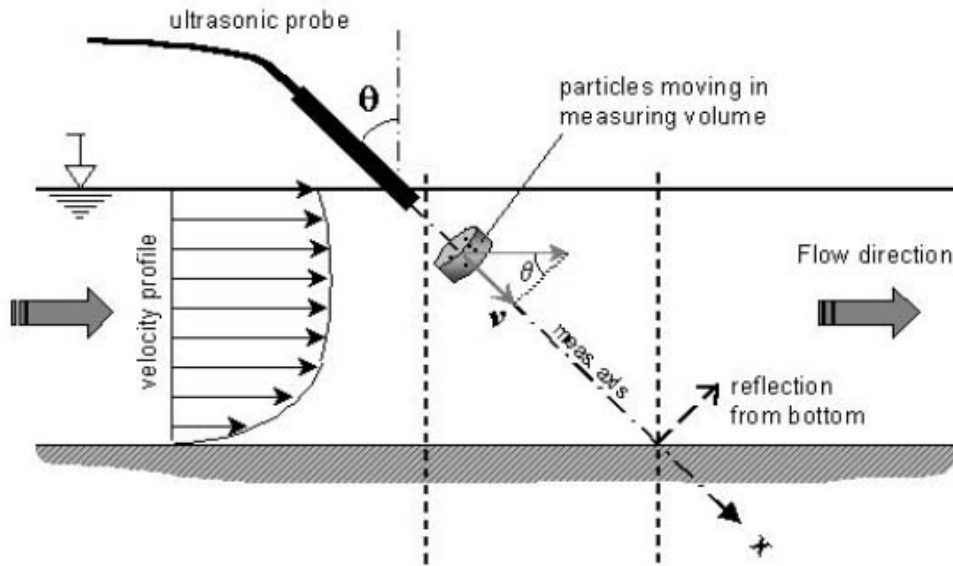
Figure 4.2 Sketch of the terms involved in a velocity profile measurement using the transducers

Figure 4.3 Description of the measurement window along the measurement axis

The channel width is related to the frequency of the emitted burst. The latter is emitted with a finite number of pulses, determining that the width of the channel can not be longer than the half of the total burst length. This is required in order to acquire information from all scatter particles contained in the volume during the reception time. Thus:

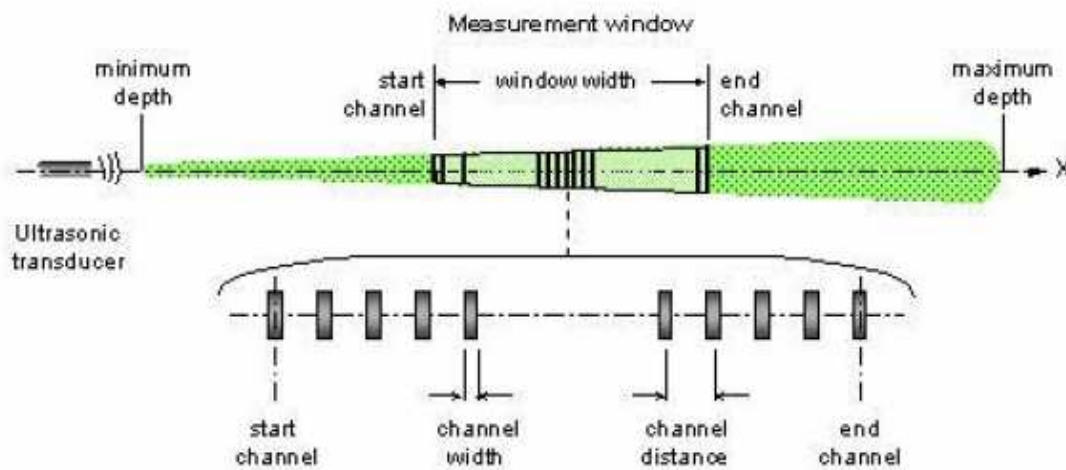$$w = \frac{n\lambda_o}{2} = \frac{cn}{2f_o} \qquad (4.10)$$

Where c is the velocity of sound which corresponds to the velocity of propagation of waves in water and n is the number of pulses of the burst. The width of the channels, the distance between each other and the total number of them determine the length along the axis where measurements are taking place, defining what is called measurement window. The echo originated by the passage of a unique burst along the measurement axis is not enough to recognize the shifted frequency. Because of this the echoed signal must be constructed using the passage of several bursts along the axis, and performing a successive and cumulative gathering of the data. This process establishes an additional limit to the measurable depth because the transducer must wait until the arriving of the last channel echo before sending another burst. The relation between both is stated in terms of the pulse repetition frequency, F_{prf}, by the following relation:

$$P_{max} \leq \frac{c}{2F_{prf}} \qquad (4.11)$$

where P_{max} is the maximum measurable depth. This relation states that the time used by a burst to reach the distance P_{max} and come back to the transducer, must be smaller, or equal in the limit, than the time between two successive burst.

4.2.4   *Transducers*

Ultrasonic transducers are devices capable of transforming a high-frequency electrical signal into high frequency mechanical vibrations. The latter generate sound waves which are transmitted through the medium surrounding the active face of the transducer (MET FLOW, 2002). Transducers work at different frequencies accordingly to their manufacture characteristics. MET FLOW has available transducer with working frequencies of 0.5, 1, 2, 4 and 8 Mhz. Generally lower frequencies are used in large-scale applications for their good propagation abilities. Higher frequencies are used for small-scale flow for which they offer good spatial resolution due to their short wavelength (MET FLOW, 2002).

The transducer selected for the experiments work at 4 Mhz, the maximum measurable depth has been set between 50 and 70 cm, using from 300 to 900 channels in different cases. The maximum flow velocity was between 350 and 400 mm/s. For the emitted burst the number of cycles was varied between 4 and 8 and the number of repetitions used to construct a profile between 32 and 64.

4.3   Bed Elevation Measurements

To measure the thickness of bed deposits, either those caused by coarse or fine sediment, a special electric device has been designed at the LNEC. It consists of a trolley mounted over rails which extended along the sides of the flume. This trolley holds all the electrical apparatus and an extensible sensor which is placed just over the bed. By means of electrical impulses this sensor is capable to detect the bed elevation variations along the flume and send the data to a computer. Figure 4.4 shows the trolley mounted over the rails with the extensible sensor.

Figure 4.4 Trolley for bed deposits thickness measurements

5. DATA TREATMENT ROUTINES

5.1 General

Although the UVP software can compute a lot of information related with the velocity profiles, it is necessary to compute other parameters specific to turbidity currents, such as the integral scales of mean velocity and turbidity current depth defined by Ellison & Turner (1959). Additionally, some velocity profiles present high levels of noise and therefore should be discarded when computing the mean profile and the mentioned parameters. In order to do this some routines have been programmed to read the files exported from UVP software, to analyze the quality of the velocity profiles and to compute the parameters of interest.

Another kind of information which requires post-process corresponds to the bed elevation profiles acquired by means of the special device developed at LNEC (here referred as bed profiler) and stored in plain text data files. The format used in these files is not suitable to directly compare the bed elevations with results coming from numerical models, since the number of points collected in each profile is not constant. Therefore to define a regular grid of information, an interpolation of each measured profile must be performed, and a reformatting of the file is performed to easily display the data.

The process of data treatment will be divided in two parts. The first part that consists in the rearranging of data exported directly from the proprietary software of UVP and the bed profiler device will be performed by routines written in Fortran90 language. The second part which includes the computing of interest parameters and results displaying will be executed by routines programmed in MATLAB.

All the routines are described in the following sections.

5.2 Profileread.exe: Reading and Writing Data Routine for Single Transducer Measurements

This routine called *profileread.exe* has been programmed in Fortran90 and is intended to read the data of a text file exported from UVP software containing the profiles information, and re-write it to a text file suitable to use in MATLAB. The process also has associated a reduction in the original file size due to the discarding of redundant information.

The routine requires the following characteristics of the exported file from UVP software:

- − File must have text format with a .txt extension, and must be saved under the name of "output.txt";
- − The option "Profile in column" and "Export header" must be checked when the file is exported from UVP Software;
- − It must include all the profiles measured by the UVP device;
- − Decimal separator character must be the point, and if commas are used as a thousands separator, they must be replaced with a null character. This is easily done with a program like Notepad.

Basically, *profileread.exe* reads the data from the output.txt file, stores it in a matrix, ask to user for new limits on the initial and final channels and profiles, and writes the new file called output_proc.txt using a simple matrix format. The detailed process is depicted in the Figure 5.1.
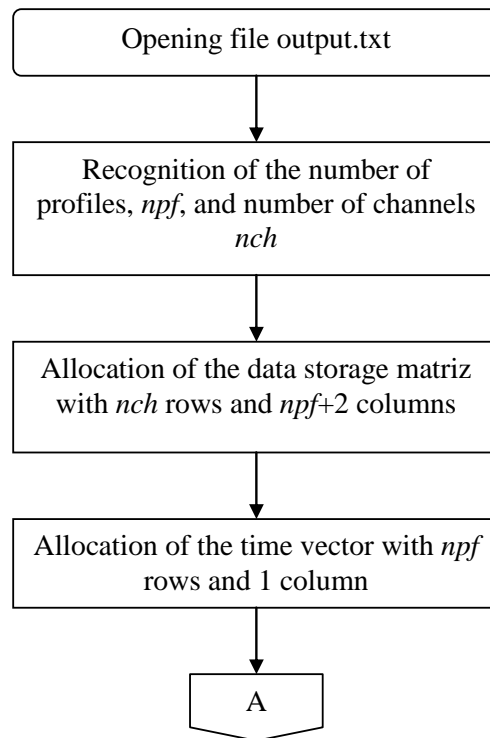

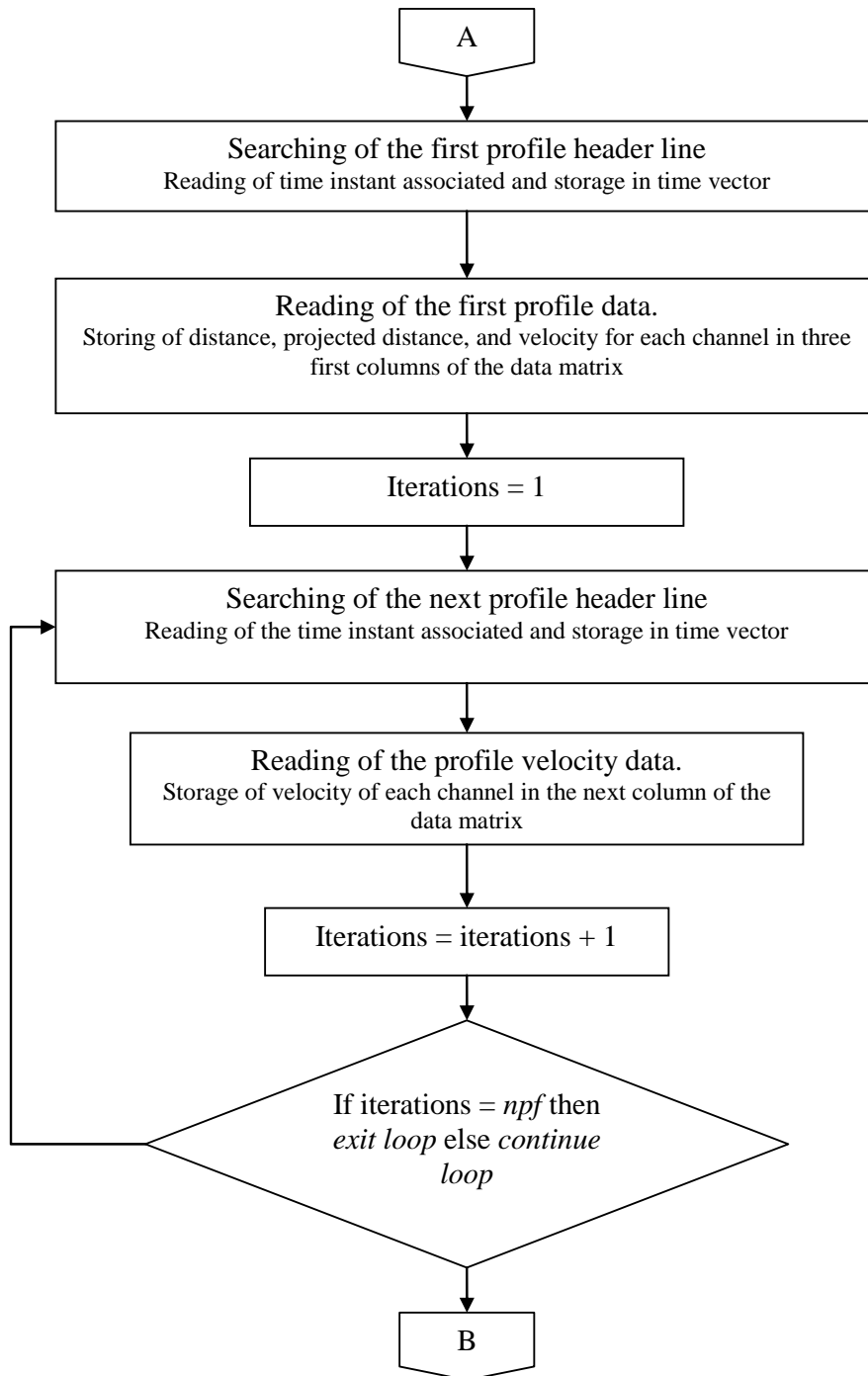**Figure 5.1 Flow diagram for the routine profileread.exe**

```
                    ┌─────────┐
                    │    A    │
                    └────┬────┘
                         │
                         ▼
   ┌─────────────────────────────────────────────────┐
   │      Searching of the first profile header line  │
   │  Reading of time instant associated and storage  │
   │                 in time vector                    │
   └─────────────────────┬───────────────────────────┘
                         │
                         ▼
   ┌─────────────────────────────────────────────────┐
   │           Reading of the first profile data.     │
   │  Storing of distance, projected distance, and    │
   │  velocity for each channel in three first columns │
   │              of the data matrix                   │
   └─────────────────────┬───────────────────────────┘
                         │
                         ▼
            ┌────────────────────────┐
            │     Iterations = 1     │
            └───────────┬────────────┘
                        │
                        ▼
   ┌─────────────────────────────────────────────────┐
   │     Searching of the next profile header line    │
   │  Reading of the time instant associated and      │
   │            storage in time vector                 │
   └─────────────────────┬───────────────────────────┘
                         │
                         ▼
   ┌─────────────────────────────────────────────────┐
   │        Reading of the profile velocity data.     │
   │  Storage of velocity of each channel in the next  │
   │           column of the data matrix               │
   └─────────────────────┬───────────────────────────┘
                         │
                         ▼
            ┌────────────────────────┐
            │  Iterations = iterations + 1 │
            └───────────┬────────────┘
                        │
                        ▼
                      ◇◇◇◇◇
            If iterations = npf then
            exit loop else continue loop
                      ◇◇◇◇◇
                         │
                         ▼
                    ┌─────────┐
                    │    B    │
                    └─────────┘
```
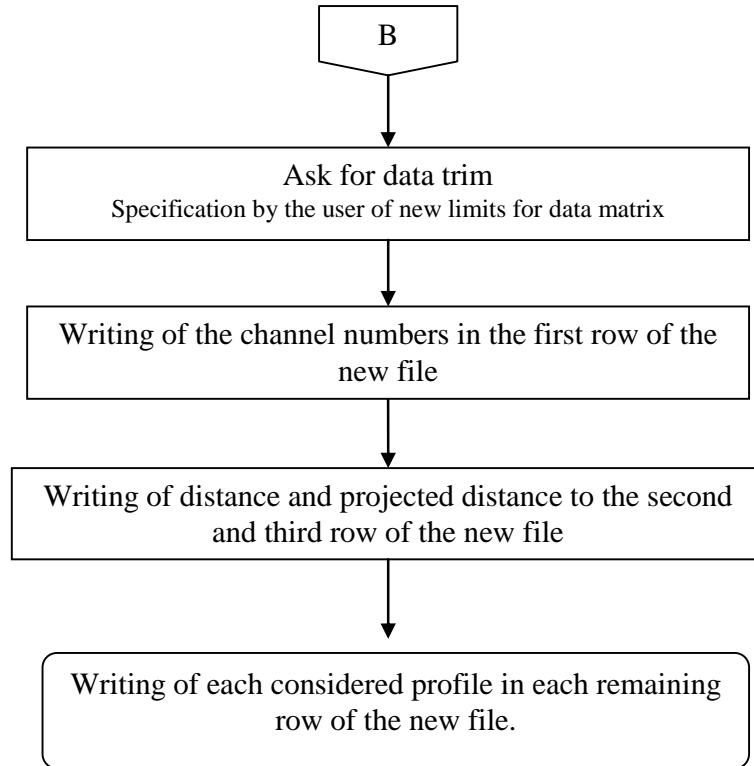
Figure 5.1 (continuation)

```
                    ┌─────────┐
                    │    B    │
                    └────┬────┘
                         │
                         ▼
┌─────────────────────────────────────────────────────┐
│                   Ask for data trim                   │
│  Specification by the user of new limits for data matrix │
└─────────────────────────┬─────────────────────────────┘
                          │
                          ▼
┌─────────────────────────────────────────────────────┐
│     Writing of the channel numbers in the first row of the │
│                       new file                        │
└─────────────────────────┬─────────────────────────────┘
                          │
                          ▼
┌─────────────────────────────────────────────────────┐
│    Writing of distance and projected distance to the second │
│              and third row of the new file            │
└─────────────────────────┬─────────────────────────────┘
                          │
                          ▼
╭─────────────────────────────────────────────────────╮
│    Writing of each considered profile in each remaining │
│                   row of the new file.                │
╰─────────────────────────────────────────────────────╯
```

Figure 5.1 (continuation)

In the output_proc.txt file the information is arranged mainly by rows. Each row will contain a number of elements equal to the number of selected channels plus 2. The first two elements of a row correspond to the profile number and the time of occurrence of that profile. The subsequent elements of the rows are the velocity values measured in that profile for each considered channel. The previous description is valid starting from the fourth row ahead. The first row starts with two zeros and after contain the description number of the considered channels; the second rows also starts with two zeros and after contain the values of the distance along the measurement axis of each associated channel; and the third row is similar but contains the values of distance projected in the direction normal to bed of each associated channel. The format of output_proc.txt for a simple time series of four profile measurements taken every 25 *ms* with a transducer oriented in the flow direction inclined 20° with respect to the normal, and containing only five channels, starting from channel 3 to channel 7 is exemplified in Figure 5.2.
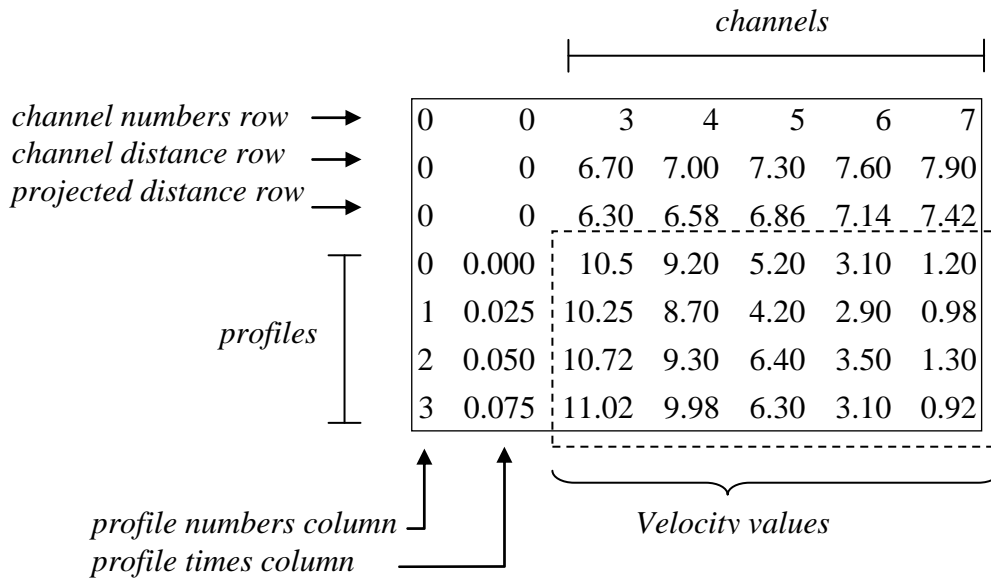
channels

channel numbers row →	0	0	3	4	5	6	7
channel distance row →	0	0	6.70	7.00	7.30	7.60	7.90
projected distance row →	0	0	6.30	6.58	6.86	7.14	7.42
profiles	0	0.000	10.5	9.20	5.20	3.10	1.20
	1	0.025	10.25	8.70	4.20	2.90	0.98
	2	0.050	10.72	9.30	6.40	3.50	1.30
	3	0.075	11.02	9.98	6.30	3.10	0.92

profile numbers column ⌐
profile times column ⌐   *Velocity values*

Figure 5.2 Example diagram of the ouput_proc.txt file format

5.3 Mutiread.exe: Reading and Writing Data Routine for Multiple Transducers Measurements

The data format of the exported files from UVP software is slightly different when multiple transducers are involved in the measurements. As the experiments will always be performed using more than one transducer, the treatment of the data in this case requires some minor modifications on the routine developed for 1 single transducer.

When multiple transducers are used, the acquisition of profiles is always sequential in time. This means that no matter how many profiles are considered to be measured by each transducer they will be always successive in time. Measurements are performed in cycles. In each cycle, each transducer measures a preset number of profiles. In addition a time delay can be specified for each transducer, meaning the time that the next transducer should wait between the end of the actual data acquisition and the beginning of its own process.

The number of cycles and profiles measured by each transducer are stored in the description lines of the exported data file. After these lines, the format of each measured profile is identical to the used in the case of single transducer measurements. In this way, the only improvement needed to treat the data coming from a multiple transducer process is to identify the source of each measured profile, accordingly to the number of cycles and number of profiles to measure for each transducer.

Again two routines will be used: *multiread.exe* and *multidata.m*. The first is programmed in Fortran90 and performs the reading of the data from the exported UVP file (output.txt) and writes it to another file in matricial format (output_proc.txt), this routine will be described in

the following paragraphs. The second routine is programmed in MATLAB and uses the written file to perform the analysis of the data and will be described in 5.4.

In comparison to the case of single transducer measurements, the routine of reading data from the UVP software exported file, remains nearly identical, with the only exception that the number of cycles and the specific number of profiles measured by each transducer must be identified. As each transducer can be placed using a different angle, this information has to be also stored.

The information of each transducer related to cycle execution will be stored in additional rows at the beginning of the output_proc.txt file. The number of transducers and an identification number will be stored now in the first row of the output file. In this way the original format of the output_proc.txt file changes with respect to Figure 5.2. Using the same example and now considering three transducers labeled with numbers 6, 7 and 8 the output file will look as presented in Figure 5.3. A detailed description is given in Figure 5.4.

The specific information in the file output_proc.txt is the following: in the first row are stored the number of transducers, the total number of cycles and after the identification number for each transducer. The second row contains initially two zeros, no information associated, after the numbers of the selected channel are listed. The third row has the same structure with two initial zeros but instead of the channel number the distances along the axis associated to each one are listed. Starting from the fourth row, there is one row for each transducer used in the measurements, listing in first place the number of profile measured in each cycle, in the second place the angle with respect to the normal of the bed is specified, and in the remaining spaces the projected distance of each channel is listed. After these rows begins the representation of the profiles using an identical format with respect to the case of single transducer.

The identification of the origin for individual profiles is performed in later stages by the MATLAB routine accordingly to the information related to each cycle.

3	2	6	7	8	0	0
0	0	3	4	5	6	7
0	0	6.70	7.00	7.30	7.60	7.90
50	20	6.30	6.58	6.86	7.14	7.42
50	20	6.30	6.58	6.86	7.14	7.42
50	20	6.30	6.58	6.86	7.14	7.42
0	0.000	10.5	9.20	5.20	3.10	1.20
1	0.025	10.25	8.70	4.20	2.90	0.98
2	0.050	10.72	9.30	6.40	3.50	1.30
⋮	⋮	⋮	⋮	⋮	⋮	⋮

Figure 5.3 Common format of the output_proc.txt file for multiple transducers
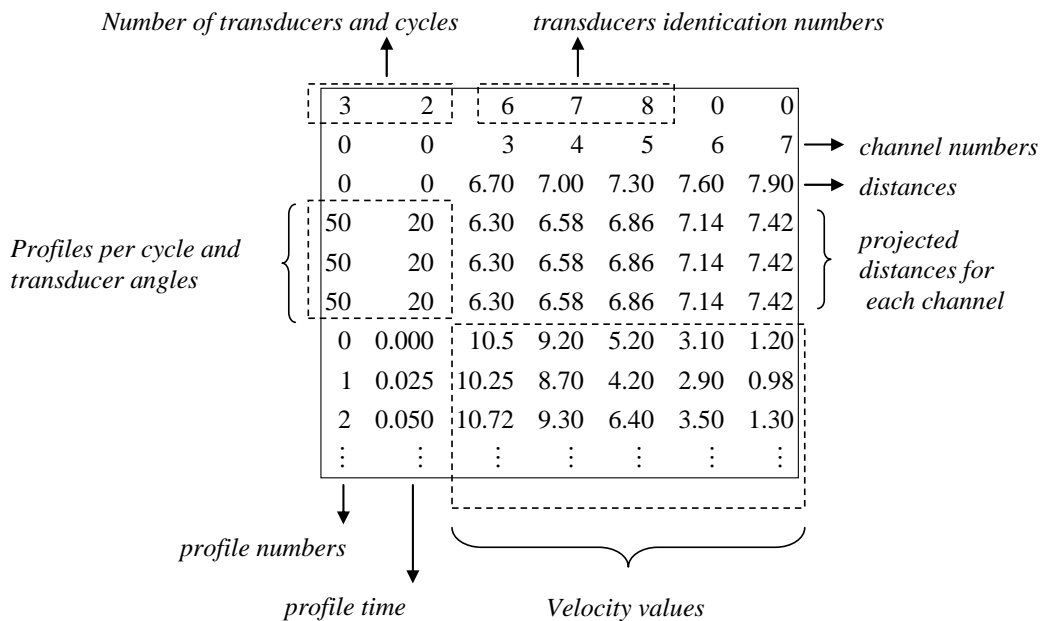
Figure 5.4 Detailed description of the data in output_proc.txt file

5.4   Multidata.m: MATLAB Routine for Data Processing of Multiple Transducers

The MATLAB routine *mutidata.m* is intended for viewing and analyzing the velocity profiles obtained from the UVP software. Initially the user is requested to specify which transducer will be analyzed. After selecting the target transducer the routine presents the following series of operations to be performed through a pop up list menu:

− *Redefine data limits*: Its principal objective is to allow the user to define the channels which will delimit the mean velocity profile from which the integral scales will be computed and to define the range of profiles considered in the computation of the mean profile.

− *Compute integral scales*: Computes the mean velocity profile and the integrals scales of velocity and depth for the turbidity current.

− *See data evolution in time*: Plots the considered velocity profiles sequentially in time, in order to have an idea of the flow behavior. It also saves an animation of the evolution in *avi* format.

- *Filter profiles*: Performs the elimination of aliased and noise corrupted profiles accordingly to predefined criteria.

- *Save data*: Stores in a data matrix internal to the routine, only those profiles that have been selected in the filtering process and writes three files: *T#_mean.dat* where the mean velocity profile and its standard deviation is written, *T#_prof.dat* where all the velocity profiles used for the calculation of the mean are stored and *T#_scal.dat* where the resulting integral scales are stored. In all the files the symbol # represents the number of the transducer under analysis given in the UVP software.

- *Channel series analysis*: It computes the mean velocity in function of the time for five user selected channels. It is intended in order to give a better idea of when the turbidity current becomes steady, and to select properly the minimum time instant for which a profile can be considered in the re-computation of the mean velocity profile.

- *Recompute mean and integral scales*: Performs the calculation of the mean velocity profile and the associated integrals scales using the profiles present in the data matrix whose time of acquisition is grater than the specified by the user. After the calculations it writes two new data files. *T#_mean2.dat* and *T#_scal2*.dat where the re-computed values are stored.

- *Take manual control*: Allow the user to review and export figures of interest. The user can come back to the routine typing *return* in the MATLAB command line.

The order of the operations has been established in this way trying to follow the natural sequence of the velocity data treatment process. The user can select a single process or a set of them through the list. If the option "*Take manual control*" has not been selected by the user, the routine shows again the same pop up list menu after all the selected tasks have been performed. If "*Take manual control*" has been selected the user is allowed to inspect figures more accurately, to export them and after continue analyzing the data. The flow diagram of the routine is depicted in Figure 5.5.

```
┌─────────────────────────────────────────┐
│       Opening file output_proc.txt       │
└─────────────────────────────────────────┘
                    │
                    ▼
┌─────────────────────────────────────────┐
│          Obtaining relevant data.        │
│ Number of profiles, number of transducers, starting and ending │
│ channels and profiles, number of cycles and transducer angles. │
└─────────────────────────────────────────┘
                    │
                    ▼
           ╱─────────────────────╲
          ╱   Asking for the number of ╲
          ╲   the transducer to analyze ╱
           ╲─────────────────────╱
                    │
                    ▼
┌─────────────────────────────────────────┐
│   Rearrange data into the single transducer │
│           format (Figure 4.2)            │
└─────────────────────────────────────────┘
                    │
                    ▼
┌─────────────────────────────────────────┐
│   Pop up list menu for specify operations │
│              to perform                   │
└─────────────────────────────────────────┘
                    │
                    ▼
           ◇─────────────────────◇
          ◇   If no operation selected ◇
          ◇   exit else continue        ◇
           ◇─────────────────────◇
                    │
                    ▼
┌─────────────────────────────────────────┐
│        Perform selected operations       │
└─────────────────────────────────────────┘
                    │
                    ▼
        ◇─────────────────────────────◇
       ◇   If "Take manual control" was ◇
       ◇  selected wait the user type "return" ◇
        ◇─────────────────────────────◇

   ▽C      ▽B           ▽A                    ▽D
```

Figure 5.5 Flow diagram for the multidata.m routine
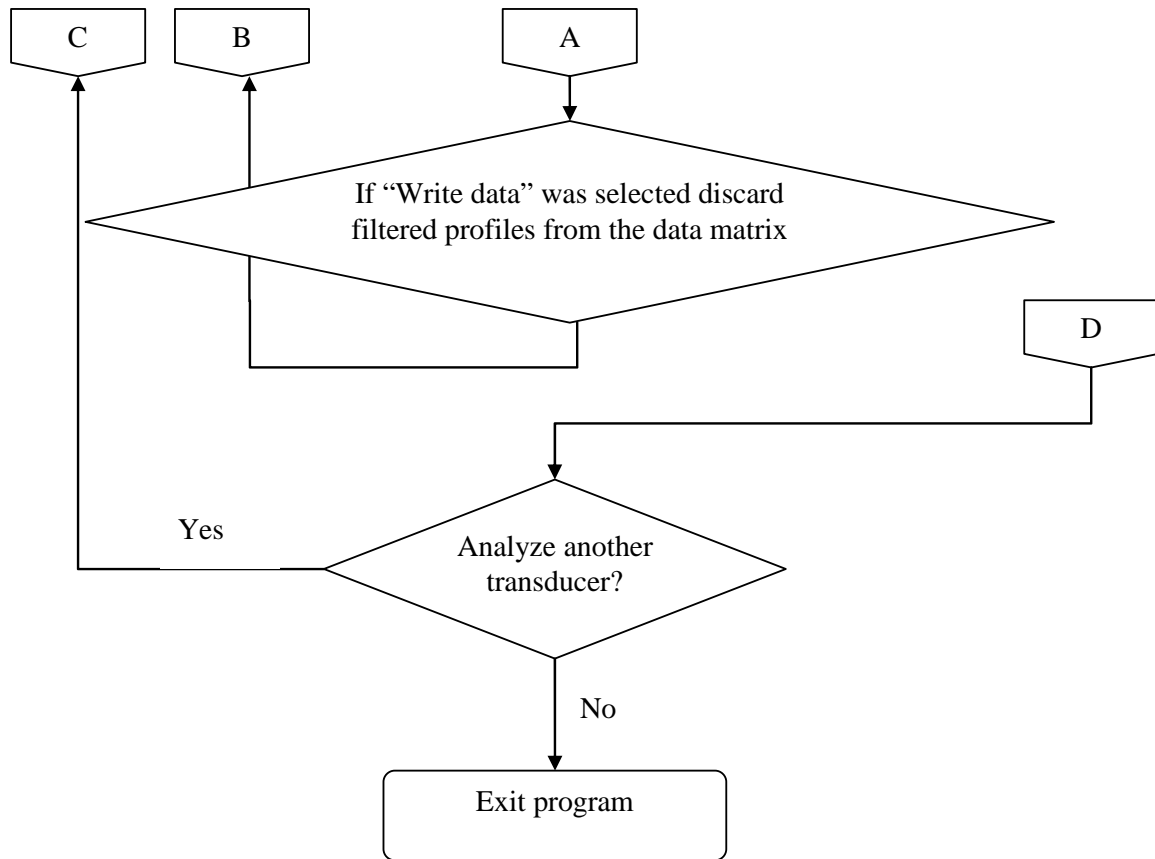
Figure 5.5 (Continuation)

Mathematical formulations of the operations that compute the mean velocity and integral scales from the data and perform the filtering process are described below.

5.4.1 *Computing Integral Scales*

The mean velocity profile is computed from the following equation:

$$\bar{u}_i = \frac{1}{npf} \sum_{j=1}^{npf} u_{i,j} \tag{5.1}$$

Where the index *i* specifies the associated channel and the index *j* the considered profile. $u_{i,j}$ is the velocity registered at the channel *i* for the profile *j* and *npf* is the total number of profiles considered.

After the mean velocity profile has been computed, the following momentums of the velocity are calculated using a trapezoidal approximation:

$$UH = \int_o^\infty \bar{u}(z)dz \approx \sum_{i=1}^{nch-1} \frac{\bar{u}_i + \bar{u}_{i+1}}{2} \left(z_{i+1} - z_i \right) \tag{5.2}$$

$$U^2H = \int_o^\infty \overline{u}^2(z)dz \approx \sum_{i=1}^{nch-1} \frac{\overline{u}_i^2 + \overline{u}_{i+1}^2}{2}\left(z_{i+1} - z_i\right) \tag{5.3}$$

Where i is the channel index, nch is the number of channels, z_i is the elevation with respect to the bed of the channel i, and $\overline{u}_i$ the mean velocity computed for that channel.

Using (5.2) and (5.3) the integrals scales for depth averaged velocity and turbidity current depth are obtained as:

$$U = \frac{U^2H}{UH} \tag{5.4}$$

$$H = \frac{(UH)^2}{U^2H} \tag{5.5}$$

5.4.2 *Filtering Profiles*

There are several intrinsic noise sources present in the acquisition of data that are identified in Shahram (2005):

- Discretization error due to 8 bits of resolution of the A/D converter in the Met-flow instrument.
- Noise due to incorrect timing issues in hardware/software.
- Ultrasound noise due to reverberation in walls, absence of reflectors in the fluid, multiple reflections near the walls, ultrasound absorption, diffraction scattering from air bubbles, several scatterers occupying the same measurement volume, too many or too few scattering particles and other anomalies.
- Less accurate profiles when using the time domain Doppler shift algorithm a low F_{prf} value due to less profile averaging.
- Severely distorted velocity profiles if the echo amplification values gainMax and gainMin are chosen incorrectly.
- Random measurement noise from sources beyond the control of personal in charge (e.g. Gaussian white noise, electrical disturbance, thermal noise etc.).

This states the need for filtering profiles to eliminate corrupt data which could alter the value of the turbidity current integral scales.

The first problem to be treated is the occurrence of aliasing, which basically consists in the erroneous estimation of the signal phase and the occurrence of a velocity value outside the velocity range stated by the measurement parameters configuration of the UVP device. Since

the mean values of velocity are well represented by a long series, even in the eventual presence of aliasing, the elimination of profiles whit this phenomena is made only to guaranteed data consistency.

Commonly aliasing is represented as high spikes of velocity going to the limit of the measurable range. An example is presented in Figure 5.6.
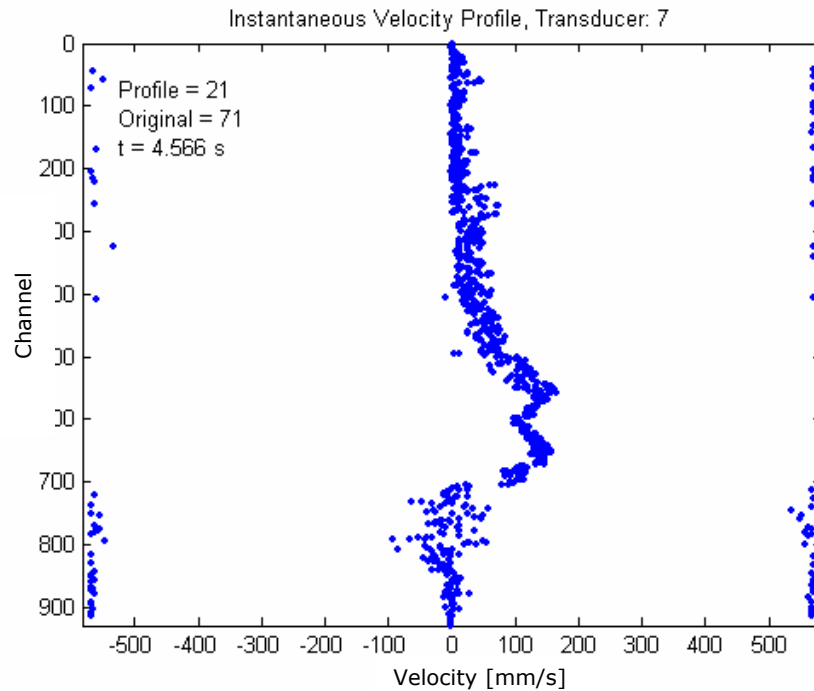
Figure 5.6 Aliasing of the velocity values in a profile of a measurement series

In the routine the elimination of aliasing is available to the user by selecting the *Filtering profiles* options. The maximum velocity considering all the profiles is stored by the routine, and then a percentage value is requested to the user. Any profile containing a velocity value greater than this percentage of the maximum velocity is considered to present aliasing and is eliminated from the mean velocity profile calculation. In this way if no aliasing was detected in the inspection of the data time evolution, it is enough to provide the routine with a value greater than 100 to avoid the filtering of correct data.

An additional tool is available to filter data corrupted by the noise sources described above. This is based on the original procedure proposed by Shahram (2005), which was oriented to the filtering of profiles in a steady state laminar flow measurement. In that case, it was valid to assume that all the profiles could be well approximated by different polynomials of the same grade. The original procedure consisted in the following steps:

- Fit a polynomial of a grade N to each velocity profile using a least mean square criterion. In this way a group of N+1 coefficients a_k with k going from 0 to N were calculated for each profile.
- The set of coefficients $\{a_k\}$, k: 0…N for all profiles was saved
- The mean value μ_k and the standard deviation σ_k for each set $\{a_k\}$ k:0…N, were computed.
- For each profile the sum $S =\#\{a_k; \; a_k \geq \mu_k + \sigma_k \;\; OR \;\; a_k \leq \mu_k - \sigma_k\}$ where the # sign means number of occurrences.
- Discard any profile for which the value of S was greater than a user defined number between 0 and N+1.

As the turbidity current flow is a turbulent process, it is difficult to predict a shape for the trend of the velocity profiles. Keeping in mind that acoustic noise will originate a greater variance in the velocity measurements; the methodology of Shahram (2005) has been slightly adapted in order to obtain a final mean velocity profile with a better resolution of the velocity variance. The proposed procedure is the following:

- Compute the mean velocity profile using all the profiles available.
- Starting on grade three and with a maximum grade defined by the user, several polynomials are fitted to the mean profile using a least square criterion. The grade of the polynomial with the minimum error is selected.
- Fit a polynomial of the selected grade to each considered profile.
- Perform the same operations considered in the original procedure of Shahram (2005) for the polynomial coefficients and the discarding of profiles.

With this procedure profiles are discarded using the same criterion originally proposed by Shahram (2005) but where the grade of the fitted polynomials has been determined using the original mean velocity profile. The maximum value for the S parameter is also defined by the user at the beginning of the process.

5.4.3   *Channel Velocity Series Analysis*

As described before, this option of the routine is intended to have a better idea of when the mean velocity value of a channel becomes nearly steady with the addition of new profiles, and to use this time as an estimation of the end of strong unsteady processes in the turbidity current.

The mean velocity of a channel j is computed as following:

$$\bar{u}_j(t) = \frac{1}{t-t_o} \int_{t_o}^{t} u_j(t)dt \approx \frac{1}{t-t_o} \sum_{t=t_o}^{t} \frac{u_{j,i} + u_{j,i+1}}{2} \left(t_{i+1} - t_i\right) \qquad (5.6)$$

Where the index *i* refers to the measured profile, and t_o is the time of the first profile considered.

5.4.4 *Procedure for Data Processing*

This section describes the proposed procedure for data treatment using the *multiread.m* routine. The processing of the data obtained through the different experiments presented in Chapter 6 resulted in a series of steps leading to a quite standard procedure which is described below. The symbol # has been used to represent the number of the transducer under analysis.

1. After typing in the MATLAB command line "mutidata" the routine shows a pop up dialog asking for the number of the transducer to be analyzed. The available transducers are listed in the input field title.

2. After selecting a transducer, the routine asks for the orientation of it with respect to the flow direction. If the transducer is facing the flow, then the number 1 must be entered, otherwise the number -1 must be entered in order all velocities be plotted as positive in figures and animations.

3. The main menu of the routine is shown. All the options are available. Select *See data evolution in time*. The routine will create an animation called *T#_AVI_.avi*. Go to the work folder and rename it manually to *T#_AVI1_original.avi*. In this animation, for each profile is shown the following information: the relative number of the profile between those registered by the transducer, the original number of the profile in the whole sequence of the data acquisition and the time at which the profile was registered.

4. Inspecting the video animation the user can define the first and last profile with valid measurement. The relative and original number and the acquisition time of the these profiles is registered.

5. Select *Redefine data limits* and enter the relative number of the profiles determined in the previous step.

6. Select *Compute integrals scales*. The routine will generate two images:
   T#_IMG1_mean__v-chx.bmp
   T#_IMG2_mean__v-x.bmp

Rename manually these images to
> *T#_IMG1_mean_original_v-chx.bmp*
> *T#_IMG2_mean_original_v-x.bmp*

7. Select *Take manual control*, using the zoom tool in the previous images, the bottom of the flume can be located in the mean velocity profile. Normally the bottom position can be assessed projecting visually the slope of the velocity profile near the bottom. To measure the distance between the transducer face and the bottom of the flume during the experiment can also be useful as help. Save each image of the bottom region as:
> *T#_IMG3_mean_original_bottom_v-chx.bmp*
> *T#_IMG4_mean_original_bottom_v-x.bmp*

8. Select *Redefine data limits*. Enter the number of the limiting profiles and of the bottom channel.

9. Select *See data evolution in time*. The routine will create the *T#_AVI_.avi* animation. Rename this file as *T#_AVI2_window.avi*

10. Select *Compute integrals scales*. The routine will create the images *T#_IMG1_mean__v-chx.bmp* and *T#_IMG2_mean__v-x.bmp*. Rename these images to:
> *T#_IMG5_mean_window_v-chx.bmp*
> *T#_IMG6_mean_window_v-x.bmp*

11. Select *Filter profiles*. The routine shows a pop up dialog asking for the filtering parameters. At the end of the process the routine computes automatically the mean profile and the integrals scales using only those profiles kept after the filtering profiles, it shows and saves these results in the figures:
> *T#_IMG7_mean_window_filtered_v-chx.bmp*
> T*#_IMG8_mean_window_filtered_v-x.bmp*

12. Select *Save data* and after select *See data evolution in time*. Rename the created *T#_AVI_.avi* to *T#_AVI3_window_filtered.avi*

13. Select *Channel series analysis*. A pop up menu is shown requesting the user to define five channels to analyze. A figure showing the mean velocity of each channel in function of time is saved under the name of *T#_IMG9_channel_series.bmp*. Using this figure the user can select a time to define the instant where the mean velocity is approximately constant.

14. Select *Recompute mean and integral scales*. Using the time defined in step 13, the routine will compute the mean velocity profile and the associated integral scales using only those profiles that have been registered after this instant of time. The result are shown and saved to the following images:

   T#_IMG9a_mean_recomputed_v-chx.bmp

   T#_IMG9a_mean_ recomputed_v-x.bmp

15. An alternative procedure is to compute the mean velocity profile and integral scales using the region of the profile where only positive mean velocities are present. In order to do this, select *Take manual control*, search in the *T#_IMG9a_mean_recomputed_v-chx.bmp* figure for the channel where velocity equals zero, near the region belonging to the turbidity current interface. Type *return* in the command line, and go to *Redefine data limits*; enter this channel number for the upper limit, and the one of the bottom for the lower limit. The limits for the profiles should already be set by the filtering process. Then select *Recompute mean an integral scales*. Using the same time entered for step 14.

5.5   Bedread.exe and Bedread.m: Bed Elevation Data Processing Routines

Bed elevations profiles are registered and stored in plain text data files with *dat* extension. The original file includes, for every profile, a heading row indicating the date when profile was started to be measured, in the following format:

* yyyy/mm/dd hh:xx:ss *

Where *yyyy* represents the year, *mm* the month, *dd* the day, *hh* the hour in 24 hrs format, *xx* the minutes and *ss* the seconds. After this heading row, there is a variable number of them containing each one a (*x,z*) pair, where *x* is the longitudinal coordinate in meters and *z* is the vertical coordinate in millimeters. An example of the file is presented in Figure 5.7.
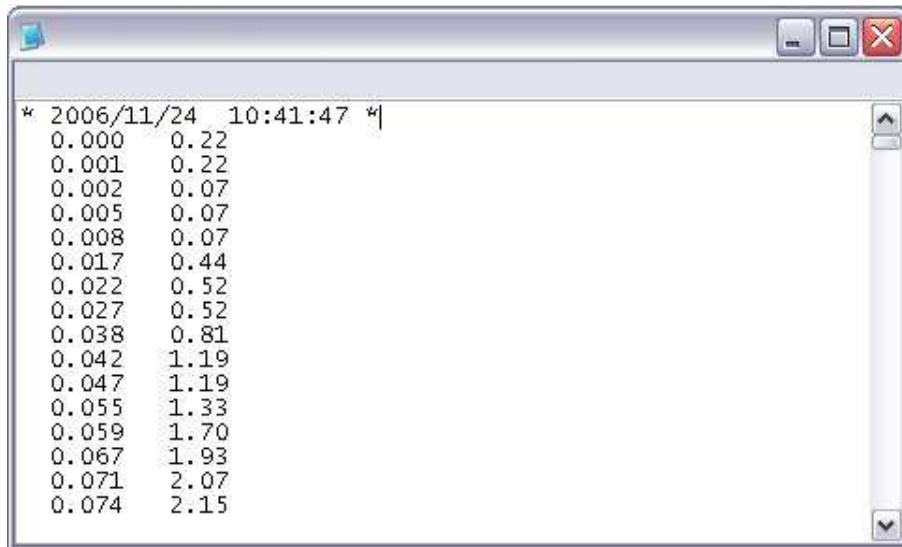
Figure 5.7 Example of the original file containing bed elevation data

The number of (*x,z*) pairs stored for each profiles depends on the velocity at which the measuring device is displaced in the longitudinal direction. By this reason there is a variable number of registered point from one profile to another.

As a way to compare with a uniform grid, which is the common case used in numerical simulations, every read profile is interpolated to obtain the elevation at a regular interval defined by the user.

The data treatment is performed by a Fortran90 routine called *bedread.exe*. This routine reads all the profiles and generates a new file with a matricial format suitable to plot on MATLAB or Excel. The final file is called *bed_proc.dat* and its format is described in Figure 5.8.

0	t_1	t_2	$\ldots$	$\ldots$	t_i	$\ldots$	$\ldots$	t_{np}
x_1	$z_{1,1}$	$z_{2,1}$	$\ldots$	$\ldots$	$z_{i,1}$	$\ldots$	$\ldots$	$z_{np,1}$
x_2	$z_{1,2}$	$z_{2,2}$	$\ldots$	$\ldots$	$z_{i,2}$	$\ldots$	$\ldots$	$z_{np,2}$
x_3	$z_{1,3}$	$z_{2,3}$	$\ldots$	$\ldots$	$z_{i,3}$	$\ldots$	$\ldots$	$z_{np,3}$
x_4	$z_{1,4}$	$z_{2,4}$	$\ldots$	$\ldots$	$z_{i,4}$	$\ldots$	$\ldots$	$z_{np,4}$
$\vdots$	$\vdots$	$\vdots$			$\vdots$			$\vdots$
x_j	$z_{1,j}$	$z_{2,j}$	$\ldots$	$\ldots$	$z_{i,j}$	$\ldots$	$\ldots$	$z_{np,j}$
$\vdots$	$\vdots$	$\vdots$			$\vdots$			$\vdots$
$\vdots$	$\vdots$	$\vdots$			$\vdots$			$\vdots$
x_{ng}	$z_{1,ng}$	$z_{2,ng}$	$\ldots$	$\ldots$	$z_{j,ng}$	$\ldots$	$\ldots$	$z_{np,ng}$

Figure 5.8 General format of the bed_proc.dat file

As depicted in Figure 5.8, bed elevation profiles are arranged in columns. The value of t_1 is always zero and all remaining times are expressed in seconds with respect to the time at which the initial bed profile was executed. The value of x1 is also always zero, and the difference between two successive coordinates is always constant and equal to the user selected discretization.

A second routine that reads this file and plot the profiles has been created in MATLAB. The routine is called *bedread.m*. Figure 5.9 and Figure 5.10 present examples of the plotted profiles. A video animation called *bed.avi* is also created, presenting the bed elevation profiles sequentially.
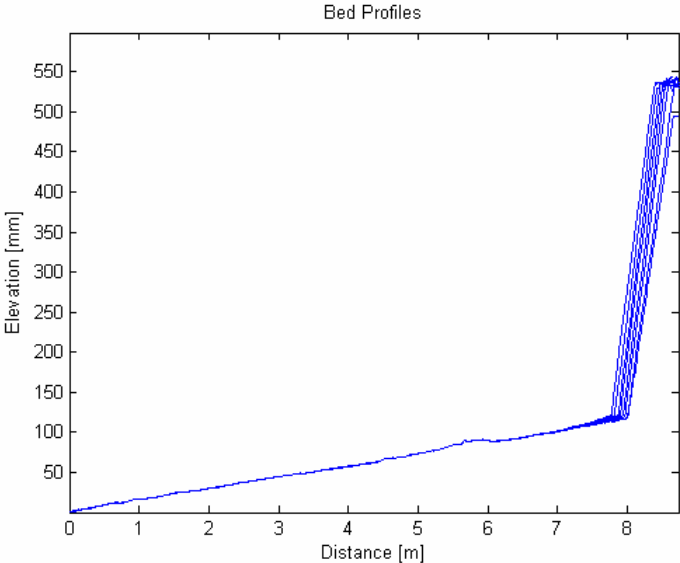
Figure 5.9 Plot of successive bed elevation profiles in a sand delta progradation experiment
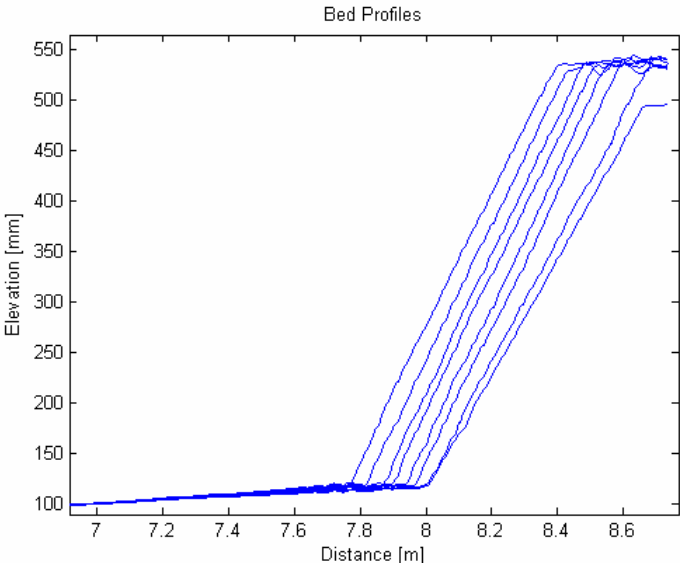
Figure 5.10 Zoom to the delta zone of Figure 5.9

6. EXPERIMENTAL DATA

This chapter presents the velocity measurements taken during the experiment carried out on the 19th of March of 2007 and the corresponding post-processing using the routines depicted in Chapter 5. For one of the transducers all the steps and figures are presented as an example of the procedure of velocity data treatment described in section 5.4.4. For the sake of brevity, the data pertaining to remaining transducers of this experiment will be resumed to the final mean velocity profiles and the parameters used in the process will be presented by means of tables. The transducer chosen to exemplify the procedure is transducer number 4. The experiment has been selected because is one of the latest performed during this work and its data has been processed including all the considerations arisen during the development of the routines.

The processed data for the all the other experiments is presented in Chapter 9 "Appendix: Experimental Data Treatment". The experiments have been titled under the performing data.

6.1   Experiment 2007.03.19

The discharge of the turbidity current mixture was set to 18.5% of the maximum measurable discharge by the flowmeter, corresponding to 0.71 l/s. The design value for the volumetric fine sediment concentration was 0.7%. The number of transducers used was 7, each one with a measuring window of 549.82 mm equivalent to the maximum measurable depth. In this window a total of 360 channels were used. The number of profiles measured by each transducer in one cycle was 3 and the duration of each cycle considering all the transducer was estimated in 3 s. The total number of profiles measured during the experiment was 4158.

The information given in the previous paragraph will be resumed by means of Table 6.1. The position along the channel, with respect to the zero position marked on one of the rails that supports the bed deposit measurement trolley, is described in Table 6.2 as well as the distance between the face of each transducer and the channel bottom.

Table 6.1 Experiment parameters

Discharge [%]	18.5
Discharge [l/s]	0.71
Volumetric fine sediment concentration [%]	0.7
Number of transducers	7
Maximum Depth	549.82 mm
Total number of channels	360
Profiles measured in each transducer per cycle	3
Estimated total cycle time [s]	3
Total number of measured profiles	4158

Table 6.2 Description of the position and distance to the bottom for each transducer

Transducer nº	1	2	3	4	5	6	7
Longitudinal location [m]	8.4	8.0	7.0	6.0	5.0	3.0	1.0
Transducer angle [º]	10	10	20	20	20	20	20
Bottom distance [mm]	152	302	389	399	408	430	460
Projected bottom distance [mm]	150	297	366	375	383	404	432

6.1.1   *Velocity Measurements Transducer 4*

The first step taken to analyze the data was to elaborate the video animation of all profiles registered by the transducer. Inspecting this animation it was possible to establish that the first profile with valid data corresponded to profile number 66 (number 471 in the whole velocity data set) registered at 67.541 s, and the last registered profile, before the arrival of the returning internal hydraulic jump, was profile number 542 (number 3791 in the whole velocity data set) registered at 543.48 s.

With these two profile numbers, the data limits are redefined and the integral scales together with the mean velocity profile are computed. The images showed in Figure 6.1 are obtained:
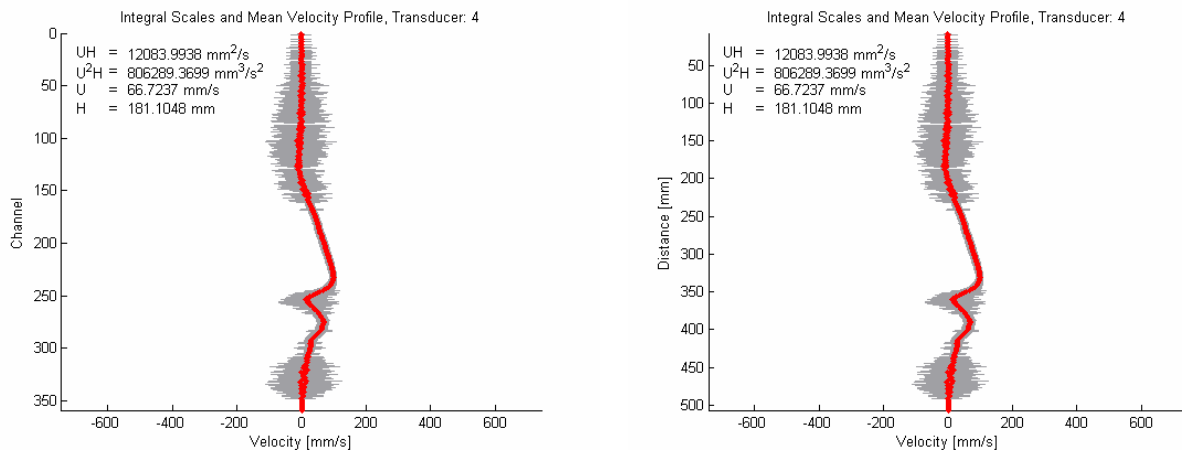
Figure 6.1 Original mean velocity profiles for transducer 4

In these images, the near bottom zone is inspected using the MATLAB zoom tool and two new figures are stored accordingly to the names described in section 5.4.4. Figure 6.2 shows a zoom to the bottom zone, with these images the number of the channel representing the bottom is estimated, the selected channel number is 254 located at a vertical projected distance of 360.814 mm from the face of the transducer.
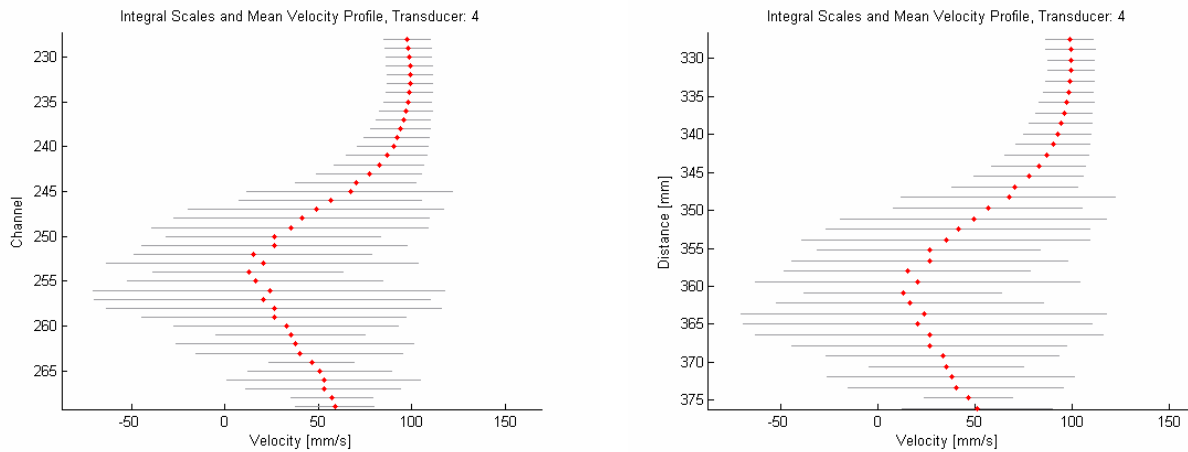
Figure 6.2 Zoom to bottom regien in the mean velocity profile for transducer 4

The data limits are redefined once more time, and a new video animation is created. The resulting mean velocity profiles and integral scales of consider such limits is presented in Figure 6.3.
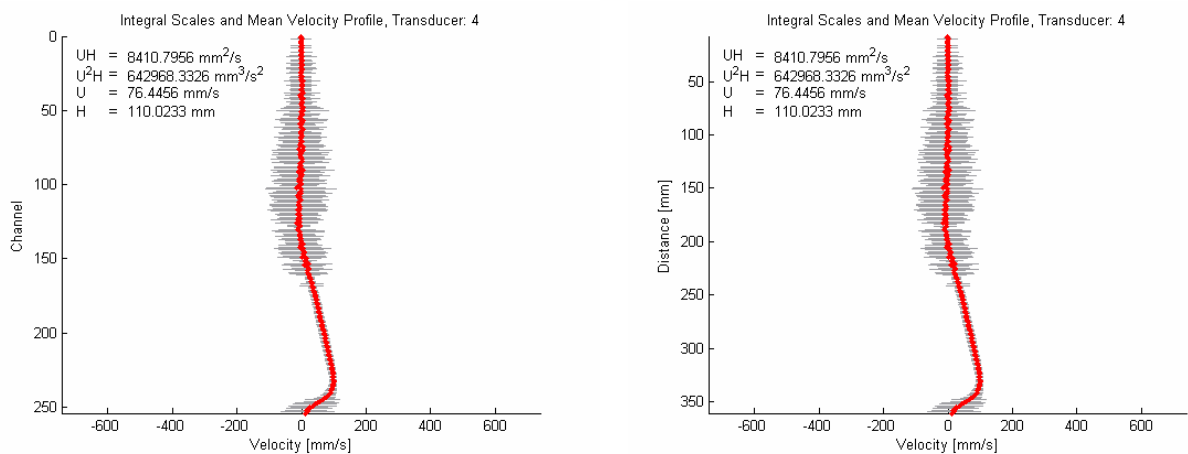
Figure 6.3 Mean velocity profile and integral scales with the new data limits defined

Inspecting the animation generated in the previous step some profiles affected by aliasing are found. The filtering profiles module is selected. To eliminate aliased profiles a value of 90% is given for the maximum velocity. In order to eliminate noise corrupted profiles, the best adjustment to mean velocity profile will be determined using a maximum polynomial grade of 7, and a threshold number of 4 coefficients outside the range of the group will be allowed as described in section 5.4.2. Figure 6.4 shows the obtained mean velocity and integral scales.
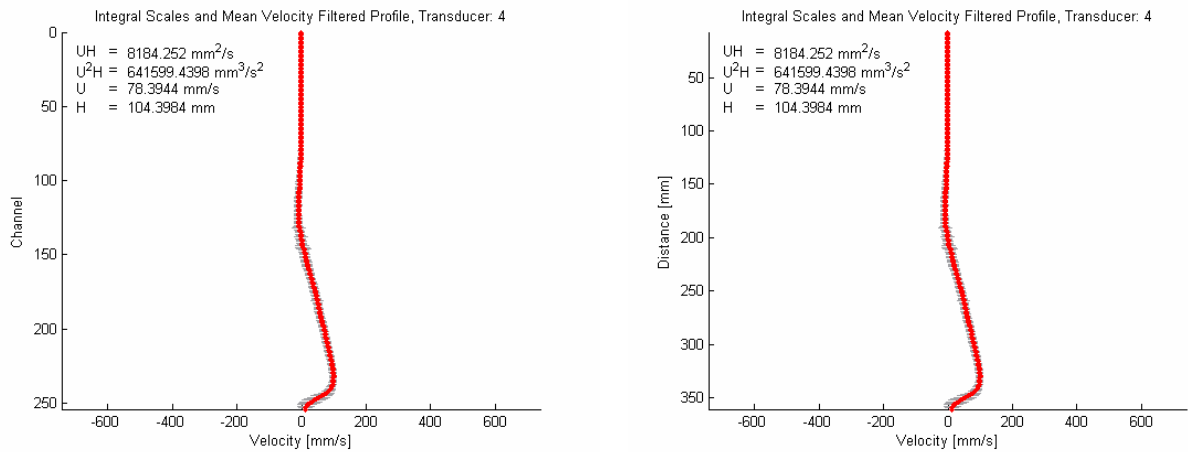
Figure 6.4 Mean velocity profile and integral scales obtained after the filtering process

In the filtering process a total number of 373 profiles were included. The details concerning which profiles were included can be found in the text files stored after selecting the *save data* option.

The channel analysis tool is now used to evaluate the steadiness of the profiles included in the calculus. Channels 150, 170, 190, 230 and 245 were analyzed. From channels 190 and 245 it can be seen that starting from t = 250 s the mean velocity of each channel does not present great variations (See Figure 6.5).
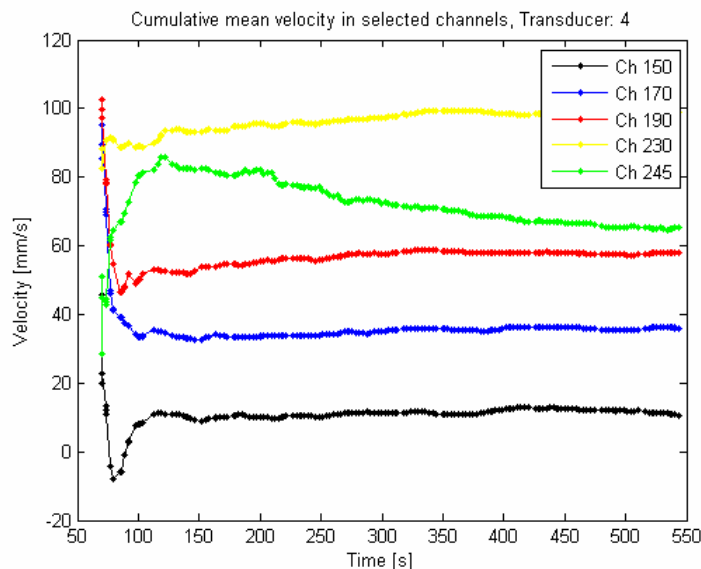
Figure 6.5 Channel mean velocity analysis for transducer 4

Thus t = 250 s is used to recomputed the mean velocity profile. The result of excluding the profiles registered before this time is shown in Figure 6.6.
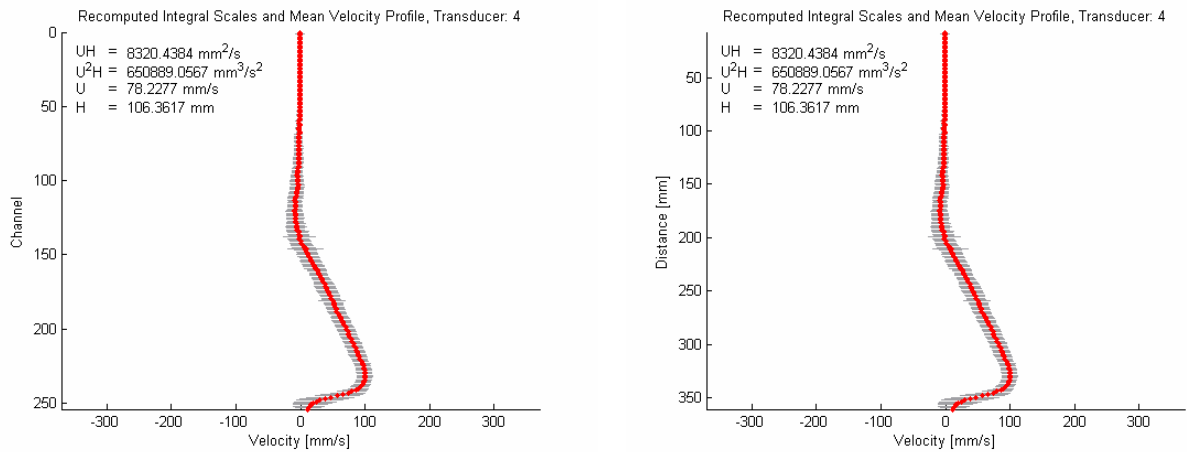
Figure 6.6 Mean velocity profile and integral scales obtained after the excluding the profiles registered before t=250 s

Because a reversal flow zone is detected at the interface zone of the turbidity current, it is worth to analyze how the integral scales vary if only the positive velocity region is considered. The first channel of the positive velocity region is determined to be channel number 141. Redefining the data limits for channel and after that computing again the mean velocity profile and integral scales the results of are obtained.
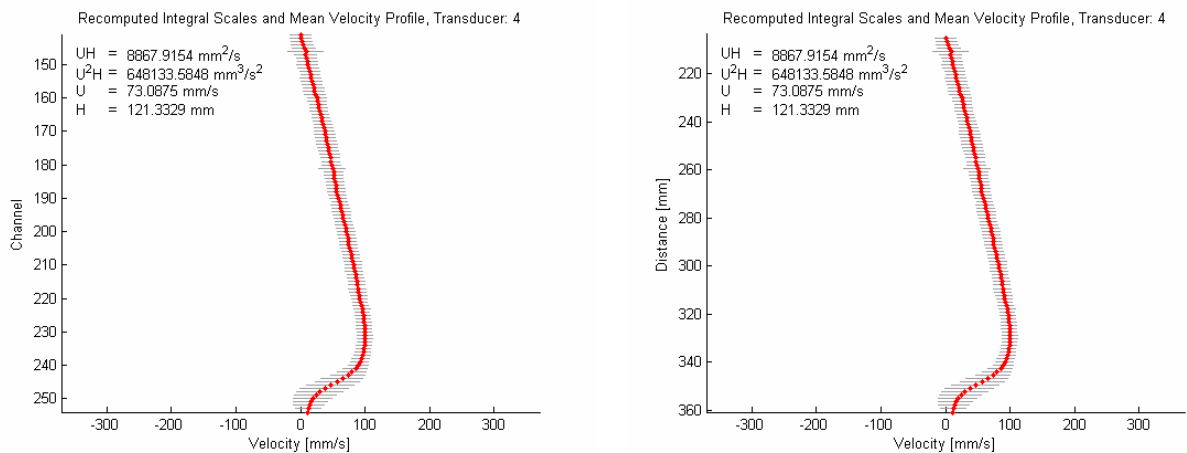
Figure 6.7 Mean velocity profile and integral scales obtained after the considering only the positive velocity region and excluding the profiles registered before t=250 s.

For the sake of brevity, all the information described in the previous paragraphs of this section will be resumed by means of tables with the format shown in. The only figures that will be included in this report are those reporting the final recomputed mean velocity profiles with and without the influence of the reversal flow zone, and only those where the velocity has been plotted against channel distance. All the remaining figures can be found in the companion digital appendix.

Table 6.3 Resume of the values used in the data processing for transducer 4

Channel number of the bottom	254
Registered distance for bottom channel	360.814 mm
First profile considered	66 originally 471 at 67.541 s
Last profile considered	542 originally 3791 at 543.48 s
Percentage of the maximum velocity for aliasing filtering	90%
Maximum grade for mean profile adjustment	7
Threshold number for polynomial coefficients (*S*)	4
Total number of profiles considered	373
Initial time selected to recompute the mean profile [s]	250
Upper channel defining positive mean velocity region	141

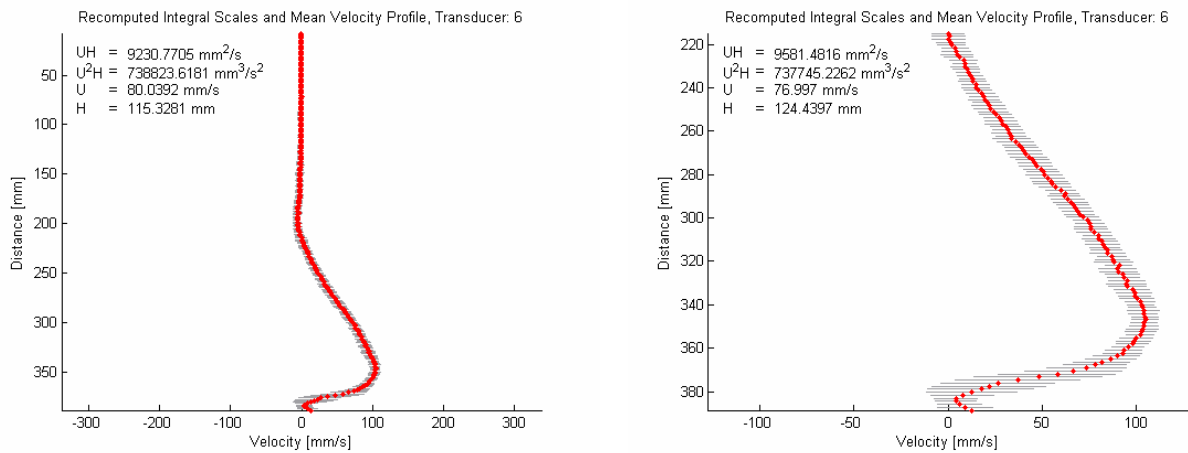## 6.1.2   *Velocity Measurements Transducer 1*
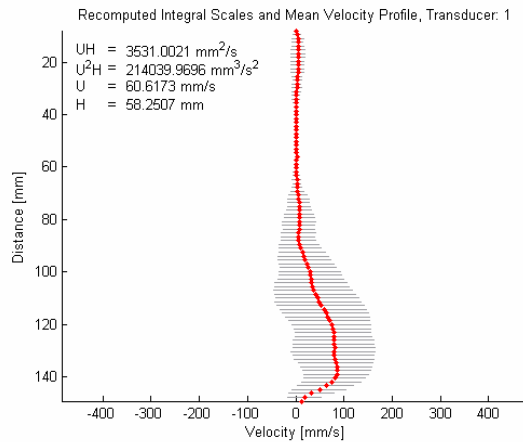
Figure 6.8 Mean velocity profile for transducer 1 after noise and aliasing filtering

Table 6.4 Resume of the values used in the data processing for transducer 1

Channel number of the bottom	97
Registered distance for bottom channel	149.307 mm
First profile considered	24 originally 168 at 24.091 s
Last profile considered	593 originally 4139 at 593.383 s
Percentage of the maximum velocity for aliasing filtering	90%
Maximum grade for mean profile adjustment	7
Threshold number for polynomial coefficients (*S*)	4
Total number of profiles considered	200
Initial time selected to recompute the mean profile [s]	394
Upper channel defining positive mean velocity region	0

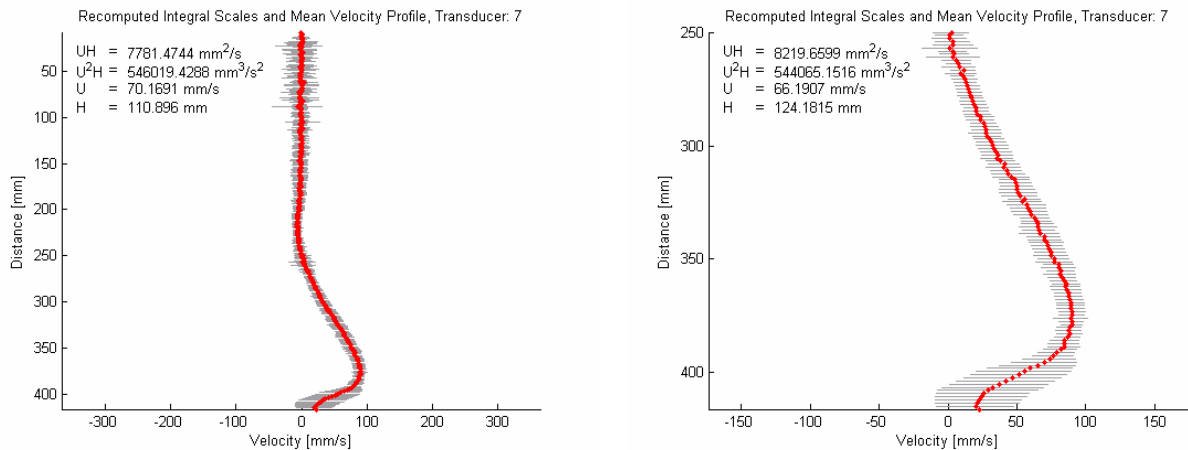### 6.1.3   *Velocity Measurements Transducer 2*
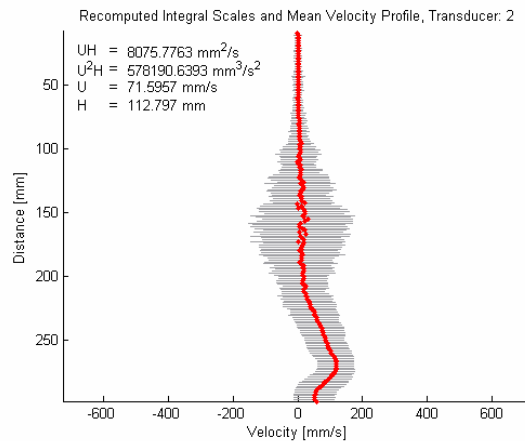
Figure 6.9 Mean velocity profile for transducer 2 after noise and aliasing filtering

Table 6.5 Resume of the values used in the data processing for transducer 2

Channel number of the bottom	199
Registered distance for bottom channel	297.973 mm
First profile considered	33 originally 234 at 33.555 s
Last profile considered	593 originally 4142 at 593.814 s
Percentage of the maximum velocity for aliasing filtering	90%
Maximum grade for mean profile adjustment	7
Threshold number for polynomial coefficients (*S*)	4
Total number of profiles considered	395
Initial time selected to recompute the mean profile [s]	200
Upper channel defining positive mean velocity region	0

6.1.4   *Velocity Measurements Transducer 3*
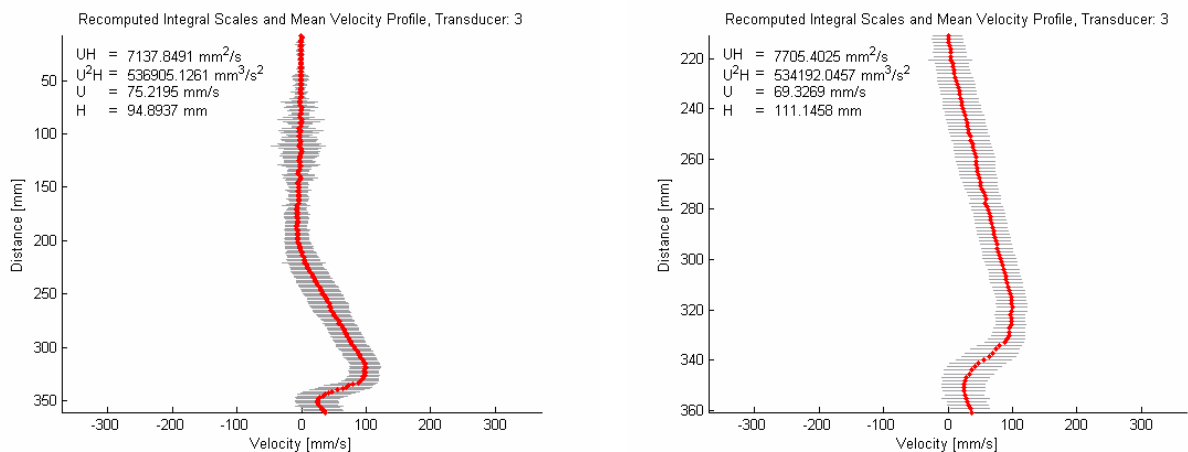
Figure 6.10 Mean velocity profile for transducer 3 after noise and aliasing filtering

Table 6.6 Resume of the values used in the data processing for transducer 3

Channel number of the bottom	254
Registered distance for bottom channel	360.814 mm
First profile considered	45 originally 321 at 46.031 s
Last profile considered	593 originally 4145 at 594.244 s
Percentage of the maximum velocity for aliasing filtering	90%
Maximum grade for mean profile adjustment	7
Threshold number for polynomial coefficients (*S*)	4
Total number of profiles considered	368
Initial time selected to recompute the mean profile [s]	250
Upper channel defining positive mean velocity region	146

6.1.5   *Velocity Measurements Transducer 5*
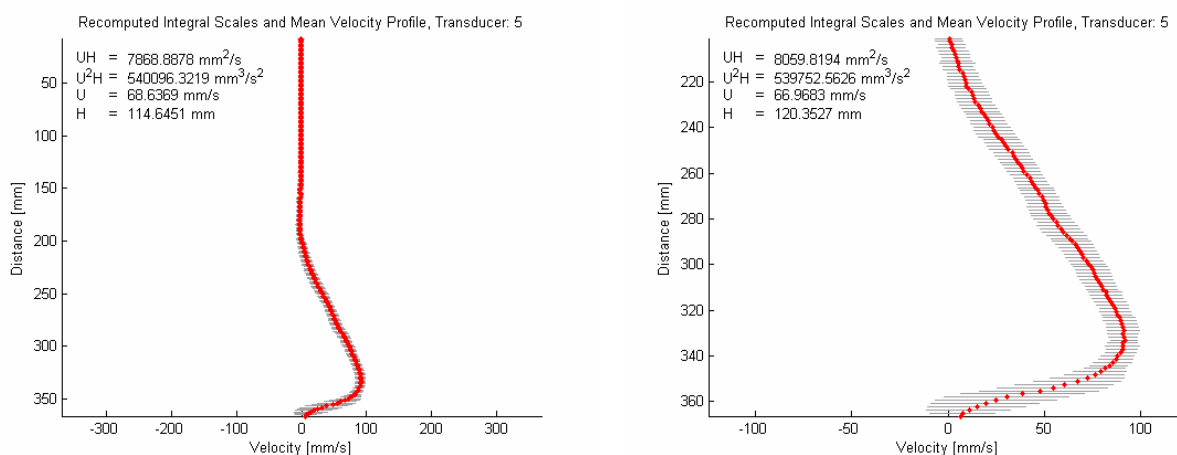
Figure 6.11 Mean velocity profile for transducer 5 after noise and aliasing filtering

Table 6.7 Resume of the values used in the data processing for transducer 5

Channel number of the bottom	258
Registered distance for bottom channel	366.377 mm
First profile considered	82 originally 580 at 83.097s
Last profile considered	497 originally 3479 at 498.739 s
Percentage of the maximum velocity for aliasing filtering	90%
Maximum grade for mean profile adjustment	7
Threshold number for polynomial coefficients (*S*)	4
Total number of profiles considered	327
Initial time selected to recompute the mean profile [s]	250
Upper channel defining positive mean velocity region	139

6.1.6 Velocity Measurements Transducer 6

Figure 6.12 Mean velocity profile for transducer 6 after noise and aliasing filtering

Table 6.8 Resume of the values used in the data processing for transducer 6

Channel number of the bottom	274
Registered distance for bottom channel	388.629 mm
First profile considered	114 originally 813 at 116.584 s
Last profile considered	435 originally 3060 at 438.805 s
Percentage of the maximum velocity for aliasing filtering	90%
Maximum grade for mean profile adjustment	7
Threshold number for polynomial coefficients (S)	4
Total number of profiles considered	238
Initial time selected to recompute the mean profile [s]	250
Upper channel defining positive mean velocity region	149

6.1.7 Velocity Measurements Transducer 7

Figure 6.13 Mean velocity profile for transducer 7 after noise and aliasing filtering

Table 6.9 Resume of the values used in the data processing for transducer 7

Channel number of the bottom	294
Registered distance for bottom channel	415.053 mm
First profile considered	150 originally 1068 at 153.151 s
Last profile considered	376 originally 2644 at 379.075 s
Percentage of the maximum velocity for aliasing filtering	90%
Maximum grade for mean profile adjustment	7
Threshold number for polynomial coefficients (S)	4
Total number of profiles considered	150
Initial time selected to recompute the mean profile [s]	250
Upper channel defining positive mean velocity region	174

7. CONCLUSIONS AND RECOMMENDATIONS

7.1 Experimental Facility and Measuring Instrumentation

The first part of the experimental work consisted in a familiarization with the experimental facility and measuring instrumentation. Several activities were developed as part of this, which were very helpful in defining the better way to focus the development of the data treatment routines.

Among these activities, the calibration process of control valves in the principal flume lead to a recommendation to implement an overflow weir at the downstream end of the channel, in order to have a better control over the water surface levels in the reservoir part. The large extension of the channel and the slow response of the discharge evacuated by the downstream control valve to water depth variations, resulted in that the response of the water levels was extremely slow, becoming very difficult to set a stable one. This fact could be assessed by inspecting a simple integral continuity equation for the channel:

$$\frac{\partial V}{\partial t} = Q_i - Q_o \qquad (7.1)$$

Where V is the water volume, Q_i is the inflow discharge and Q_o the outflow discharge. If the discharge difference is represented by $\Delta Q(t)$, and the chain rule is invoked, it is obtained that:

$$\frac{\partial V}{\partial H}\frac{\partial H}{\partial t} = \frac{\partial H}{\partial t} = \Delta Q(t) \;\; \Rightarrow \;\; \frac{\partial H}{\partial t} = \frac{\Delta Q(t)}{A_s(t)} \qquad (7.2)$$

Where H is the depth of water in the channel and A_s is the surface area of the flowing water. To have an estimation; a difference of 0.1 l between the inflow and outflow discharge, and assuming that the water surface area is approximately constant and equal to the length of the channel times its width, i.e. 5 m^2, results in a depth rate of approximately 1 mm/min. If the experiment have a duration of 15 minutes this means a total level variation of 1.5 cm, even when a very small difference in the discharges is being assumed.

To assure a small difference between the initial and final water surface level in the channel, it was looked for the better way to made quickly tend ΔQ to zero, and the implementation of the overflow weir was proposed, because this lead to a faster response of the outflow discharge to the water surface level variations.

At the downstream end of the channel, a thin metallic gate played the role of a vertical wall. Due to this, the projected weir was conceived as one of the thin wall type and performed by

means of a rectangular window on the gate. The width of the weir was estimated following a simple discharge equation (7.3):

$$Q_o = m \cdot L_w \cdot H_w \sqrt{2gH_w} \tag{7.3}$$

Where m is the discharge coefficient, L_w is the width of the weir, H_w the water head over the weir and g the gravity acceleration. Using a value of 0.434 (ideal case, no energy losses) for the discharge coefficient, m, the relation between L_w and H_w was plotted for two representative discharges, 1 l/s and 3 l/s in Figure 7.1.
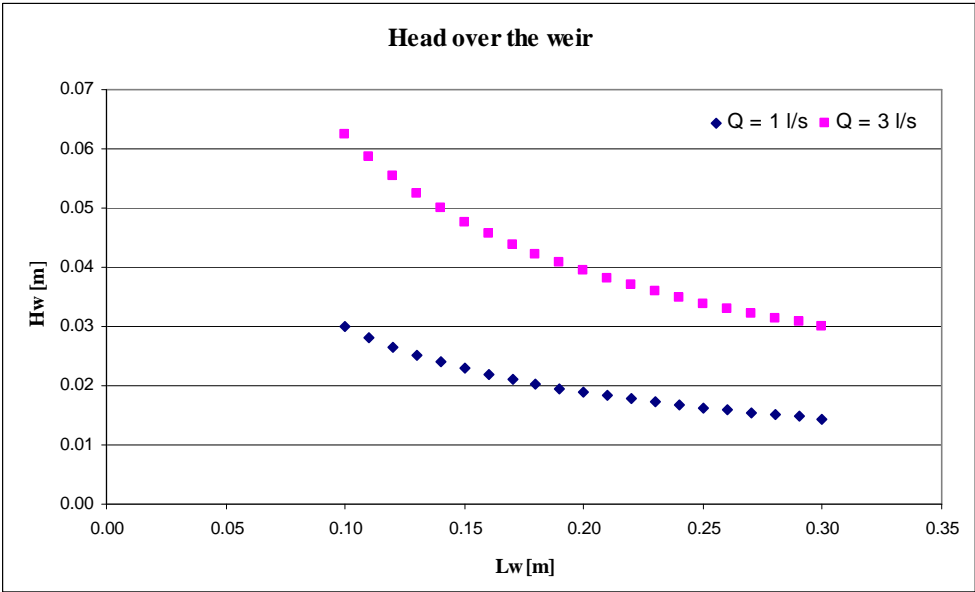
Figure 7.1 Relation between L_w and H_w for two different discharges

The final width was selected in order to have a small difference between the maximum and minimum surface water level in the channel (water head over the weir). The selected value corresponded to 25 cm and the bottom of the rectangular window was located on the gate in order to obtain the desired water surface levels on the channel.

In another area of the experimental facility, some ideas were also given in designing the system to inject the turbidity current mixture to the main channel. Specifically, pointing out the necessity of a recirculation circuit to the mixture tank which could be directed at some point to the main channel. This was sought in order to have an instance for set the mixture discharge without major difficulties. The system was proposed with two branches after the main control valve: a returning branch and an injection branch, both of them provided with control valves to allow or deny the flow. It was supposed that both branches should be as symmetrical as possible to minimize the difference in the energy losses for a given discharge; however, even when the final injection system had to be adjusted to the facility characteristics

in decline of symmetry, the differences in the energy losses showed to be practically negligible for the range of mixture discharges used.

Also regarding the mixture injection system, it was suggested to dissipate the momentum of the inflowing jet at the upstream end of the channel. This was finally implemented by means of a rectangular counter-clock wise inclined plate in front of the jet.

7.2   Data Treatment Routines

In this work several routines for the data treatment of velocity and bed deposits thickness were developed. The implementation of these routines was made as long as the insight of the experimental facility was gained. This fact leaded to several modifications and upgrades which ended in the two main routines for the purpose of the experiments: *multidata.m* and *bedread.m*.

The more used of these two routines was *multidata.m* because of the experiments involved mainly turbidity current velocity measurements. The routine was programmed with a user friendly orientation keeping in mind that this would contribute to the efficiency in the post process and analysis of the obtained data, and that would allow future applications in other experimental facilities. The description of the routines presented in Chapter 5 was oriented to allow the usage of the routine by any user without the necessity of reviewing the code.

The program code for all routines is included in the companion CD-ROM.

7.3   Experimental Data

In Chapter 6 the final results of the data treatment profile were presented in the form of figures and tables, these were obtained following the procedure described in section 5.4.4 for the majority of the experiment included this report.

Through the analysis of the velocity profiles, two main issues can be cited. In the first place it was observed some anomalies in the mean velocity profiles associated to the transducer placed in position 5. Considering the typical shape of a velocity profile described in literature, this anomaly consisted of a region towards the bottom where velocities were lower than the expected, giving an irregular shape to mean velocity profile. After considering several options it was evaluated the possibility of a region in the channel wall with a higher characteristic roughness. With this suspicion the engineer in charge asked that the whole channel wall were smoothed. This caused a considerable improvement in the behavior of the velocities in the questioned region.

The second fact detected in the final stages of the work corresponds to the behavior of the velocities near the bottom, registered by the UVP device when quite faster turbidity currents

were developed along the experiment. Inspecting figures as the one of section 6.1 it can be seen that the velocity near the bottom is quite different of zero, and thus the channel representing the bottom becomes difficult to determine.

The experiment under analysis corresponds to the one with the biggest value for the designed fine sediment concentration. The phenomenon can be explained by the spreading that affects the burst along the measurement axis. This determines that channels near the bottom are wider, and when the concentration is bigger, there are more reflecting particles with a non-zero velocity contained on it. For this reason it is recommended that in future experiments that involve fine sediment concentration higher that 0.7% the location of the transducers be as closer as possible to the bottom of the flume.

Finally it is worth to note that the parameters used for filtering the velocity profile were decided after a quick analysis, and they have shown a good behavior through all the experiment where data was subjected to analysis. It has been observed that the mean velocity profile and the integrals scales are more sensitive to the limits of the data included in the analysis than to the amount of profiles included on it. This is stated based in the small variation that show these parameters to the exclusion of aliased profiles. However it would be useful to have an analysis of the effect of changing the filtering parameter over the mean velocity profile and the integral scales.

Lisboa, Laboratório Nacional de Engenharia Civil, Março de 2007
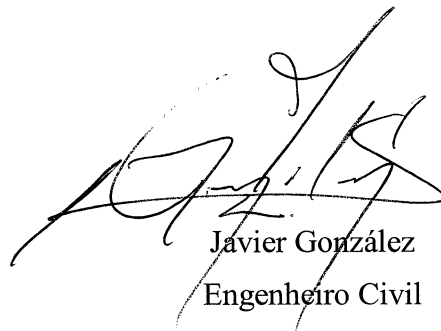
<table>
<tr><td>VISTO</td><td>AUTORIA</td></tr>
<tr><td>João Soromenho Rocha</td><td>Javier González</td></tr>
<tr><td>Chefe do Núcleo de Recursos Hídricos e Estruturas Hidráulicas</td><td>Engenheiro Civil</td></tr>
</table>

Rafaela de Saldanha Matos

Directora do Departamento de Hidráulica e Ambiente

8. REFERENCES

Altinakar, M.S. (1993). "Weakly Depositing Turbidity Currents on Small Slopes", PhD Thesis N° 738, École Polytechnique Fédérale de Lausanne, EPFL, Switzerland.

Ellison, T., and Turner, J. (1959). "Turbulent entrainment in Stratified flows." Journal of Fluid Mechanics, Vol. 6, pp. 423-448.

De Cesare, G. (1998). "Reservoir Sedimentation by Turbidity Currents", PhD Thesis N° 1820, École Polytechnique Fédérale de Lausanne, EPFL, Switzerland.

Garcia, M.H. (1990). "Depositing and Eroding Sediment-driven Flows: Turbidity Currents" Ph.D Thesis, University of Minnesota, Minneapolis, 179 p.

García, M. H. (1993). "Hydraulic Jumps in Sediment-driven Bottom Currents." Journal of Hydraulic Engineering, ASCE, Vol. 119, No. 10, pp. 1094-1117.

Kostic, S., and Parker, G. (2003a). "Progradational Sand-Mud Deltas in Lakes and Reservoirs. Part 1. Theory and Numerical Modeling." Journal of Hydraulic Research, Vol 41, No. 2, pp.127-140.

Kostic, S., and Parker, G. (2003b). "Progradational Sand-Mud Deltas in Lakes and Reservoirs. Part 2. Experiments and Numerical Simulation." Journal of Hydraulic Research, Vol. 41, No 2, pp. 141-152.

MET FLOW (2002). "UVP Monitor Model UVP-DUO with Software Version 3" User's Guide.

Oehy, C. (2003). "Effects of Obstacles and Jets on Reservoir Sedimentation Due to Turbidity Currents", PhD Thesis N° 2684, École Polytechnique Fédérale de Lausanne, EPFL, Switzerland.

Toniolo, H. (2003). "Depositional Turbidity Currents in Diapiric Minibasins on the Continental Slope: Experiments and Numerical Simulation." Chapter 3 of Ph.D. Thesis, University of Minnesota, 233 p.

Shahram, I. (2005). "Signal Processing and Analysis of Ultrasonic Velocity Profiling (UVP) Measurements". *Master Thesis*. Chalmers University of Technology, Göteborg, Sweden. 71 p.

9. APPENDIX: EXPERIMENTAL DATA TREATMENT

The velocity data obtained and processed for the majority of the experiments carried out during the project is presented here. Some of the initial experiments were treated using a different procedure of that described in section 5.4.4 and thus the associated figures and descriptions do not follow strictly the proposed steps.

9.1 Experiment 2007.02.06

This experiment was performed using a discharge equal to 33% of the maximum measurable discharge in the flowmeter, equivalent to 1.28 l/s. No clean water flow, constant initial water surface at the downstream end. The volumetric concentration of fine sediment was measured to be 0.28%

Seven transducers were used. For each one, the longitudinal position with respect to the zero point on the channel, the distance between the transducer and the channel bottom measured along the beam axis, and the projection of this distance on the normal to the bed direction are presented in Table 9.1.

A total of 360 channels were used in a window measurement of 539.37 mm. A total 800 profiles were registered by each transducer.

Table 9.1 Description of the position and distance to the bottom for each transducer

Transducer nº	1	2	3	4	5	6	7
Longitudinal location [m]	8.4	8.0	7.0	6.0	5.0	3.0	1.0
Transducer angle [º]	10	10	20	20	20	20	20
Bottom distance [mm]	155	270	347	364	380	416	440
Projected bottom distance [mm]	153	266	326	342	357	391	413

9.1.1   *Velocity measurements transducer 1*
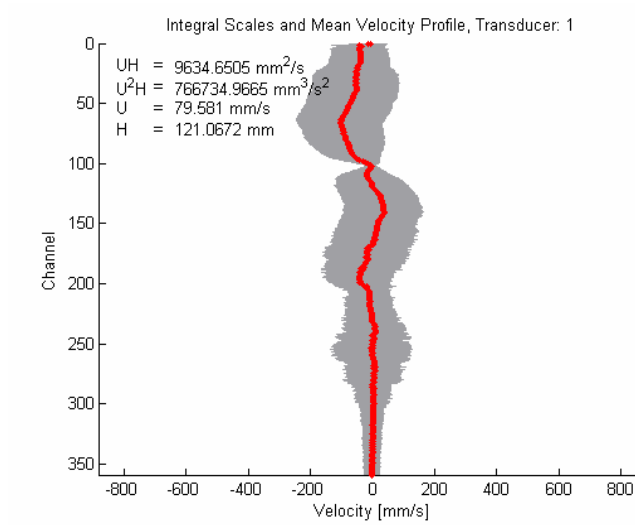
Figure 9.1 Original mean velocity profile and integral scales, transducer 1: velocity against channel number
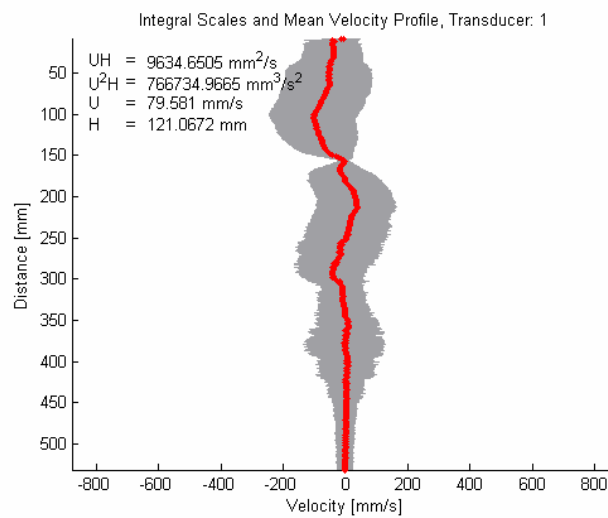
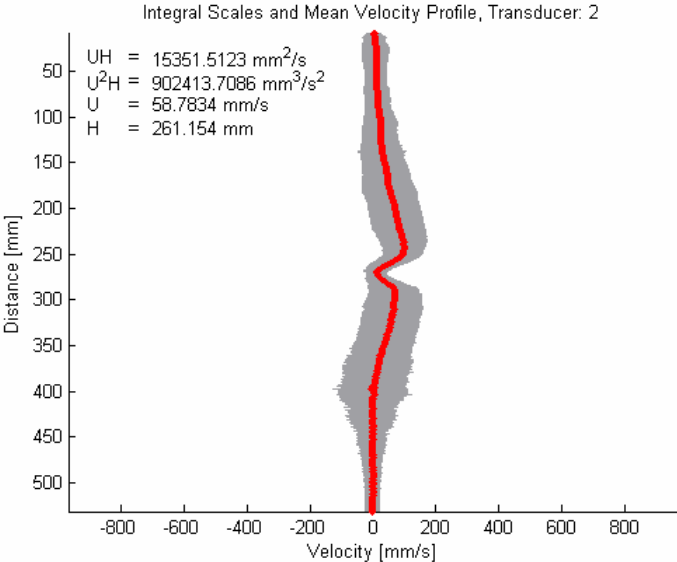**Figure 9.2 Original mean velocity profile and integral scales, transducer 1: velocity against channel distance**

From the data evolution animation and Figure 9.1 it can been seen that the channel bottom is being detected between channel 100 and 103, which are being located at a distance of 156.06 mm and 160.49 mm in the measurement axis, and a projected distance of 153.67 mm and 158.05 mm.
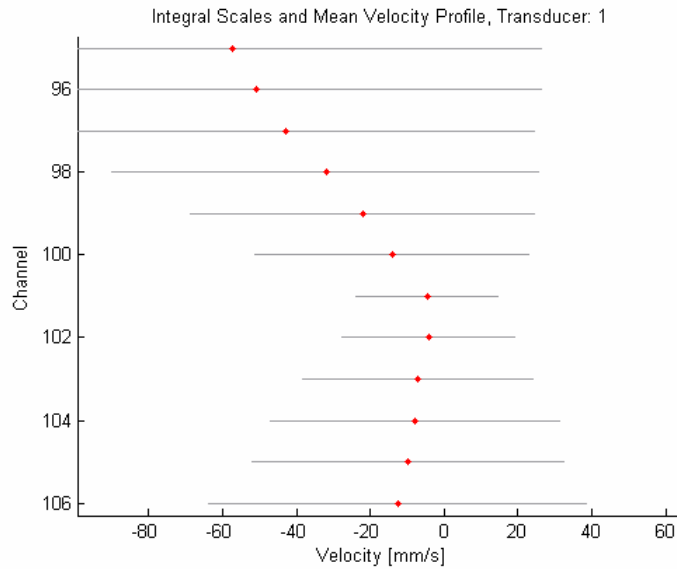
Figure 9.3 Original mean velocity profile transducer 1: zoom to the channel bottom zone

Even when mean velocity is not null in this domain window, channel 101 and 102 are the closer to zero velocity, and channel 101 is the one with the smaller variance. This channel is selected to as the last one to compute the integral scales in further analysis. The registered distance of this channel from the transducer is 157.53 mm and the projected one is 155.14 mm. As can be seen in Table 9.1 the measured bottom distance along the beam axis is 155 mm. The difference is small and can be attributed to the accuracy on the manual measurement or a difference in the actual sound velocity used in the measurement. In the latter case, the effect of having such a difference in sound velocity over current velocity measurement is negligible (Best et al. 2001).

From an inspection of the measured velocity profile evolution, it can be seen that the initial 16 profiles were registered before the arrival of the current. By this reason they will be excluded from the mean velocity profile and integral scales calculation. Figure 9.4 shows the resulting mean profile without any filtering process.
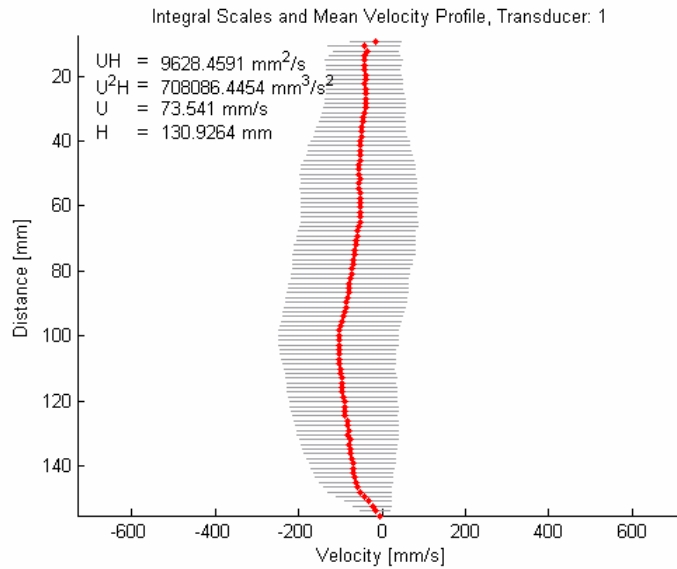
Figure 9.4 Mean velocity profile for transducer 1 considering channel 0 to 101 and profiles 16 to 799

The velocity data defined by the selected channels and profiles is inspected using a video animation where no aliasing can be found. After evaluating the best parameters for performing the noise filtering process a polynomial grade of 7 is selected and a threshold number of 4 coefficients is selected (S = 4 see section 5.4.2). At this stage the *multidata.m* was corrected to present the correct sign of velocity accordingly to the flow direction. The correction is made in terms of the orientation of the transducer. The result is presented in Figure 9.5.
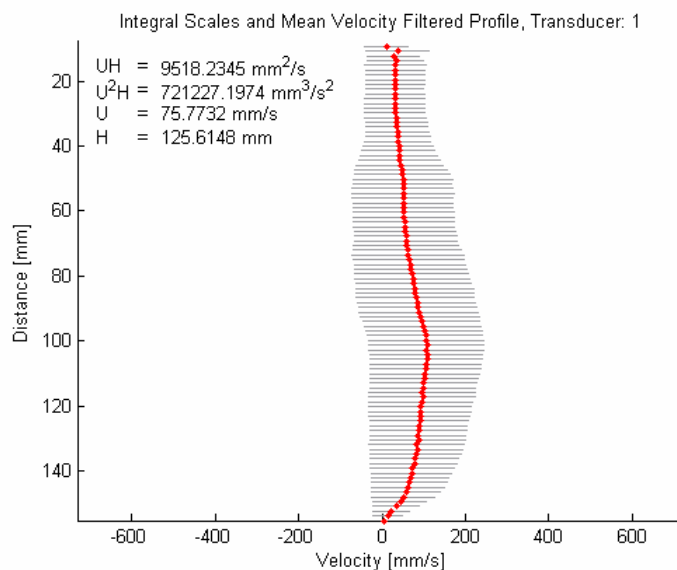
Figure 9.5 Mean velocity profile for transducer 1 after noise filtering

A total of 593 velocity profiles ware kept after the filtering process. The principal effect is a reduction in the standard deviation of the velocity of the upper part of the profile, as a small reduction in the values of the mean velocity for upper channels.

Final values of the mean velocity and standard deviation have been stored in the file *T1_mean.dat*. Values of the integral scales are stored in the file *T1_scal.dat* and the whole set of profiles considered after the filtering process is stores in the file *T1_prof.dat*, this structure will be followed for remaining transducers changing the number in the files name accordingly to transducer number.

9.1.2 *Velocity Measurements transducer 2*

The same procedure described in section is followed. Analogous images are shown below:

Figure 9.6 Original mean velocity profile and integral scales, transducer 2: velocity against channel distance
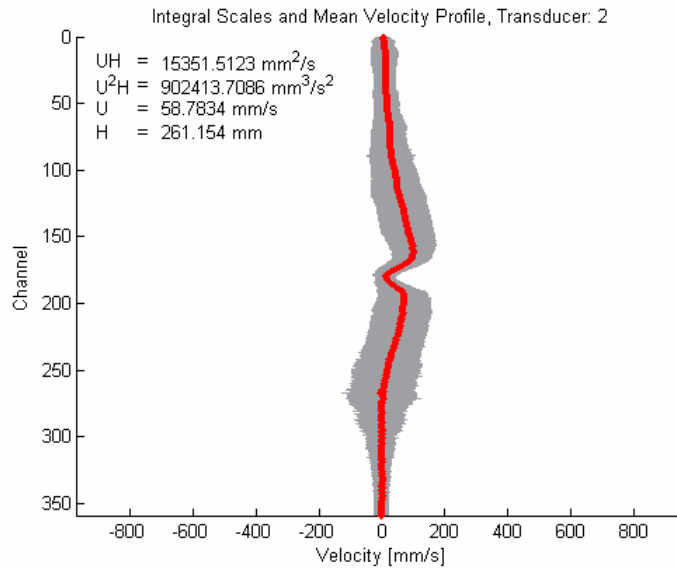
Figure 9.7 Original mean velocity profile and integral scales, transducer 2: velocity against channel number
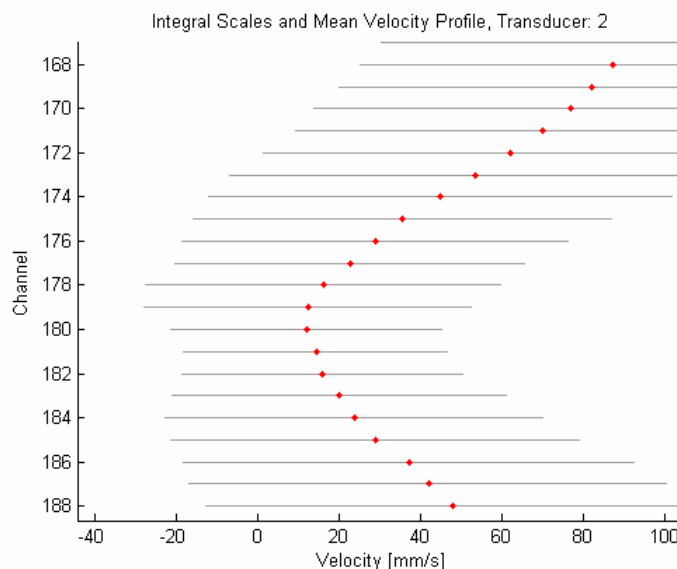
Figure 9.8 Original mean velocity for transducer 2: zoom to the channel bottom zone

Inspecting the channel distances it is found that channel 180 is at 274.45 mm from the transducer, corresponding to a projected normal distance of 270.28 mm. These values are in good agreement with the in situ measured distance to the bottom. By these reasons it will be signed as the position of the channel bottom.

Again, the first profile with turbidity current velocity measurement is profile number 16. First 15 profiles will be excluded from the analysis. The fact of profile number 16 being the first with velocity measurements attributable to the pass of the turbidity current will be retained for further analysis, it could indicate that the arriving of the turbidity current occurred during the

second measurement cycle, but was only registered when the third cycle started. Integrals scales computed using the selected profiles and channel window, without any filtering process is shown in Figure 9.9.
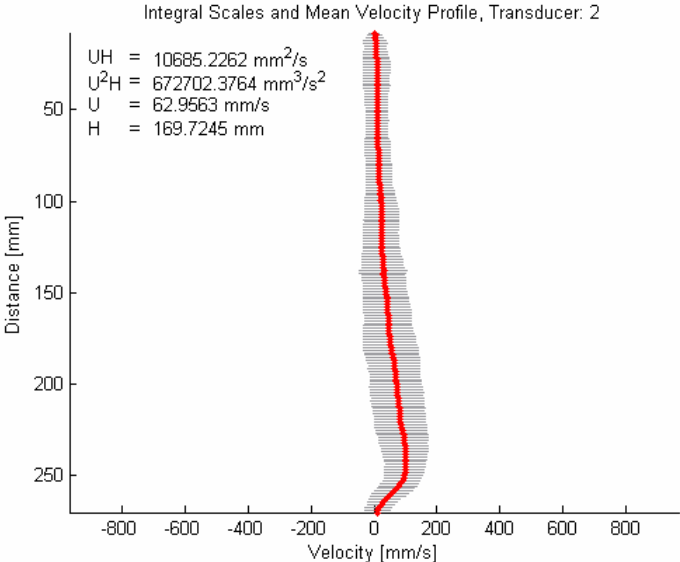
Figure 9.9 Mean velocity profile for transducer 2 considering channel 0 to 180 and profiles 16 to 799

Some profiles were detected to present aliasing; therefore a threshold of the 90% of the maximum velocity was used to eliminate them. To filter noise the same parameters for transducer 1 were used. A total of 536 profile were considered finally. The result is presented and it can be observed that the effect of the filtering process is similar to the obtained on transducer 1.
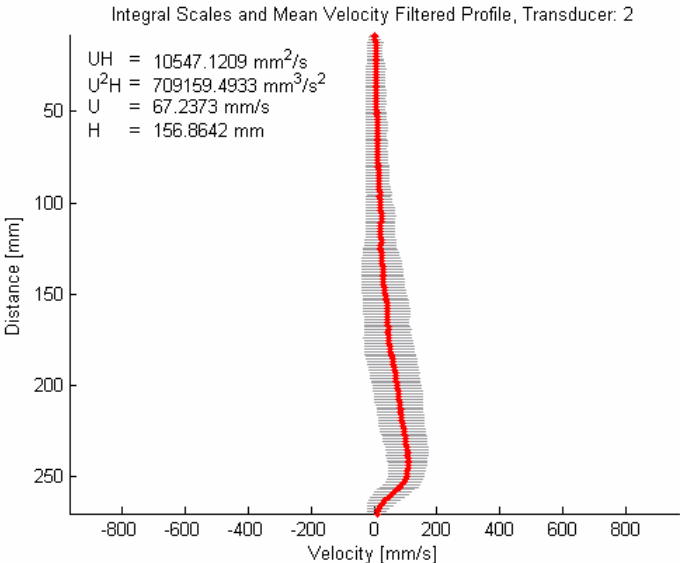
Figure 9.10 Mean velocity profile for transducer 2 after noise and aliasing filtering

9.1.3 *Velocity measurements transducer 3*

For the following transducers it will be presented only the last mean profile obtained after the filtering process. Remaining considerations like channel chosen of the bottom, initial profile and total number of profiles considered for the final mean profile will be resumed in a table.
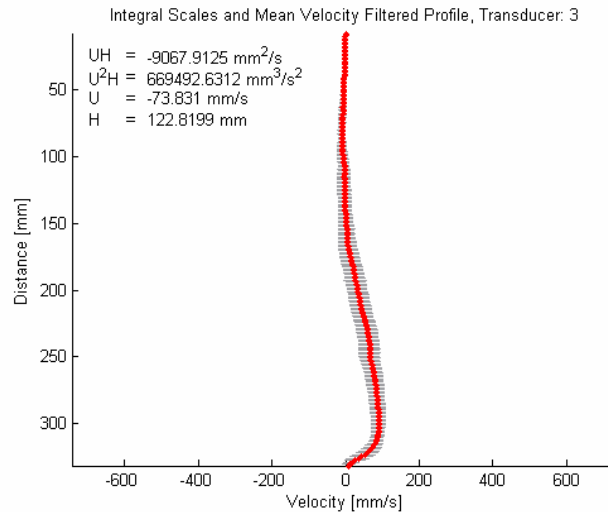
Figure 9.11 Mean velocity profile for transducer 3 after noise and aliasing filtering

Table 9.2 Resume of the values used in the data processing for transducer 3

Channel number of the bottom	233
Registered distance for bottom channel	332 mm
First profile considered	58 originally 410 at 39.508 s
Last profile considered	799 originally 5567 at 537.011 s
Percentage of the maximum velocity for aliasing filtering	90%
Maximum grade for mean profile adjustment	7
Threshold number for polynomial coefficients (S)	4
Total number of profiles considered	493

9.1.4 *Velocity measurements transducer 4*

Table 9.3 Resume of the values used in the data processing for transducer 4

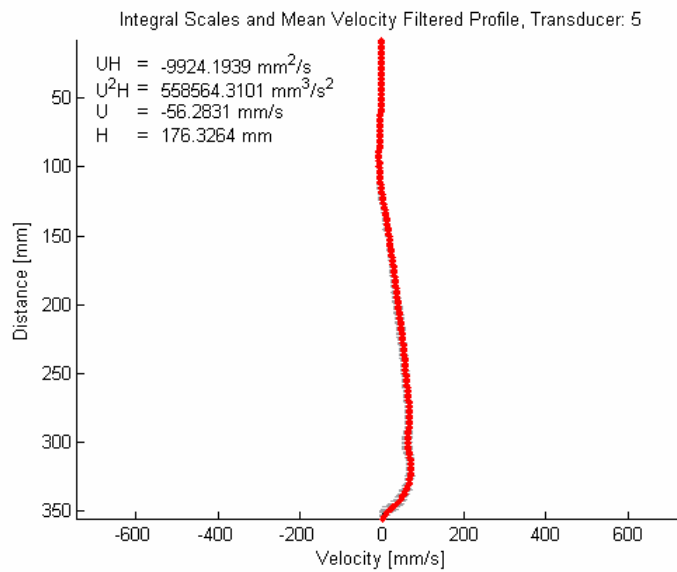|	
Channel number of the bottom	246
Registered distance for bottom channel	349.68 mm
First profile considered	88 originally 640 at 61.759 s
Last profile considered	799 originally 5575 at 537.783 s
Percentage of the maximum velocity for aliasing filtering	90%
Maximum grade for mean profile adjustment	7
Threshold number for polynomial coefficients (S)	4
Total number of profiles considered	488
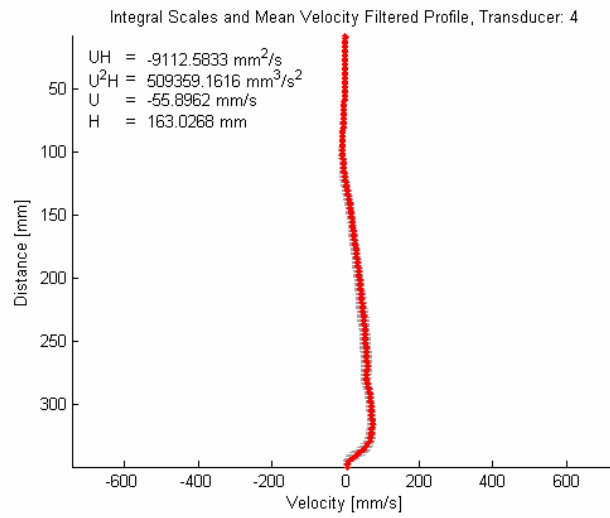
Figure 9.12 Mean velocity profile for transducer 4 after noise and aliasing filtering
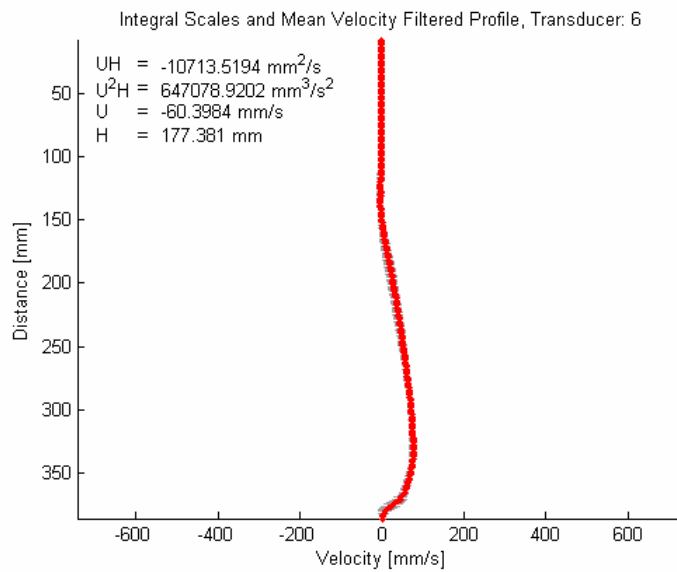
9.1.5 _Velocity measurements transducer 5_

Figure 9.13 Mean velocity profile for transducer 5 after noise and aliasing filtering

Table 9.4 Resume of the values used in the data processing for transducer 5

Channel number of the bottom	250
Registered distance for bottom channel	355.251 mm
First profile considered	120 originally 872 at 84.147 s
Last profile considered	799 originally 5583 at 538.555 s
Percentage of the maximum velocity for aliasing filtering	90%
Maximum grade for mean profile adjustment	7
Threshold number for polynomial coefficients (*S*)	4
Total number of profiles considered	474

9.1.6 *Velocity measurements transducer 6*

Integral Scales and Mean Velocity Filtered Profile, Transducer: 6

UH = -10713.5194 mm²/s
U^2H = 647078.9202 mm³/s²
U = -60.3984 mm/s
H = 177.381 mm

Figure 9.14 Mean velocity profile for transducer 6 after noise and aliasing filtering

Table 9.5 Resume of the values used in the data processing for transducer 6

Channel number of the bottom	272
Registered distance for bottom channel	385.847 mm
First profile considered	176 originally 1272 at 122.746 s
Last profile considered	728 originally 5136 at 495.617 s
Percentage of the maximum velocity for aliasing filtering	90%
Maximum grade for mean profile adjustment	7
Threshold number for polynomial coefficients (*S*)	4
Total number of profiles considered	442

Some profiles belonging to the formation of the internal hydraulic jump were detected in this transducer data set, starting specifically at profile 729. These profiles were excluded from the calculation of the final mean velocity profile.
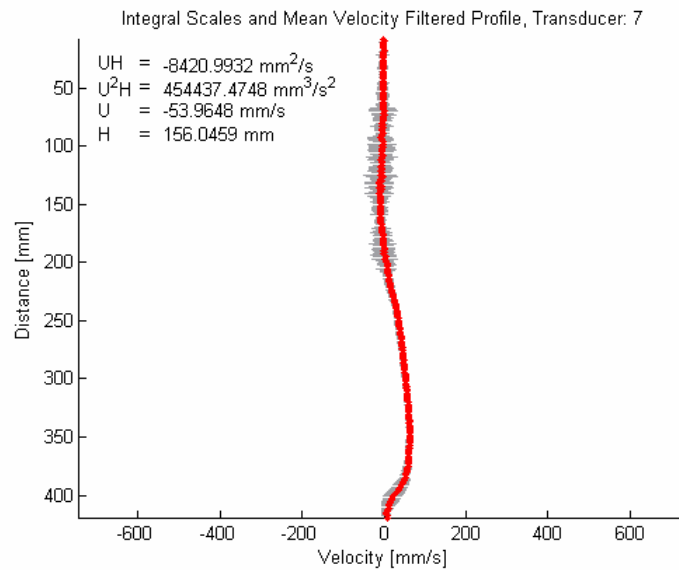
9.1.7 *Velocity measurements transducer 7*

Integral Scales and Mean Velocity Filtered Profile, Transducer: 7

UH = -8420.9932 mm^2/s
U^{2}H = 454437.4748 mm^3/s^2
U   = -53.9648 mm/s
H   = 156.0459 mm

Figure 9.15 Mean velocity profile for transducer 7 after noise and aliasing filtering

Table 9.6 Resume of the values used in the data processing for transducer 7

Channel number of the bottom	296
Registered distance for bottom channel	419.225 mm
First profile considered	240 originally 1728 at 166.749 s
Last profile considered	635 originally 4475 at 431.747 s
Percentage of the maximum velocity for aliasing filtering	90%
Maximum grade for mean profile adjustment	7
Threshold number for polynomial coefficients (*S*)	4
Total number of profiles considered	317

Some profiles belonging to the formation of the internal hydraulic jump were detected in this transducer data set, starting specifically at profile 636. These profiles were excluded from the calculation of the final mean velocity profile.

9.2   Experiment 2007.02.12

For the sake of brevity the principal parameters of each experiments will be described using the format shown by Table 9.7. The signaled volumetric fine sediment concentration corresponds to the design value.

Table 9.7 Principal parameters used in experiment 2007.02.12

Discharge [%]	18.5
Discharge [l/s]	0.71
Volumetric fine sediment concentration [%]	0.11
Number of transducers	7
Maximum Depth	549.82 mm
Total number of channels	360
Profiles measured in each transducer per cycle	3
Estimated total cycle time [s]	3
Total number of measured profiles	3360

Table 9.8 Description of the position and distance to the bottom for each transducer

Transducer n°	1	2	3	4	5	6	7
Longitudinal location [m]	8.4	8.0	7.0	6.0	5.0	3.0	1.0
Transducer angle [°]	10	10	20	20	20	20	20
Bottom distance [mm]	152	296	345	359	377	425	441
Projected bottom distance [mm]	150	292	324	337	354	399	414

In this experiment, starting from the analysis of transducer 3 the *multidata.m* routine was modified to include an analysis of the cumulative mean velocity evolution in five user selected channels. This was done in order to facilitate the selection of a time instant when strong unsteady conditions of the turbidity current were absent and the computed mean values were truly representative.

9.2.1   *Velocity measurements transducer 1*

Table 9.9 Resume of the values used in the data processing for transducer 1

|	
Channel number of the bottom	98
Registered distance for bottom channel	153 mm
First profile considered	36 originally 252 at 36.137 s
Last profile considered	479 originally 3341 at 478.95 s
Percentage of the maximum velocity for aliasing filtering	90%
Maximum grade for mean profile adjustment	7
Threshold number for polynomial coefficients (*S*)	4
Total number of profiles considered	303
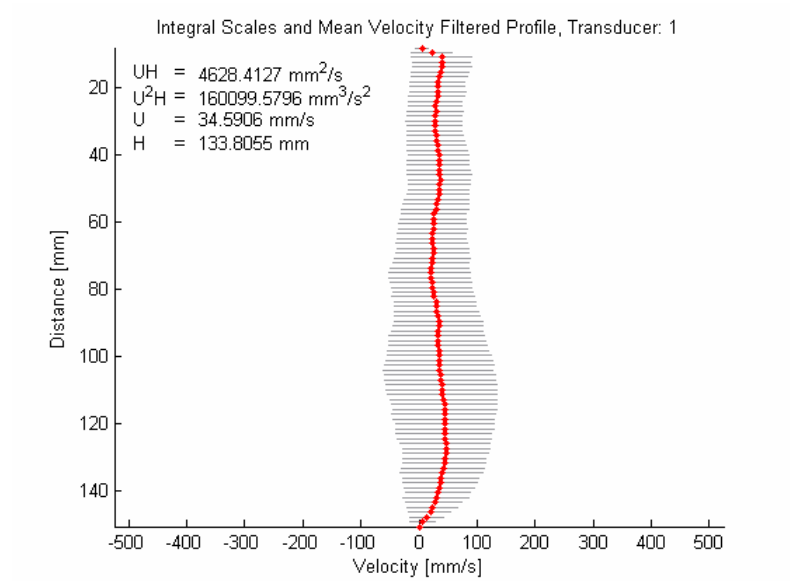
Figure 9.16 Mean velocity profile for transducer 1 after noise and aliasing filtering
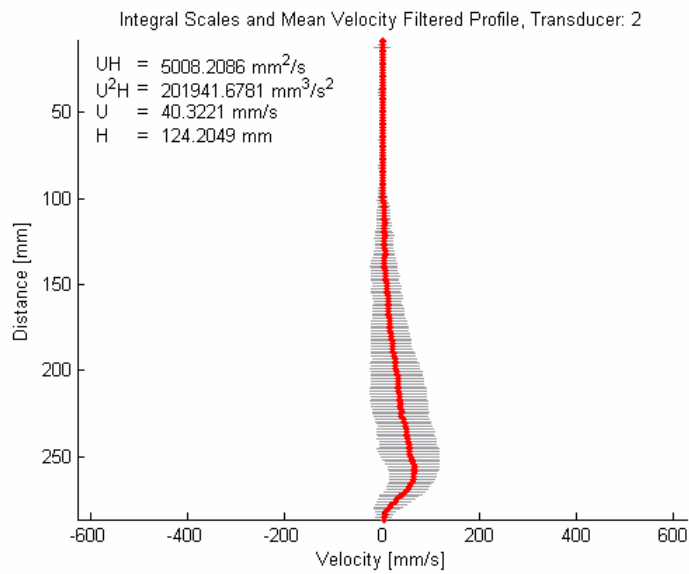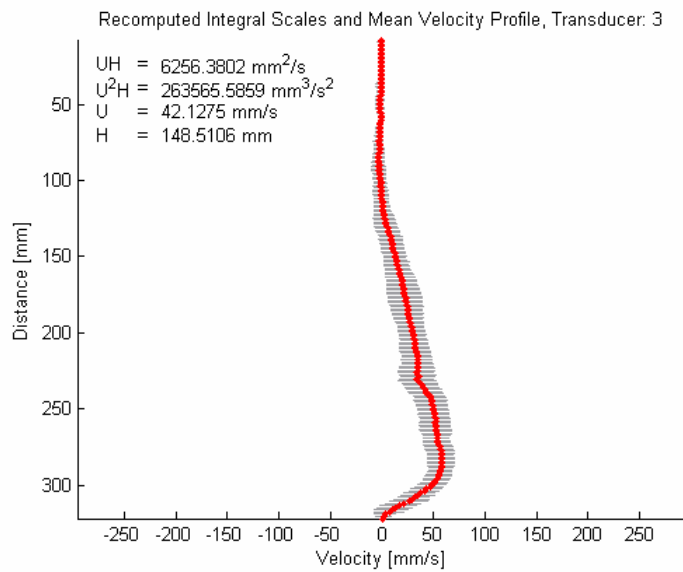
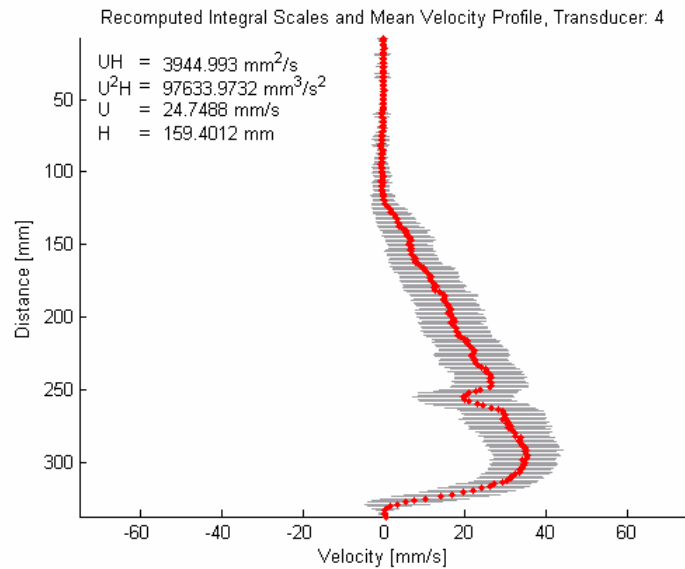### 9.2.2 *Velocity measurements transducer 2*

Figure 9.17 Mean velocity profile for transducer 2 after noise and aliasing filtering

Table 9.10 Resume of the values used in the data processing for transducer 2

Channel number of the bottom	191
Registered distance for bottom channel	290.73 mm
First profile considered	36 originally 255 at 36.567 s
Last profile considered	479 originally 3344 at 479.381 s
Percentage of the maximum velocity for aliasing filtering	90%
Maximum grade for mean profile adjustment	7
Threshold number for polynomial coefficients (*S*)	4
Total number of profiles considered	295

9.2.3   *Velocity measurements transducer 3*

Figure 9.18 Mean velocity profile for transducer 3 after noise and aliasing filtering

Table 9.11 Resume of the values used in the data processing for transducer 3

Channel number of the bottom	226
Registered distance for bottom channel	342.053 mm
First profile considered	51 originally 363 at 52.064 s
Last profile considered	479 originally 3347 at 479.811 s
Percentage of the maximum velocity for aliasing filtering	90%
Maximum grade for mean profile adjustment	7
Threshold number for polynomial coefficients (*S*)	4
Total number of profiles considered	292
Initial time selected to recompute the mean profile [s]	215

9.2.4 *Velocity measurements transducer 4*

Recomputed Integral Scales and Mean Velocity Profile, Transducer: 4

$UH = 3944.993$ mm^2/s
$U^2H = 97633.9732$ mm^3/s^2
$U = 24.7488$ mm/s
$H = 159.4012$ mm

Figure 9.19 Mean velocity profile for transducer 4 after noise and aliasing filtering

Table 9.12 Resume of the values used in the data processing for transducer 4

Channel number of the bottom	237
Registered distance for bottom channel	337.171mm
First profile considered	84 originally 597 at 85.61 s
Last profile considered	479 originally 3350 at 480.241 s
Percentage of the maximum velocity for aliasing filtering	90%
Maximum grade for mean profile adjustment	7
Threshold number for polynomial coefficients (*S*)	4
Total number of profiles considered	273
Initial time selected to recompute the mean profile [s]	235

9.2.5 *Velocity measurements transducer 5*

Table 9.13 Resume of the values used in the data processing for transducer 5

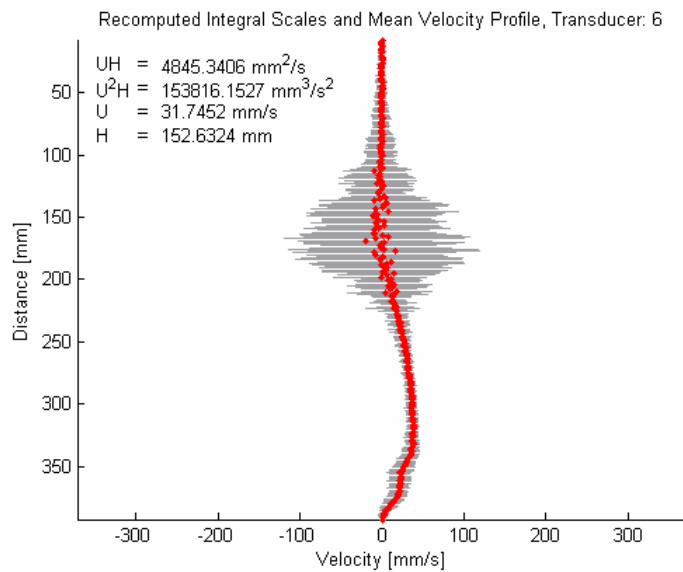|	
Channel number of the bottom	246
Registered distance for bottom channel	349.688 mm
First profile considered	117 originally 831 at 119.166 s
Last profile considered	479 originally 3353 at 480.671 s
Percentage of the maximum velocity for aliasing filtering	90%
Maximum grade for mean profile adjustment	7
Threshold number for polynomial coefficients (*S*)	4
Total number of profiles considered	300
Initial time selected to recompute the mean profile [s]	275
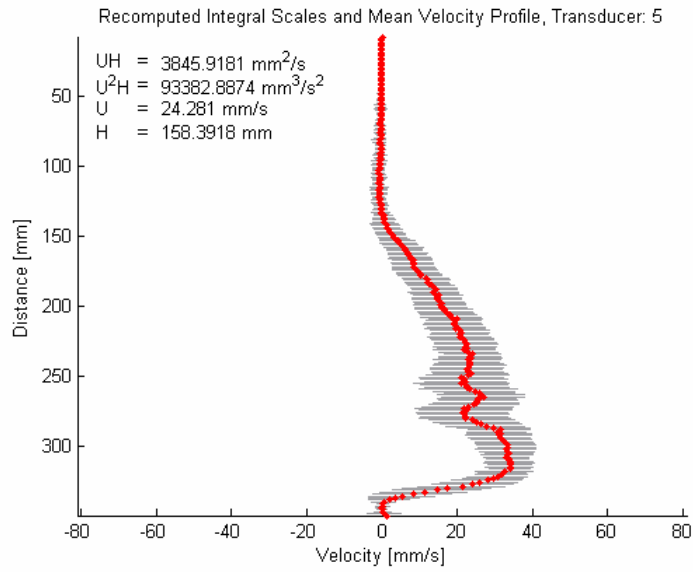
Figure 9.20 Mean velocity profile for transducer 5 after noise and aliasing filtering

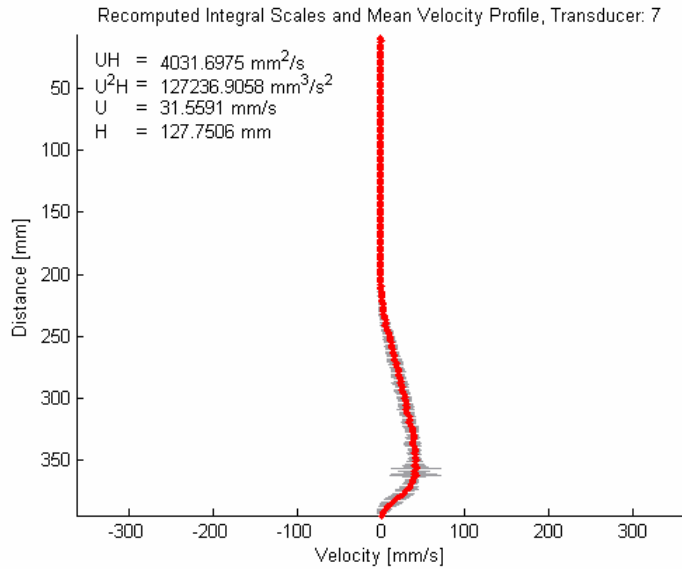### 9.2.6 *Velocity measurements transducer 6*

Figure 9.21 Mean velocity profile for transducer 6 after noise and aliasing filtering

Table 9.14 Resume of the values used in the data processing for transducer 6

Channel number of the bottom	277
Registered distance for bottom channel	392.801 mm
First profile considered	177 originally 1254 at 179.824 s
Last profile considered	479 originally 3356 at 481.101 s
Percentage of the maximum velocity for aliasing filtering	80%
Maximum grade for mean profile adjustment	7
Threshold number for polynomial coefficients (*S*)	4
Total number of profiles considered	229
Initial time selected to recompute the mean profile [s]	260

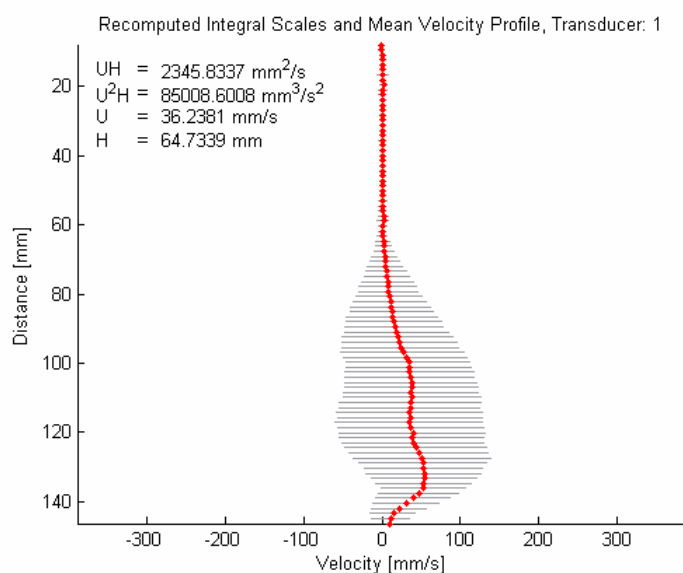## 9.2.7 *Velocity measurements transducer 7*

Figure 9.22 Mean velocity profile for transducer 7 after noise and aliasing filtering

Table 9.15 Resume of the values used in the data processing for transducer 7

Channel number of the bottom	278
Registered distance for bottom channel	394.192 mm
First profile considered	240 originally 1698 at 243.494 s
Last profile considered	479 originally 3359 at 481.532 s
Percentage of the maximum velocity for aliasing filtering	90%
Maximum grade for mean profile adjustment	7
Threshold number for polynomial coefficients (*S*)	4
Total number of profiles considered	220
Initial time selected to recompute the mean profile [s]	310

9.3 Experiment 2007.02.14

Discharge [%]	18.8
Discharge [l/s]	0.71
Volumetric fine sediment concentration [%]	0.5
Number of transducers	7
Maximum Depth	549.82 mm
Total number of channels	360
Profiles measured in each transducer per cycle	3
Estimated total cycle time [s]	3
Total number of measured profiles	3360

Table 9.16 Description of the position and distance to the bottom for each transducer

Transducer n°	1	2	3	4	5	6	7
Longitudinal location [m]	8.4	8.0	7.0	6.0	5.0	3.0	1.0
Transducer angle [º]	10	10	20	20	20	20	20
Bottom distance [mm]	152	274	358	366	378	420	437
Projected bottom distance [mm]	150	270	336	344	355	395	411

9.3.1 *Velocity measurements transducer 1*

Recomputed Integral Scales and Mean Velocity Profile, Transducer: 1

UH = 2345.8337 mm^2/s
U^2H = 85008.6008 mm^3/s^2
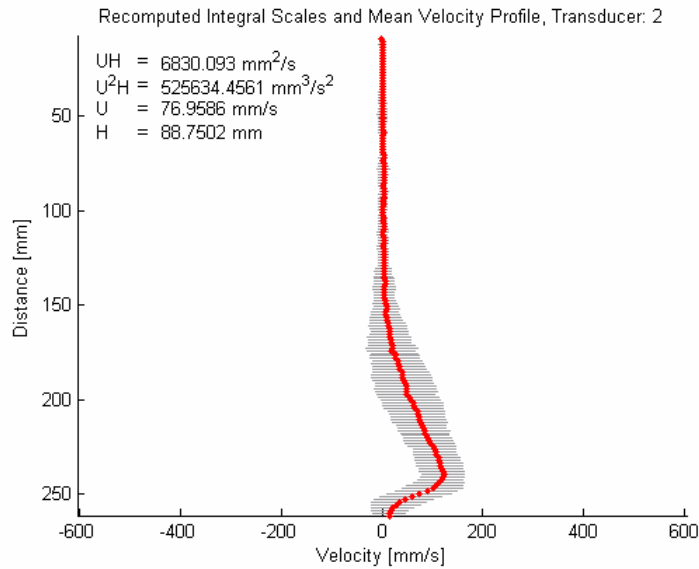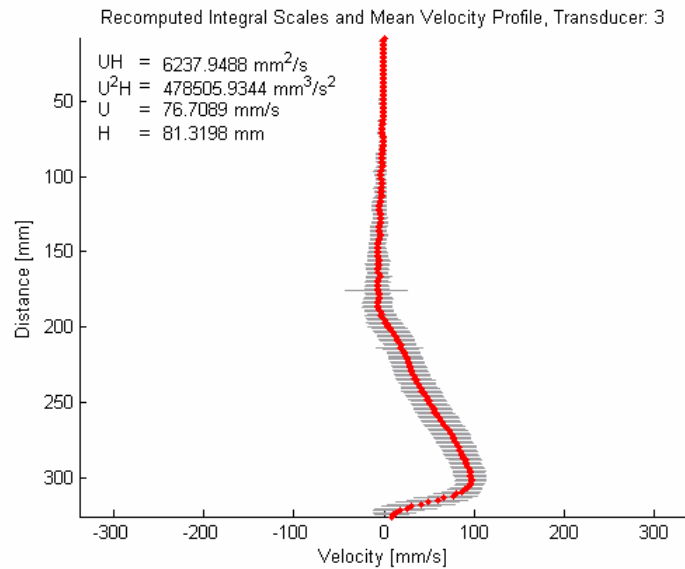U = 36.2381 mm/s
H = 64.7339 mm

Figure 9.23 Mean velocity profile for transducer 1 after noise and aliasing filtering

Table 9.17 Resume of the values used in the data processing for transducer 1

Channel number of the bottom	95
Registered distance for bottom channel	mm
First profile considered	21 originally 147 at 21.08 s
Last profile considered	479 originally 3341 at 478.95 s
Percentage of the maximum velocity for aliasing filtering	90%
Maximum grade for mean profile adjustment	7
Threshold number for polynomial coefficients (*S*)	4
Total number of profiles considered	309
Initial time selected to recompute the mean profile [s]	180

9.3.2 *Velocity measurements transducer 2*

Figure 9.24 Mean velocity profile for transducer 2 after noise and aliasing filtering

Table 9.18 Resume of the values used in the data processing for transducer 2

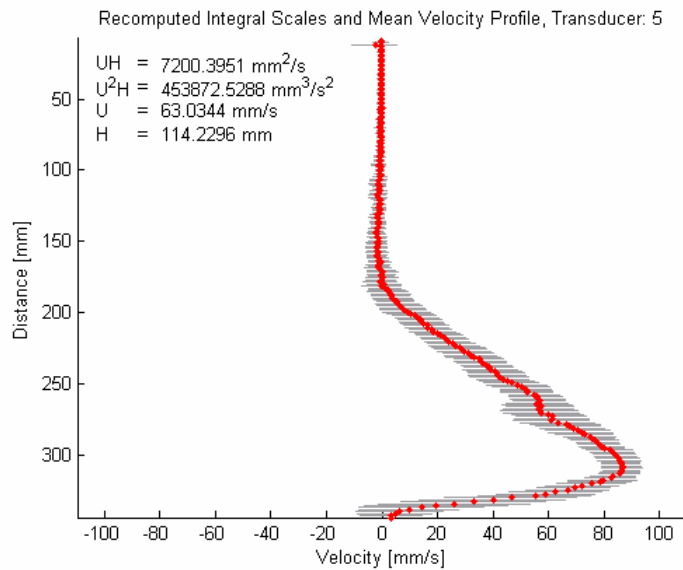|	
Channel number of the bottom	174
Registered distance for bottom channel	261.535 mm
First profile considered	30 originally 213 at 30.544 s
Last profile considered	479 originally 3344 at 479.381 s
Percentage of the maximum velocity for aliasing filtering	90%
Maximum grade for mean profile adjustment	7
Threshold number for polynomial coefficients (*S*)	4
Total number of profiles considered	312
Initial time selected to recompute the mean profile [s]	200

9.3.3 Velocity measurements transducer 3

Figure 9.25 Mean velocity profile for transducer 3 after noise and aliasing filtering

Table 9.19 Resume of the values used in the data processing for transducer 3

Channel number of the bottom	229
Registered distance for bottom channel	326.045 mm
First profile considered	45 originally 321 at 46.031 s
Last profile considered	479 originally 3347 at 479.811 s
Percentage of the maximum velocity for aliasing filtering	90%
Maximum grade for mean profile adjustment	7
Threshold number for polynomial coefficients (S)	4
Total number of profiles considered	311
Initial time selected to recompute the mean profile [s]	235

9.3.4 Velocity measurements transducer 4

Table 9.20 Resume of the values used in the data processing for transducer 4

Channel number of the bottom	237
Registered distance for bottom channel	337.171 mm
First profile considered	60 originally 429 at 61.519 s
Last profile considered	479 originally 3350 at 480.241 s
Percentage of the maximum velocity for aliasing filtering	90%
Maximum grade for mean profile adjustment	7
Threshold number for polynomial coefficients (S)	4
Total number of profiles considered	314
Initial time selected to recompute the mean profile [s]	260
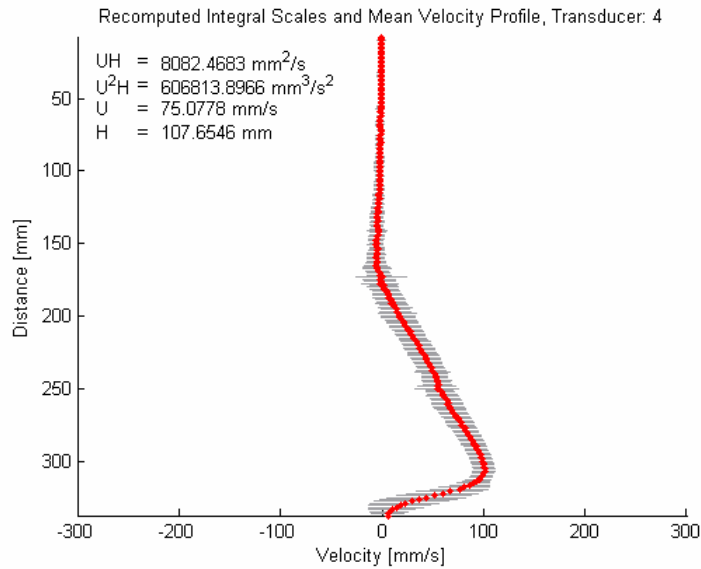
Figure 9.26 Mean velocity profile for transducer 4 after noise and aliasing filtering

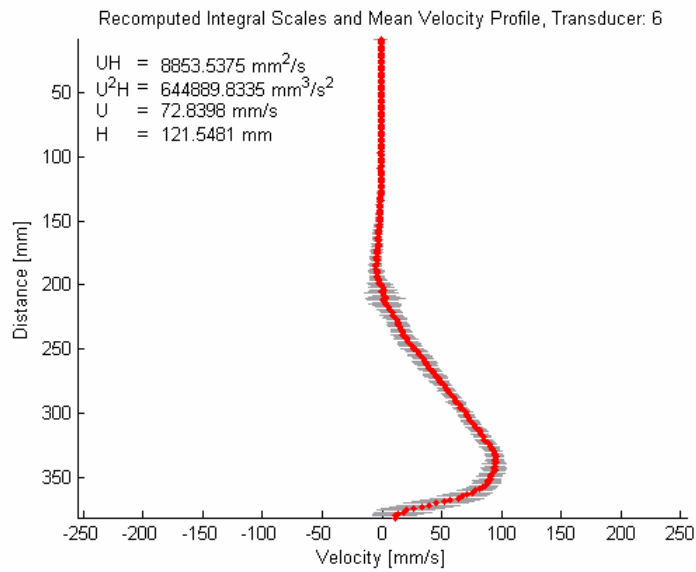## 9.3.5 *Velocity measurements transducer 5*

Figure 9.27 Mean velocity profile for transducer 5 after noise and aliasing filtering

Table 9.21 Resume of the values used in the data processing for transducer 5

Channel number of the bottom	242
Registered distance for bottom channel	344.13 mm
First profile considered	78 originally 558 at 80.017 s
Last profile considered	479 originally 3353 at 480.671 s
Percentage of the maximum velocity for aliasing filtering	90%
Maximum grade for mean profile adjustment	7
Threshold number for polynomial coefficients (*S*)	4
Total number of profiles considered	345
Initial time selected to recompute the mean profile [s]	310

9.3.6 *Velocity measurements transducer 6*

Figure 9.28 Mean velocity profile for transducer 6 after noise and aliasing filtering

Table 9.22 Resume of the values used in the data processing for transducer 6

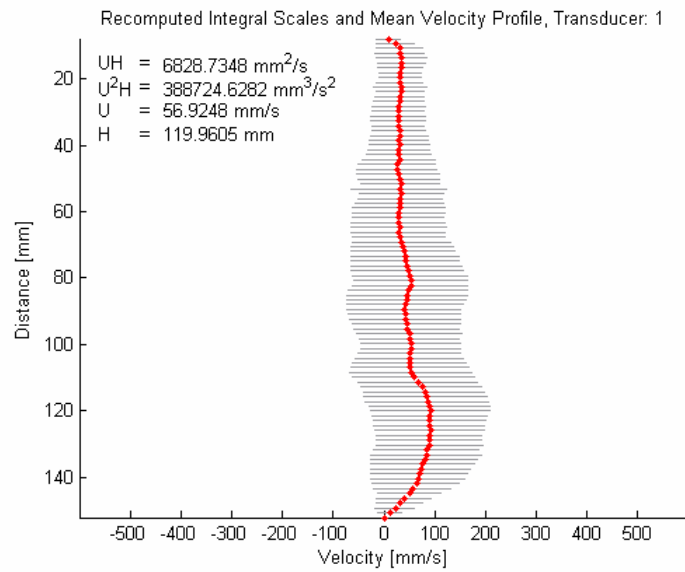|	
Channel number of the bottom	269
Registered distance for bottom channel	381.68 mm
First profile considered	115 originally 814 at 116.653 s
Last profile considered	437 originally 3062 at 438.942 s
Percentage of the maximum velocity for aliasing filtering	90%
Maximum grade for mean profile adjustment	7
Threshold number for polynomial coefficients (*S*)	4
Total number of profiles considered	243
Initial time selected to recompute the mean profile [s]	260

9.3.7 *Velocity measurements transducer 7*

Table 9.23 Resume of the values used in the data processing for transducer 7

Channel number of the bottom	276
Registered distance for bottom channel	391.41 mm
First profile considered	153 originally 1089 at 156.163 s
Last profile considered	381 originally 2685 at 385.03 s
Percentage of the maximum velocity for aliasing filtering	90%
Maximum grade for mean profile adjustment	7
Threshold number for polynomial coefficients (*S*)	4
Total number of profiles considered	190
Initial time selected to recompute the mean profile [s]	275
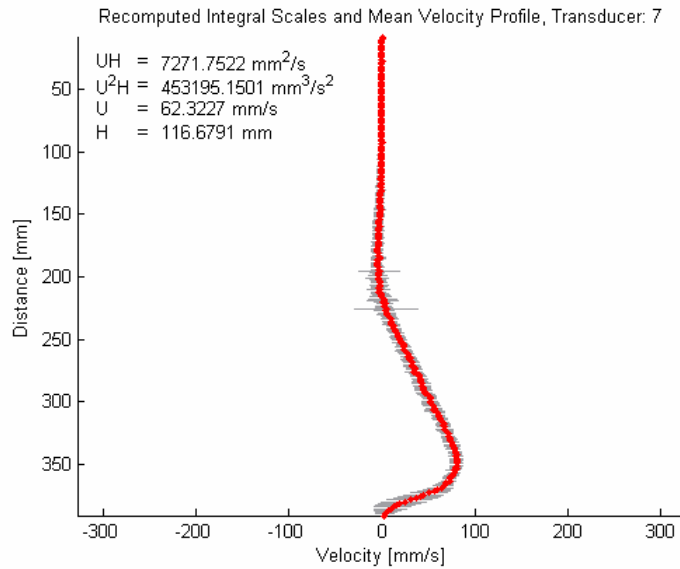
Figure 9.29 Mean velocity profile for transducer 7 after noise and aliasing filtering

9.4   Experiment 2007.02.16

Discharge [%]	26.9
Discharge [l/s]	1.05
Volumetric fine sediment concentration [%]	0.2
Number of transducers	7
Maximum Depth	549.82 mm
Total number of channels	360
Profiles measured in each transducer per cycle	3
Estimated total cycle time [s]	3
Total number of measured profiles	3360

Table 9.24 Description of the position and distance to the bottom for each transducer

Transducer n°	1	2	3	4	5	6	7
Longitudinal location [m]	8.4	8.0	7.0	6.0	5.0	3.0	1.0
Transducer angle [°]	10	10	20	20	20	20	20
Bottom distance [mm]	153	273	356	366	382	409	440
Projected bottom distance [mm]	151	269	335	344	359	384	413

9.4.1 *Velocity measurements transducer 1*

Recomputed Integral Scales and Mean Velocity Profile, Transducer: 1

UH = 6828.7348 mm²/s
U²H = 388724.6282 mm³/s²
U   = 56.9248 mm/s
H   = 119.9605 mm

Figure 9.30 Mean velocity profile for transducer 1 after noise and aliasing filtering

Table 9.25 Resume of the values used in the data processing for transducer 1

Channel number of the bottom	99
Registered distance for bottom channel	152.22 mm
First profile considered	12 originally 84 at 12.045 s
Last profile considered	479 originally 3341 at 478.95 s
Percentage of the maximum velocity for aliasing filtering	90%
Maximum grade for mean profile adjustment	7
Threshold number for polynomial coefficients (*S*)	4
Total number of profiles considered	326
Initial time selected to recompute the mean profile [s]	250

9.4.2 *Velocity measurements transducer 2*

Table 9.26 Resume of the values used in the data processing for transducer 2

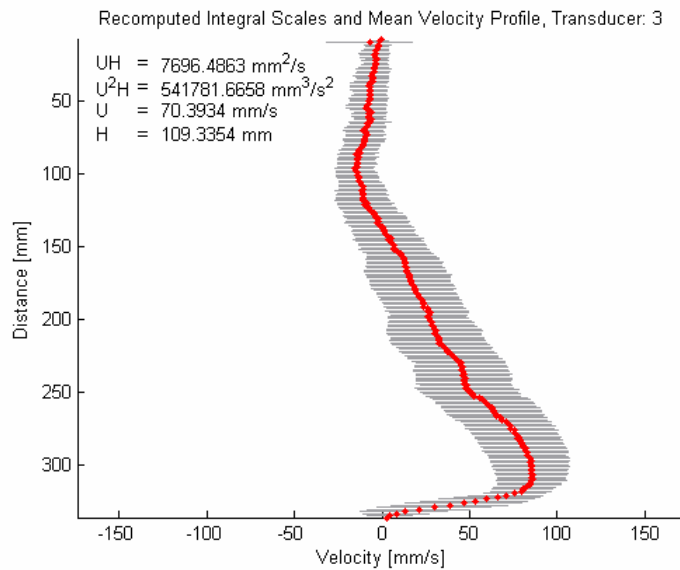|	
Channel number of the bottom	178
Registered distance for bottom channel	267.365 mm
First profile considered	24 originally 171 at 24.521 s
Last profile considered	479 originally 3344 at 479.38 s
Percentage of the maximum velocity for aliasing filtering	90%
Maximum grade for mean profile adjustment	7
Threshold number for polynomial coefficients (*S*)	4
Total number of profiles considered	313
Initial time selected to recompute the mean profile [s]	230
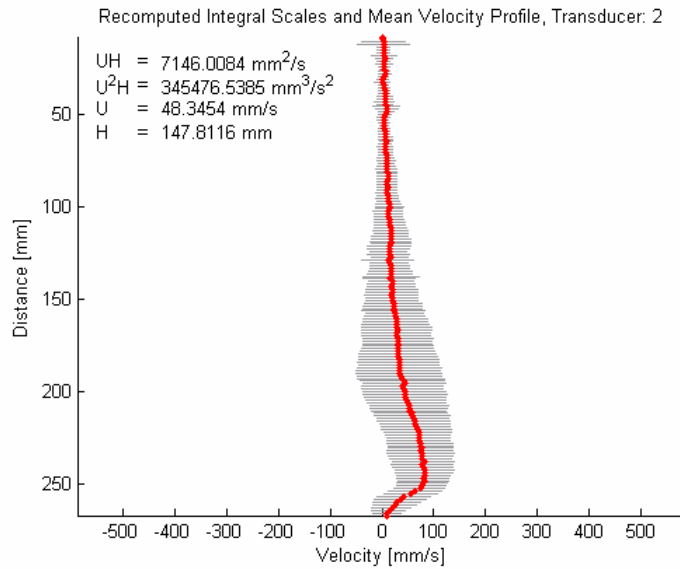
Figure 9.31 Mean velocity profile for transducer 2 after noise and aliasing filtering
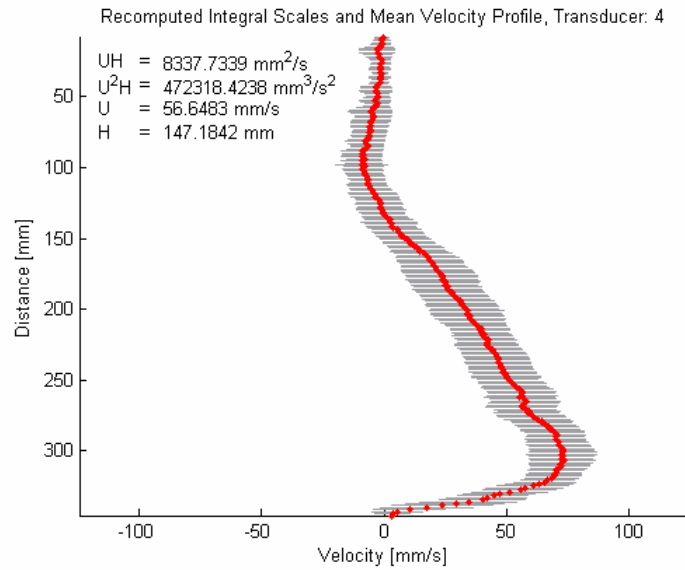
9.4.3 _Velocity measurements transducer 3_

Figure 9.32 Mean velocity profile for transducer 3 after noise and aliasing filtering

Table 9.27 Resume of the values used in the data processing for transducer 3

Channel number of the bottom	236
Registered distance for bottom channel	335.78 mm
First profile considered	42 originally 300 at 43.02 s
Last profile considered	479 originally 3347 at 479.84 s
Percentage of the maximum velocity for aliasing filtering	90%
Maximum grade for mean profile adjustment	7
Threshold number for polynomial coefficients (*S*)	4
Total number of profiles considered	294
Initial time selected to recompute the mean profile [s]	275

9.4.4 _Velocity measurements transducer 4_

Recomputed Integral Scales and Mean Velocity Profile, Transducer: 4

UH = 8337.7339 mm²/s
U²H = 472318.4238 mm³/s²
U = 56.6483 mm/s
H = 147.1842 mm

Figure 9.33 Mean velocity profile for transducer 4 after noise and aliasing filtering

Table 9.28 Resume of the values used in the data processing for transducer 4

Channel number of the bottom	243
Registered distance for bottom channel	345.515 mm
First profile considered	66 originally 471 at 67.541 s
Last profile considered	479 originally 3350 at 480.241 s
Percentage of the maximum velocity for aliasing filtering	90%
Maximum grade for mean profile adjustment	7
Threshold number for polynomial coefficients (_S_)	4
Total number of profiles considered	278
Initial time selected to recompute the mean profile [s]	250

9.4.5 _Velocity measurements transducer 5_

Table 9.29 Resume of the values used in the data processing for transducer 5

|	
Channel number of the bottom	255
Registered distance for bottom channel	362.204 mm
First profile considered	84 originally 600 at 86.04 s
Last profile considered	479 originally 3353 at 480.671 s
Percentage of the maximum velocity for aliasing filtering	90%
Maximum grade for mean profile adjustment	7
Threshold number for polynomial coefficients (_S_)	4
Total number of profiles considered	282
Initial time selected to recompute the mean profile [s]	275
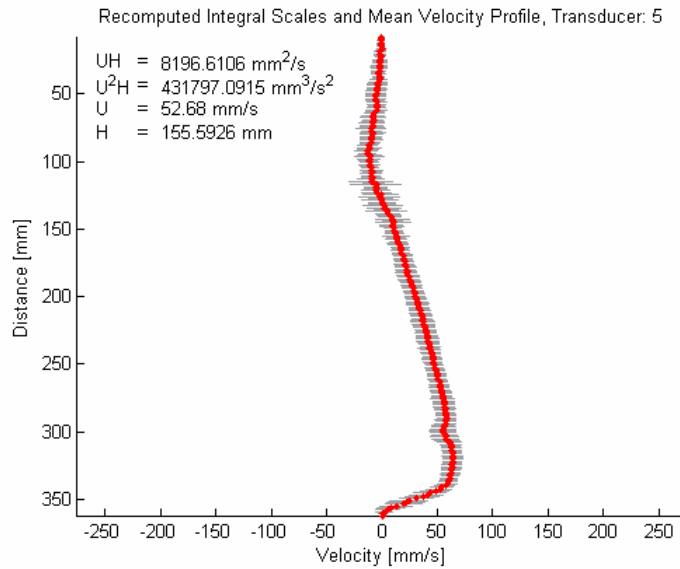
Figure 9.34 Mean velocity profile for transducer 5 after noise and aliasing filtering
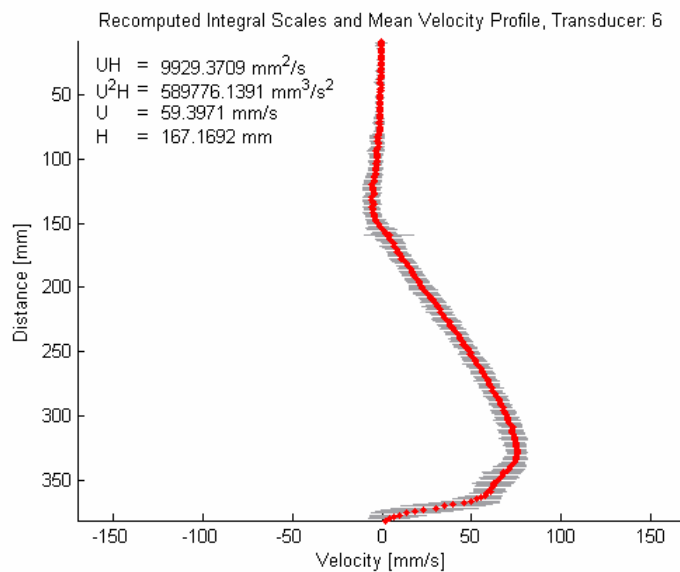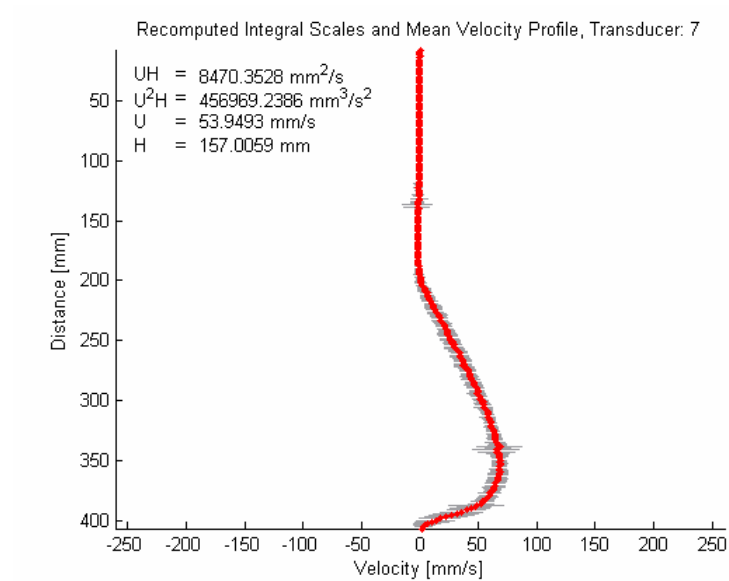
Velocity measurements transducer 6

Figure 9.35 Mean velocity profile for transducer 6 after noise and aliasing filtering

Table 9.30 Resume of the values used in the data processing for transducer 6

Channel number of the bottom	269
Registered distance for bottom channel	381.675 mm
First profile considered	129 originally 918 at 131.641 s
Last profile considered	479 originally 3356 at 481.101 s
Percentage of the maximum velocity for aliasing filtering	90%
Maximum grade for mean profile adjustment	7
Threshold number for polynomial coefficients (*S*)	4
Total number of profiles considered	276
Initial time selected to recompute the mean profile [s]	275

9.4.6 *Velocity measurements transducer 7*

Figure 9.36 Mean velocity profile for transducer 7 after noise and aliasing filtering

Table 9.31 Resume of the values used in the data processing for transducer 7

Channel number of the bottom	287
Registered distance for bottom channel	406.708 mm
First profile considered	170 originally 1196 at 171.356 s
Last profile considered	440 originally 3086 at 442.383s
Percentage of the maximum velocity for aliasing filtering	90%
Maximum grade for mean profile adjustment	7
Threshold number for polynomial coefficients (*S*)	4
Total number of profiles considered	230
Initial time selected to recompute the mean profile [s]	300

9.5   Experiment 2007.02.27

Discharge [%]	38.8
Discharge [l/s]	1.51
Volumetric fine sediment concentration [%]	0.2
Number of transducers	7
Maximum Depth	549.82 mm
Total number of channels	360
Profiles measured in each transducer per cycle	3
Estimated total cycle time [s]	3
Total number of measured profiles	4620

Table 9.32 Description of the position and distance to the bottom for each transducer

Transducer n°	1	2	3	4	5	6	7
Longitudinal location [m]	8.4	8.0	7.0	6.0	5.0	3.0	1.0
Transducer angle [º]	10	10	20	20	20	20	20
Bottom distance [mm]	148	274	343	370	373	413	448
Projected bottom distance [mm]	146	270	322	348	351	388	421

In this experiment the integral scales will also be computed considering only the region of the velocity profile which shows positive mean velocities. This is done in order to exclude the reversal flow commonly present at the turbidity current interface. Both computations, with and without this criterion, are shown through figures.

The mean velocity profiles shown in the figures are the ones that are computed with data comprised between the initial time selected to recompute the mean profile and the last profile considered in the analysis.

The channel where the positive mean velocity region starts will be included in the table. The values of the integral scales that will be stored in the file T#_scal2.dat, where the symbol # describe the number of the transducer, are those obtained considering only the region with positive mean velocity values.

9.5.1 *Velocity measurements transducer 1*

Recomputed Integral Scales and Mean Velocity Profile, Transducer: 1

$UH = 9287.6691\ mm^2/s$
$U^2H = 639074.2267\ mm^3/s^2$
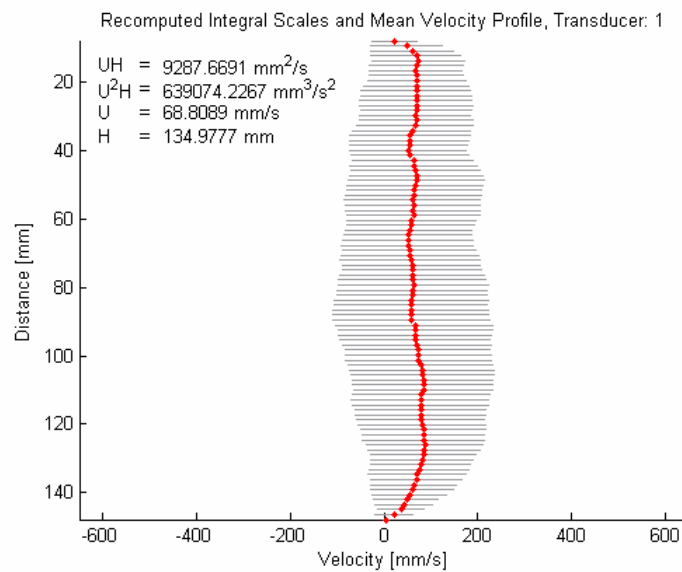$U = 68.8089\ mm/s$
$H = 134.9777\ mm$

Figure 9.37 Mean velocity profile for transducer 1 after noise and aliasing filtering

Table 9.33 Resume of the values used in the data processing for transducer 1

Channel number of the bottom	96
Registered distance for bottom channel	147.849 mm
First profile considered	12 originally 84 at 12.046 s
Last profile considered	516 originally 3612 at 517.961 s
Percentage of the maximum velocity for aliasing filtering	90%
Maximum grade for mean profile adjustment	7
Threshold number for polynomial coefficients (*S*)	4
Total number of profiles considered	385
Initial time selected to recompute the mean profile [s]	200
Upper channel defining positive mean velocity region	0

9.5.2 *Velocity measurements transducer 2*

Table 9.34 Resume of the values used in the data processing for transducer 2

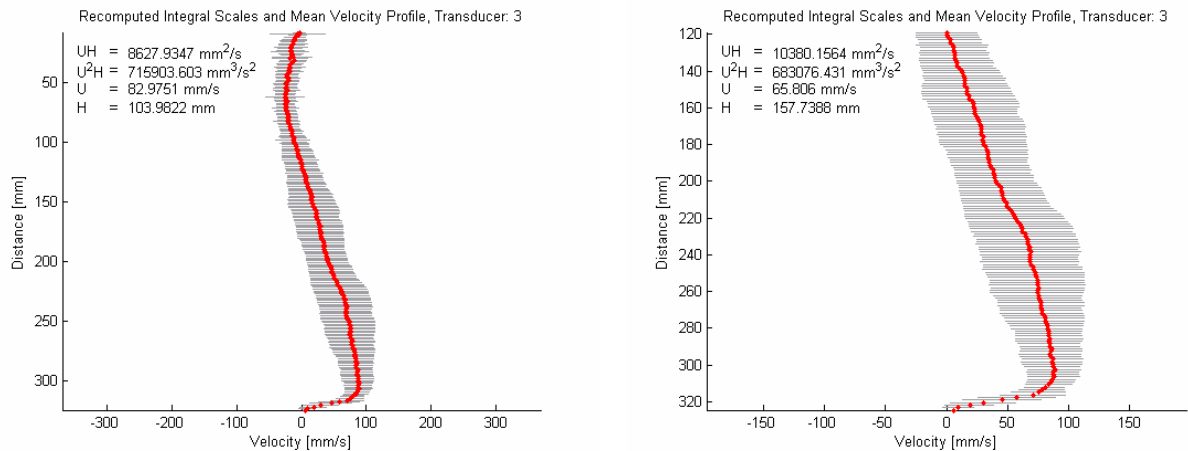|	
Channel number of the bottom	182
Registered distance for bottom channel	273.195 mm
First profile considered	12 originally 87 at 12.476 s
Last profile considered	514 originally 3595 at 514.449 s
Percentage of the maximum velocity for aliasing filtering	90%
Maximum grade for mean profile adjustment	7
Threshold number for polynomial coefficients (*S*)	4
Total number of profiles considered	364
Initial time selected to recompute the mean profile [s]	220
Upper channel defining positive mean velocity region	0
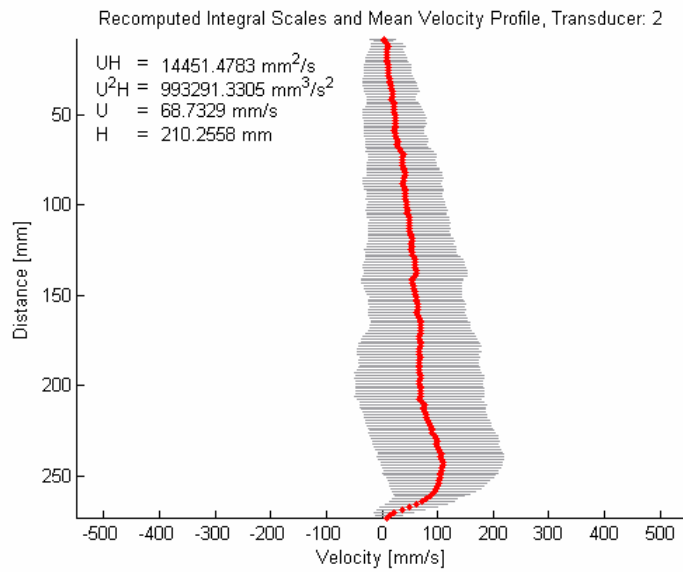
Figure 9.38 Mean velocity profile for transducer 2 after noise and aliasing filtering

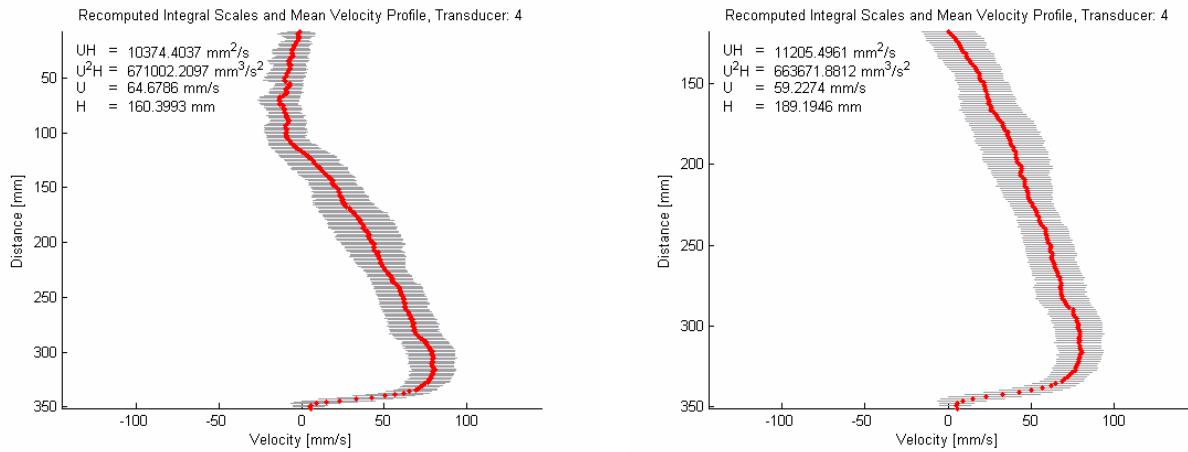## 9.5.3 *Velocity measurements transducer 3*

Figure 9.39 Mean velocity profile for transducer 3 after noise and aliasing filtering

Table 9.35 Resume of the values used in the data processing for transducer 3

Channel number of the bottom	228
Registered distance for bottom channel	324.654 mm
First profile considered	33 originally 237 at 33.986 s
Last profile considered	530 originally 3704 at 531.004 s
Percentage of the maximum velocity for aliasing filtering	90%
Maximum grade for mean profile adjustment	7
Threshold number for polynomial coefficients (*S*)	4
Total number of profiles considered	349
Initial time selected to recompute the mean profile [s]	300
Upper channel defining positive mean velocity region	80

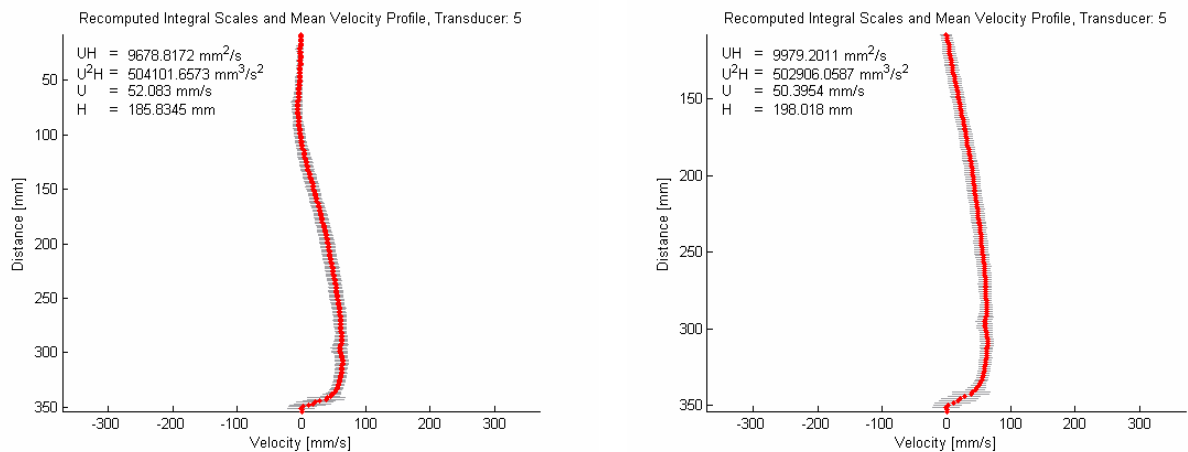### 9.5.4 Velocity measurements transducer 4

Figure 9.40 Mean velocity profile for transducer 4 after noise and aliasing filtering

Table 9.36 Resume of the values used in the data processing for transducer 4

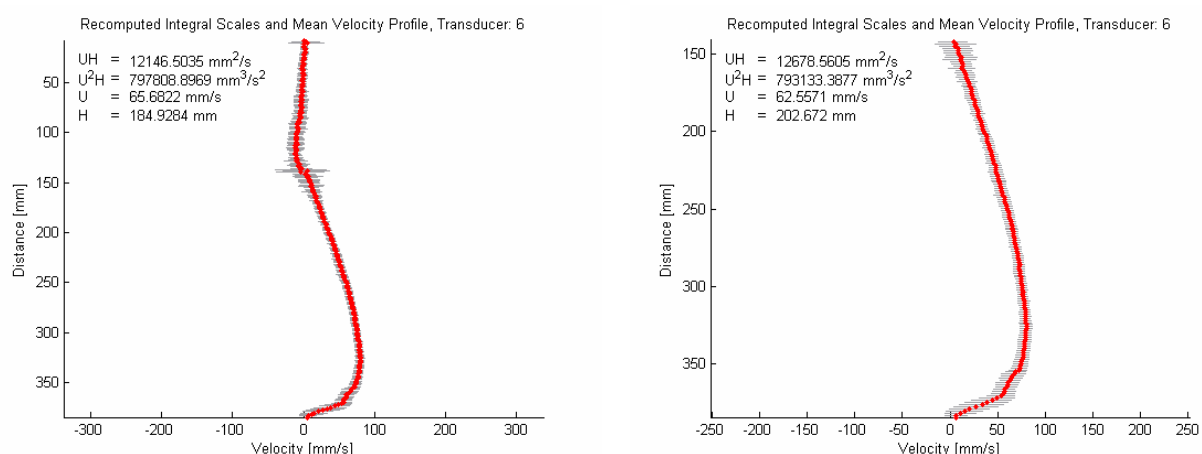|	
Channel number of the bottom	247
Registered distance for bottom channel	351.078 mm
First profile considered	54 originally 387 at 55.496 s
Last profile considered	528 originally 3705 at 531.298 s
Percentage of the maximum velocity for aliasing filtering	90%
Maximum grade for mean profile adjustment	7
Threshold number for polynomial coefficients (S)	4
Total number of profiles considered	325
Initial time selected to recompute the mean profile [s]	340
Upper channel defining positive mean velocity region	79

9.5.5 Velocity measurements transducer 5

Figure 9.41 Mean velocity profile for transducer 5 after noise and aliasing filtering

Table 9.37 Resume of the values used in the data processing for transducer 5

Channel number of the bottom	249
Registered distance for bottom channel	353.860 mm
First profile considered	75 originally 537 at 77.006 s
Last profile considered	517 originally 3625 at 519.751 s
Percentage of the maximum velocity for aliasing filtering	90%
Maximum grade for mean profile adjustment	7
Threshold number for polynomial coefficients (*S*)	4
Total number of profiles considered	333
Initial time selected to recompute the mean profile [s]	250
Upper channel defining positive mean velocity region	72

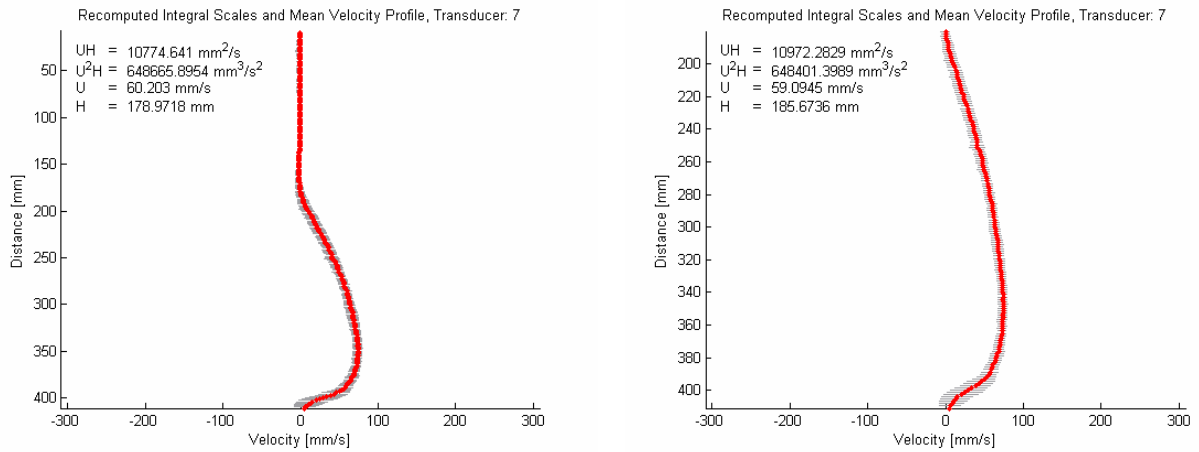### 9.5.6 *Velocity measurements transducer 6*

Figure 9.42 Mean velocity profile for transducer 6 after noise and aliasing filtering

Table 9.38 Resume of the values used in the data processing for transducer 6

Channel number of the bottom	271
Registered distance for bottom channel	384.456 mm
First profile considered	111 originally 792 at 113.573 s
Last profile considered	449 originally 3146 at 450.987 s
Percentage of the maximum velocity for aliasing filtering	90%
Maximum grade for mean profile adjustment	7
Threshold number for polynomial coefficients (*S*)	4
Total number of profiles considered	281
Initial time selected to recompute the mean profile [s]	300
Upper channel defining positive mean velocity region	96

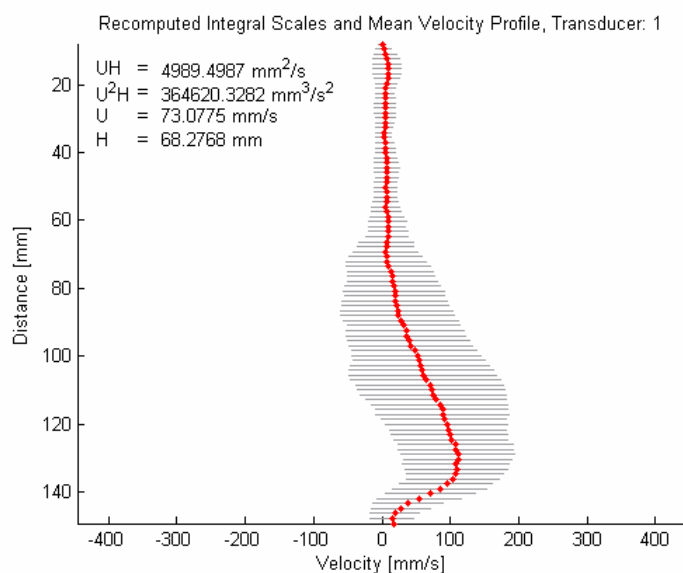### 9.5.7 *Velocity measurements transducer 7*

Figure 9.43 Mean velocity profile for transducer 7 after noise and aliasing filtering

Table 9.39 Resume of the values used in the data processing for transducer 7

Channel number of the bottom	290
Registered distance for bottom channel	410.880 mm
First profile considered	150 originally 1068 at 153.151 s
Last profile considered	398 originally 2792 at 400.223 s
Percentage of the maximum velocity for aliasing filtering	90%
Maximum grade for mean profile adjustment	7
Threshold number for polynomial coefficients (S)	4
Total number of profiles considered	217
Initial time selected to recompute the mean profile [s]	260
Upper channel defining positive mean velocity region	124

9.6   Experiment 2007.03.01

Discharge [%]	26.6
Discharge [l/s]	1.03
Volumetric fine sediment concentration [%]	0.5
Number of transducers	7
Maximum Depth	549.82 mm
Total number of channels	360
Profiles measured in each transducer per cycle	3
Estimated total cycle time [s]	3
Total number of measured profiles	4620

Table 9.40 Description of the position and distance to the bottom for each transducer

Transducer nº	1	2	3	4	5	6	7
Longitudinal location [m]	8.4	8.0	7.0	6.0	5.0	3.0	1.0
Transducer angle [º]	10	10	20	20	20	20	20
Bottom distance [mm]	151	268	357	37	373	416	448
Projected bottom distance [mm]	149	264	335	35	351	391	421

9.6.1   *Velocity measurements transducer 1*

Recomputed Integral Scales and Mean Velocity Profile, Transducer: 1

$UH = 4989.4987$ mm^2/s
$U^2H = 364620.3282$ mm^3/s^2
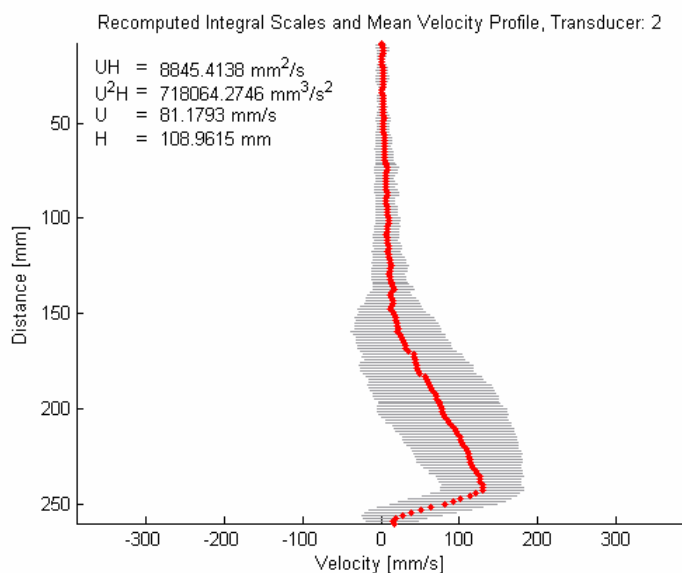$U = 73.0775$ mm/s
$H = 68.2768$ mm

Figure 9.44 Mean velocity profile for transducer 1 after noise and aliasing filtering

Table 9.41 Resume of the values used in the data processing for transducer 1

Channel number of the bottom	97
Registered distance for bottom channel	149.307 mm
First profile considered	9 originally 63 at 9.034s
Last profile considered	557 originally 3887 at 557.25 s
Percentage of the maximum velocity for aliasing filtering	90%
Maximum grade for mean profile adjustment	7
Threshold number for polynomial coefficients (*S*)	4
Total number of profiles considered	391
Initial time selected to recompute the mean profile [s]	250
Upper channel defining positive mean velocity region	0

9.6.2 *Velocity measurements transducer 2*

Recomputed Integral Scales and Mean Velocity Profile, Transducer: 2

UH = 8845.4138 mm^2/s
U^2H = 718064.2746 mm^3/s^2
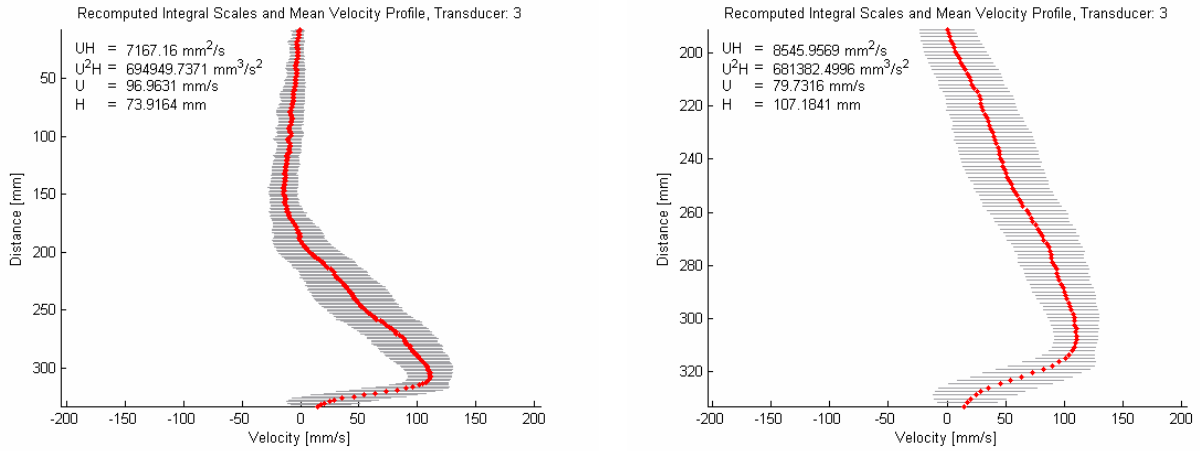U = 81.1793 mm/s
H = 108.9615 mm

Figure 9.45 Mean velocity profile for transducer 2 after noise and aliasing filtering

Table 9.42 Resume of the values used in the data processing for transducer 2

Channel number of the bottom	173
Registered distance for bottom channel	260.078 mm
First profile considered	18 originally 129 at 18.498 s
Last profile considered	557 originally 3890 at 557.68 s
Percentage of the maximum velocity for aliasing filtering	90%
Maximum grade for mean profile adjustment	7
Threshold number for polynomial coefficients (*S*)	4
Total number of profiles considered	377
Initial time selected to recompute the mean profile [s]	200
Upper channel defining positive mean velocity region	0

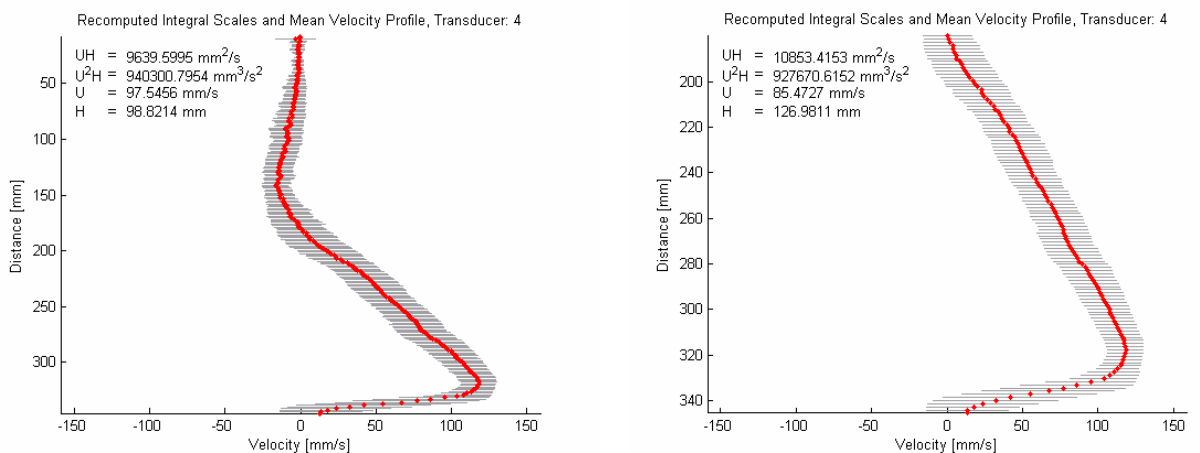## 9.6.3 *Velocity measurements transducer 3*

Figure 9.46 Mean velocity profile for transducer 3 after noise and aliasing filtering

Table 9.43 Resume of the values used in the data processing for transducer 3

Channel number of the bottom	234
Registered distance for bottom channel	332.999 mm
First profile considered	30 originally 216 at 30.974 s
Last profile considered	589 originally 4123 at 591.168 s
Percentage of the maximum velocity for aliasing filtering	90%
Maximum grade for mean profile adjustment	7
Threshold number for polynomial coefficients (*S*)	4
Total number of profiles considered	383
Initial time selected to recompute the mean profile [s]	250
Upper channel defining positive mean velocity region	132

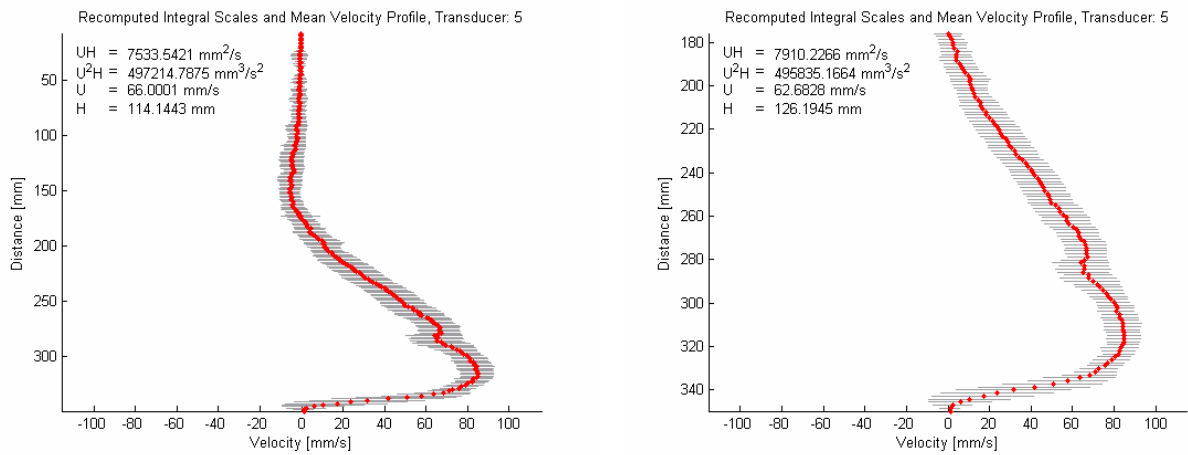## 9.6.4 *Velocity measurements transducer 4*

Figure 9.47 Mean velocity profile for transducer 4 after noise and aliasing filtering

Table 9.44 Resume of the values used in the data processing for transducer 4

Channel number of the bottom	243
Registered distance for bottom channel	345.515 mm
First profile considered	48 originally 345 at 49.473 s
Last profile considered	507 originally 3558 at 510.221 s
Percentage of the maximum velocity for aliasing filtering	90%
Maximum grade for mean profile adjustment	7
Threshold number for polynomial coefficients (*S*)	4
Total number of profiles considered	342
Initial time selected to recompute the mean profile [s]	200
Upper channel defining positive mean velocity region	124

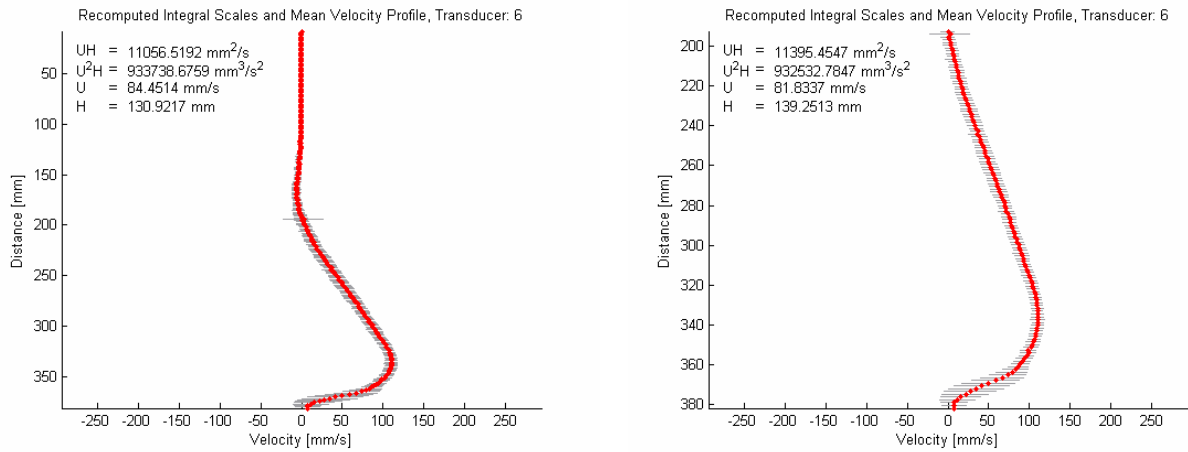### 9.6.5 *Velocity measurements transducer 5*

Figure 9.48 Mean velocity profile for transducer 5 after noise and aliasing filtering

Table 9.45 Resume of the values used in the data processing for transducer 5

Channel number of the bottom	246
Registered distance for bottom channel	349.688 mm
First profile considered	66 originally 474 at 67.972 s
Last profile considered	481 originally 3373 at 483.617 s
Percentage of the maximum velocity for aliasing filtering	90%
Maximum grade for mean profile adjustment	7
Threshold number for polynomial coefficients (*S*)	4
Total number of profiles considered	312
Initial time selected to recompute the mean profile [s]	300
Upper channel defining positive mean velocity region	121

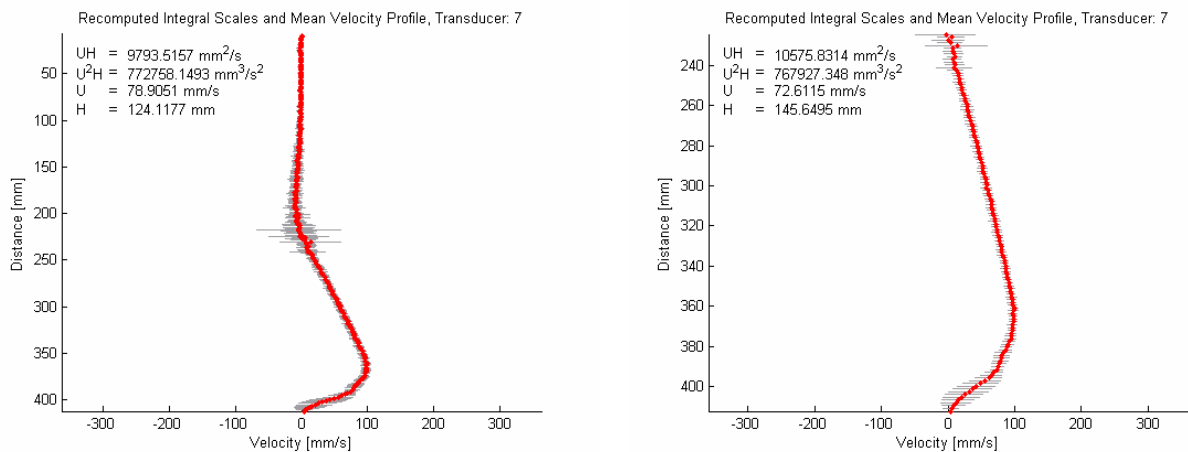### 9.6.6 Velocity measurements transducer 6

Figure 9.49 Mean velocity profile for transducer 6 after noise and aliasing filtering

Table 9.46 Resume of the values used in the data processing for transducer 6

Channel number of the bottom	269
Registered distance for bottom channel	381.675 mm
First profile considered	99 originally 708 at 101.528 s
Last profile considered	398 originally 2789 at 399.795 s
Percentage of the maximum velocity for aliasing filtering	90%
Maximum grade for mean profile adjustment	7
Threshold number for polynomial coefficients (S)	4
Total number of profiles considered	218
Initial time selected to recompute the mean profile [s]	225
Upper channel defining positive mean velocity region	133

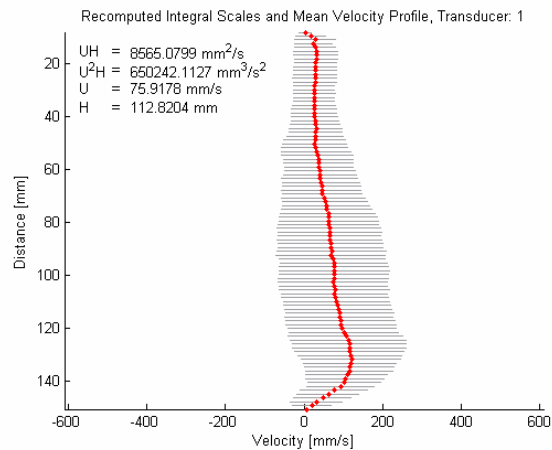### 9.6.7 Velocity measurements transducer 7

Figure 9.50 Mean velocity profile for transducer 7 after noise and aliasing filtering

Table 9.47 Resume of the values used in the data processing for transducer 7

Channel number of the bottom	291
Registered distance for bottom channel	412.271 mm
First profile considered	133 originally 943 at 135.152 s
Last profile considered	340 originally 2392 at 342.94 s
Percentage of the maximum velocity for aliasing filtering	90%
Maximum grade for mean profile adjustment	7
Threshold number for polynomial coefficients (S)	4
Total number of profiles considered	163
Initial time selected to recompute the mean profile [s]	250
Upper channel defining positive mean velocity region	156

9.7   Experiment 2007.03.05

Discharge [%]	39
Discharge [l/s]	1.52
Volumetric fine sediment concentration [%]	0.5
Number of transducers	7
Maximum Depth	549.82 mm
Total number of channels	360
Profiles measured in each transducer per cycle	3
Estimated total cycle time [s]	3
Total number of measured profiles	3360

Table 9.48 Description of the position and distance to the bottom for each transducer

Transducer n°	1	2	3	4	5	6	7
Longitudinal location [m]	8.4	8.0	7.0	6.0	5.0	3.0	1.0
Transducer angle [°]	10	10	20	20	20	20	20
Bottom distance [mm]	151	277	349	373	380	427	436
Projected bottom distance [mm]	149	273	328	351	357	401	410

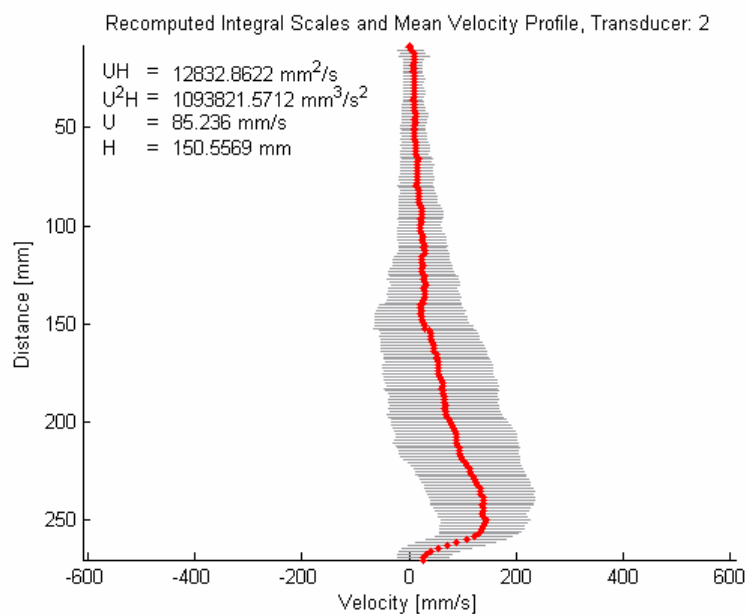### 9.7.1 *Velocity measurements transducer 1*

Figure 9.51 Mean velocity profile for transducer 1 after noise and aliasing filtering

Table 9.49 Resume of the values used in the data processing for transducer 1

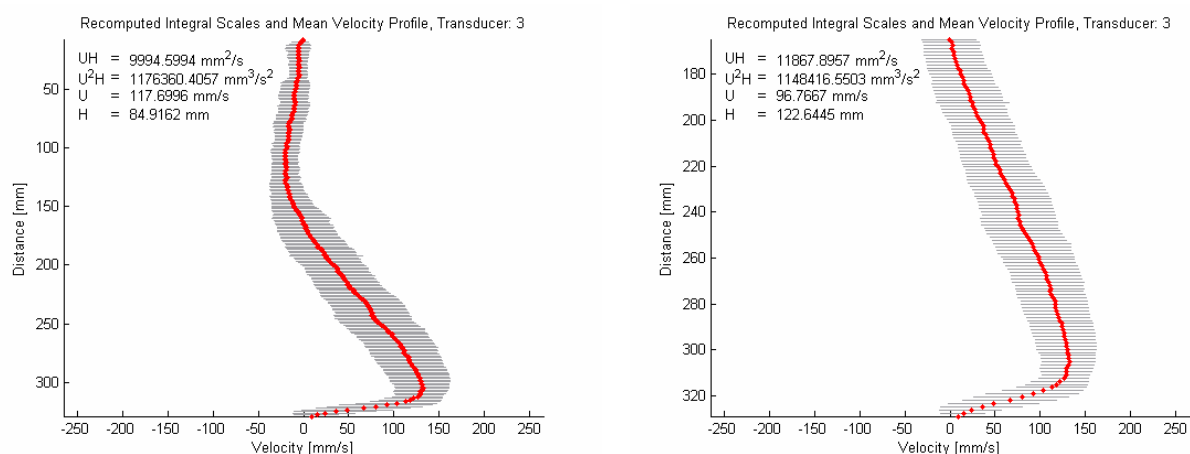|	
Channel number of the bottom	98
Registered distance for bottom channel	150.764 mm
First profile considered	6 originally 42 at 6.022 s
Last profile considered	479 originally 3341 at 478.95 s
Percentage of the maximum velocity for aliasing filtering	90%
Maximum grade for mean profile adjustment	7
Threshold number for polynomial coefficients (*S*)	4
Total number of profiles considered	355
Initial time selected to recompute the mean profile [s]	160
Upper channel defining positive mean velocity region	0

9.7.2 *Velocity measurements transducer 2*

Figure 9.52 Mean velocity profile for transducer 2 after noise and aliasing filtering

Table 9.50 Resume of the values used in the data processing for transducer 2

Channel number of the bottom	180
Registered distance for bottom channel	270.280 mm
First profile considered	12 originally 87 at 12.475 s
Last profile considered	479 originally 3344 at 479.38 s
Percentage of the maximum velocity for aliasing filtering	90%
Maximum grade for mean profile adjustment	7
Threshold number for polynomial coefficients (*S*)	4
Total number of profiles considered	317
Initial time selected to recompute the mean profile [s]	150
Upper channel defining positive mean velocity region	0

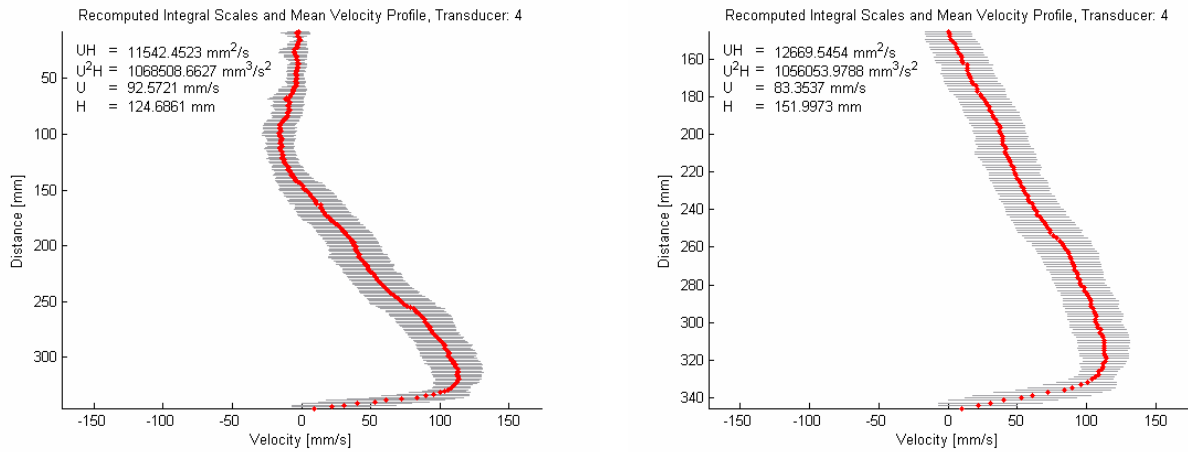### 9.7.3 *Velocity measurements transducer 3*

Figure 9.53 Mean velocity profile for transducer 3 after noise and aliasing filtering

Table 9.51 Resume of the values used in the data processing for transducer 3

Channel number of the bottom	231
Registered distance for bottom channel	328.827 mm
First profile considered	27 originally 195 at 27.963 s
Last profile considered	411 originally 2883 at 413.422 s
Percentage of the maximum velocity for aliasing filtering	90%
Maximum grade for mean profile adjustment	7
Threshold number for polynomial coefficients (*S*)	4
Total number of profiles considered	282
Initial time selected to recompute the mean profile [s]	160
Upper channel defining positive mean velocity region	113

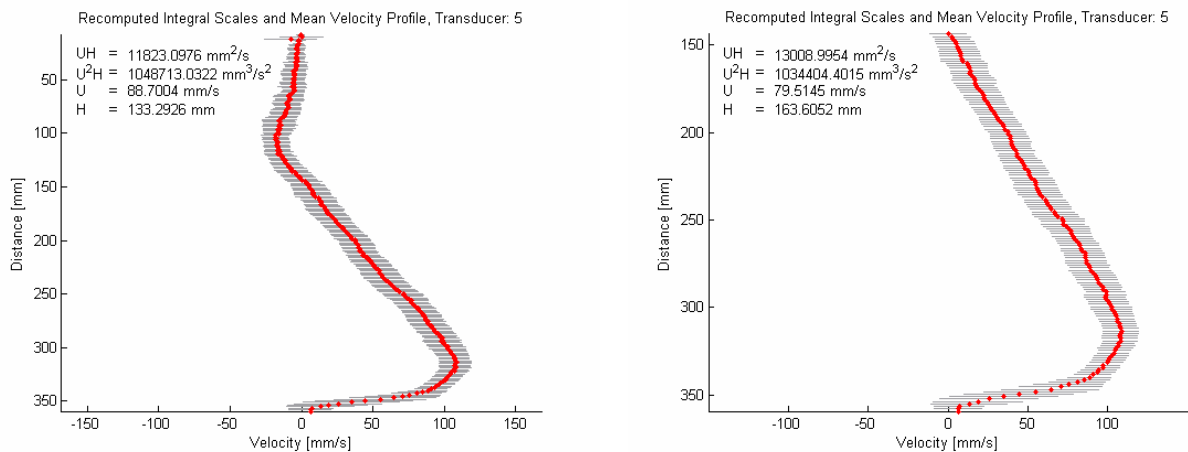## 9.7.4 *Velocity measurements transducer 4*

Figure 9.54 Mean velocity profile for transducer 4 after noise and aliasing filtering

Table 9.52 Resume of the values used in the data processing for transducer 4

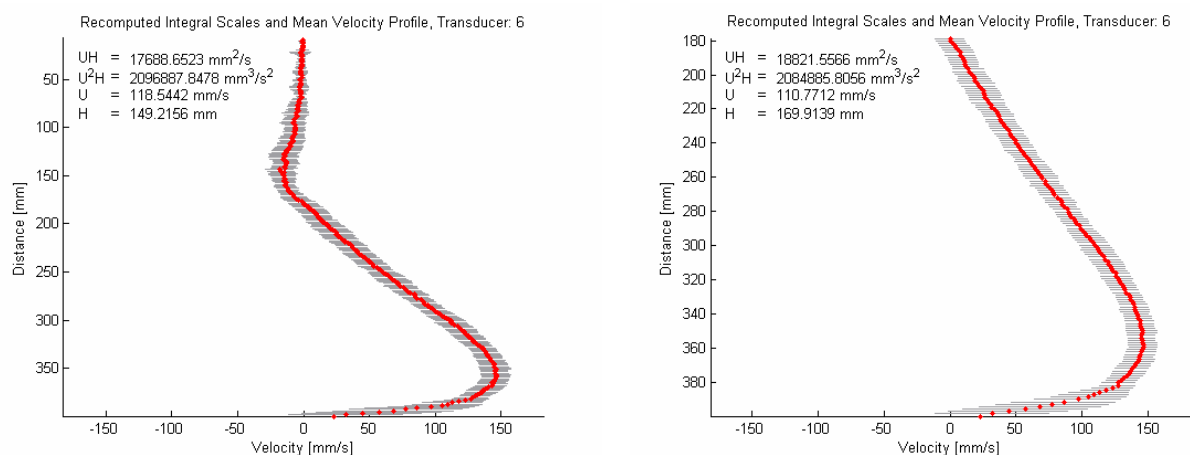|	
Channel number of the bottom	243
Registered distance for bottom channel	345.515 mm
First profile considered	39 originally 282 at 40.439 s
Last profile considered	388 originally 2917 at 389.83 s
Percentage of the maximum velocity for aliasing filtering	90%
Maximum grade for mean profile adjustment	7
Threshold number for polynomial coefficients (*S*)	4
Total number of profiles considered	241
Initial time selected to recompute the mean profile [s]	200
Upper channel defining positive mean velocity region	99

9.7.5 *Velocity measurements transducer 5*

Figure 9.55 Mean velocity profile for transducer 5 after noise and aliasing filtering

Table 9.53 Resume of the values used in the data processing for transducer 5

Channel number of the bottom	253
Registered distance for bottom channel	358.032 mm
First profile considered	55 originally 391 at 55.994 s
Last profile considered	366 originally 2574 at 369.112 s
Percentage of the maximum velocity for aliasing filtering	90%
Maximum grade for mean profile adjustment	7
Threshold number for polynomial coefficients (*S*)	4
Total number of profiles considered	219
Initial time selected to recompute the mean profile [s]	200
Upper channel defining positive mean velocity region	98

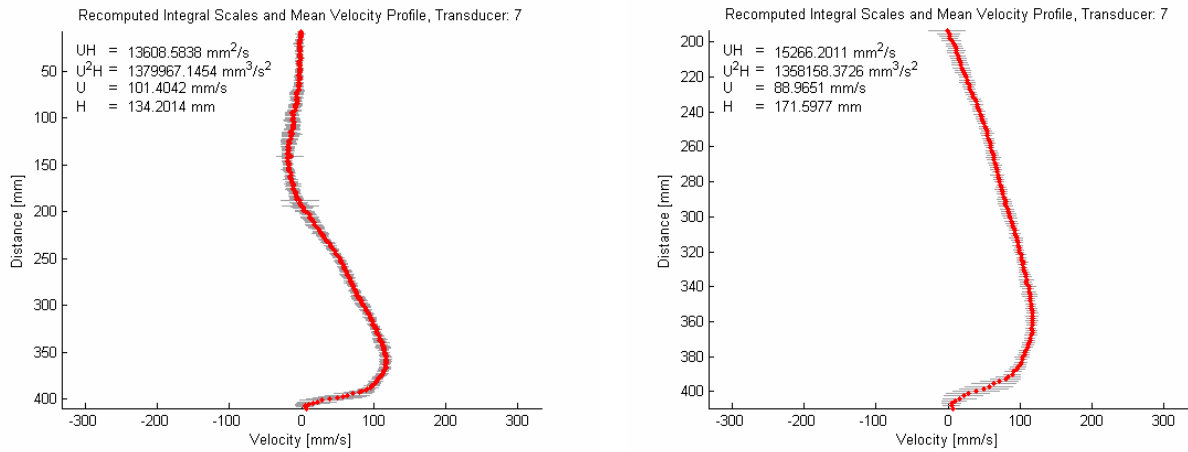## 9.7.6 *Velocity measurements transducer 6*

Figure 9.56 Mean velocity profile for transducer 6 after noise and aliasing filtering

Table 9.54 Resume of the values used in the data processing for transducer 6

Channel number of the bottom	282
Registered distance for bottom channel	399.755 mm
First profile considered	84 originally 603 at 86.47 s
Last profile considered	326 originally 2285 at 327.517 s
Percentage of the maximum velocity for aliasing filtering	90%
Maximum grade for mean profile adjustment	7
Threshold number for polynomial coefficients (*S*)	4
Total number of profiles considered	168
Initial time selected to recompute the mean profile [s]	200
Upper channel defining positive mean velocity region	123

9.7.7 Velocity measurements transducer 7

Figure 9.57 Mean velocity profile for transducer 7 after noise and aliasing filtering

Table 9.55 Resume of the values used in the data processing for transducer 7

Channel number of the bottom	289
Registered distance for bottom channel	409.490 mm
First profile considered	111 originally 795 at 114.003 s
Last profile considered	274 originally 1930 at 276.687 s
Percentage of the maximum velocity for aliasing filtering	90%
Maximum grade for mean profile adjustment	7
Threshold number for polynomial coefficients (S)	4
Total number of profiles considered	123
Initial time selected to recompute the mean profile [s]	190
Upper channel defining positive mean velocity region	134

9.8 Experiment 2007.03.07

Discharge [%]	33.3
Discharge [l/s]	1.29
Volumetric fine sediment concentration [%]	0.5
Number of transducers	7
Maximum Depth	549.82 mm
Total number of channels	360
Profiles measured in each transducer per cycle	3
Estimated total cycle time [s]	3
Total number of measured profiles	3360

Table 9.56 Description of the position and distance to the bottom for each transducer

Transducer nº	1	2	3	4	5	6	7
Longitudinal location [m]	8.4	8.0	7.0	6.0	5.0	3.0	1.0
Transducer angle [º]	10	10	20	20	20	20	20
Bottom distance [mm]	152	274	358	371	380	412	452
Projected bottom distance [mm]	150	270	336	349	357	387	425

9.8.1 *Velocity measurements transducer 1*

Recomputed Integral Scales and Mean Velocity Profile, Transducer: 1

$UH = 6739.6129$ mm^2/s
$U^2H = 575211.1862$ mm^3/s^2
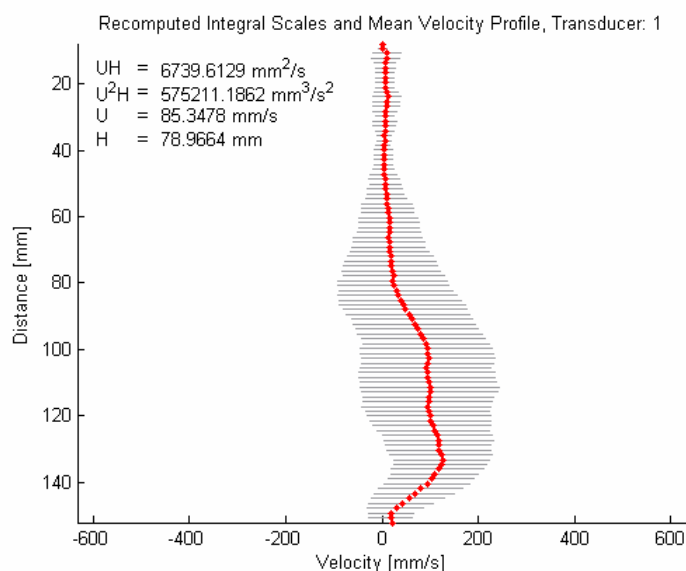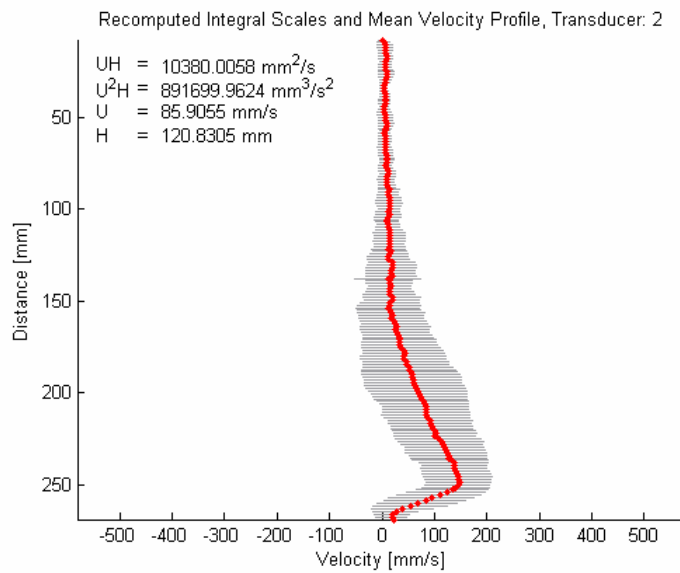$U = 85.3478$ mm/s
$H = 78.9664$ mm

Figure 9.58 Mean velocity profile for transducer 1 after noise and aliasing filtering

Table 9.57 Resume of the values used in the data processing for transducer 1

Channel number of the bottom	99
Registered distance for bottom channel	152.222 mm
First profile considered	9 originally 63 at 9.034 s
Last profile considered	479 originally 3341 at 478.95 s
Percentage of the maximum velocity for aliasing filtering	90%
Maximum grade for mean profile adjustment	7
Threshold number for polynomial coefficients (*S*)	4
Total number of profiles considered	325
Initial time selected to recompute the mean profile [s]	200
Upper channel defining positive mean velocity region	0

9.8.2 *Velocity measurements transducer 2*

Recomputed Integral Scales and Mean Velocity Profile, Transducer: 2

$UH = 10380.0058$ mm^2/s
$U^2H = 891699.9624$ mm^3/s^2
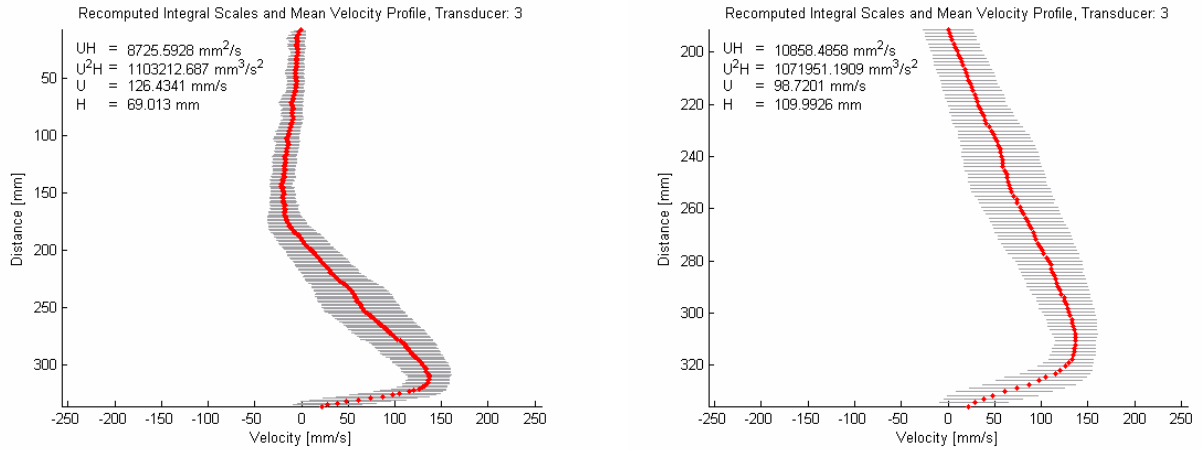$U = 85.9055$ mm/s
$H = 120.8305$ mm

Figure 9.59 Mean velocity profile for transducer 2 after noise and aliasing filtering

Table 9.58 Resume of the values used in the data processing for transducer 2

Channel number of the bottom	179
Registered distance for bottom channel	268.823 mm
First profile considered	15 originally 108 at 15.487 s
Last profile considered	479 originally 3344 at 479.381 s
Percentage of the maximum velocity for aliasing filtering	90%
Maximum grade for mean profile adjustment	7
Threshold number for polynomial coefficients (*S*)	4
Total number of profiles considered	341
Initial time selected to recompute the mean profile [s]	250
Upper channel defining positive mean velocity region	0

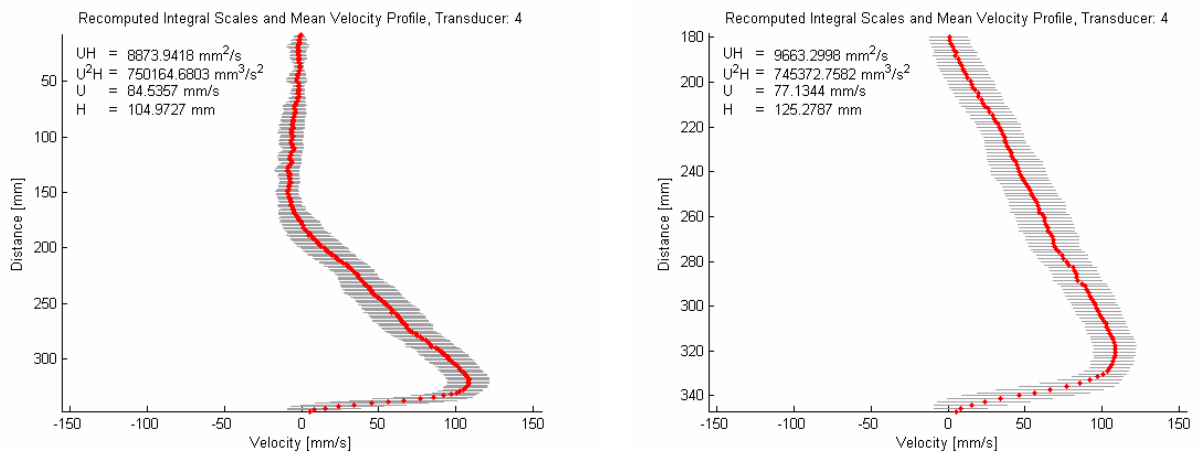## 9.8.3 Velocity measurements transducer 3

Figure 9.60 Mean velocity profile for transducer 3 after noise and aliasing filtering

Table 9.59 Resume of the values used in the data processing for transducer 3

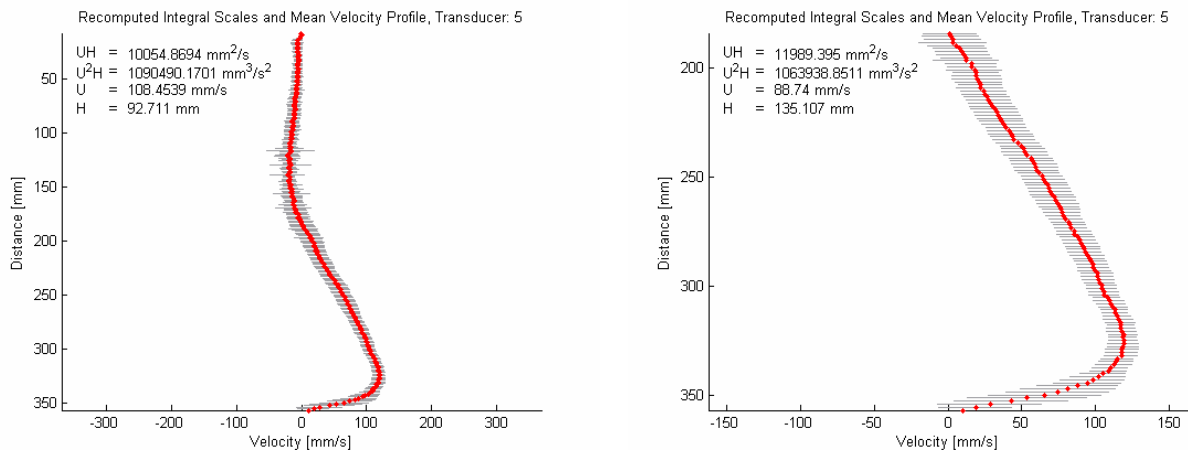|	
Channel number of the bottom	236
Registered distance for bottom channel	335.780 mm
First profile considered	30 originally 216 at 30.974 s
Last profile considered	479 originally 3347 at 479.811 s
Percentage of the maximum velocity for aliasing filtering	90%
Maximum grade for mean profile adjustment	7
Threshold number for polynomial coefficients (*S*)	4
Total number of profiles considered	332
Initial time selected to recompute the mean profile [s]	200
Upper channel defining positive mean velocity region	132

9.8.4 Velocity measurements transducer 4

Figure 9.61 Mean velocity profile for transducer 4 after noise and aliasing filtering

Table 9.60 Resume of the values used in the data processing for transducer 4

Channel number of the bottom	244
Registered distance for bottom channel	346.906 mm
First profile considered	45 originally 324 at 46.462 s
Last profile considered	455 originally 3182 at 456.15 s
Percentage of the maximum velocity for aliasing filtering	90%
Maximum grade for mean profile adjustment	7
Threshold number for polynomial coefficients (*S*)	4
Total number of profiles considered	287
Initial time selected to recompute the mean profile [s]	210
Upper channel defining positive mean velocity region	123

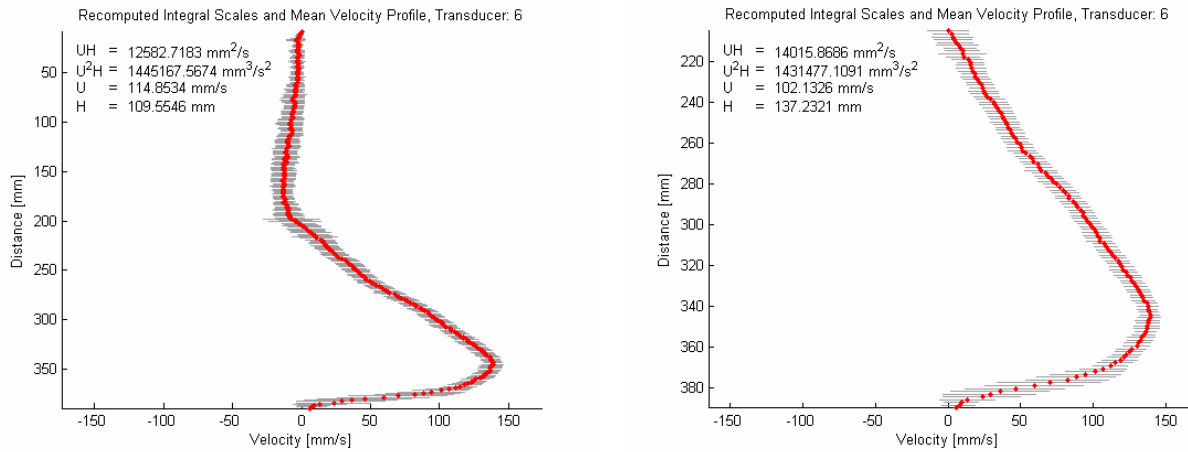### 9.8.5   *Velocity measurements transducer 5*

Figure 9.62 Mean velocity profile for transducer 5 after noise and aliasing filtering

Table 9.61 Resume of the values used in the data processing for transducer 5

Channel number of the bottom	251
Registered distance for bottom channel	356.641 mm
First profile considered	63 originally 453 at 64.96 s
Last profile considered	416 originally 2912 at 417.432 s
Percentage of the maximum velocity for aliasing filtering	90%
Maximum grade for mean profile adjustment	7
Threshold number for polynomial coefficients (*S*)	4
Total number of profiles considered	252
Initial time selected to recompute the mean profile [s]	250
Upper channel defining positive mean velocity region	127

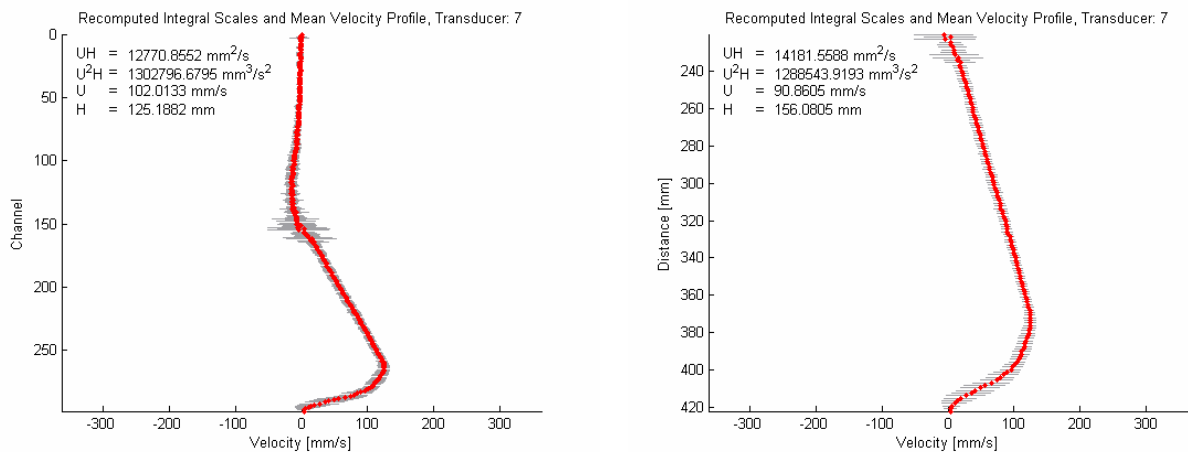## 9.8.6 *Velocity measurements transducer 6*

Figure 9.63 Mean velocity profile for transducer 6 after noise and aliasing filtering

Table 9.62 Resume of the values used in the data processing for transducer 6

Channel number of the bottom	275
Registered distance for bottom channel	390.019 mm
First profile considered	90 originally 645 at 92.493 s
Last profile considered	359 originally 2516 at 360.645 s
Percentage of the maximum velocity for aliasing filtering	90%
Maximum grade for mean profile adjustment	7
Threshold number for polynomial coefficients (*S*)	4
Total number of profiles considered	183
Initial time selected to recompute the mean profile [s]	250
Upper channel defining positive mean velocity region	142

9.8.7 *Velocity measurements transducer 7*

Figure 9.64 Mean velocity profile for transducer 7 after noise and aliasing filtering

Table 9.63 Resume of the values used in the data processing for transducer 7

Channel number of the bottom	298
Registered distance for bottom channel	422.006 mm
First profile considered	120 originally 858 at 123.037 s
Last profile considered	311 originally 2183 at 312.893 s
Percentage of the maximum velocity for aliasing filtering	90%
Maximum grade for mean profile adjustment	7
Threshold number for polynomial coefficients (S)	4
Total number of profiles considered	149
Initial time selected to recompute the mean profile [s]	200
Upper channel defining positive mean velocity region	153

9.9 Experiment 2007.03.13

Discharge [%]	33.5
Discharge [l/s]	1.3
Volumetric fine sediment concentration [%]	0.4
Number of transducers	7
Maximum Depth	549.82 mm
Total number of channels	360
Profiles measured in each transducer per cycle	3
Estimated total cycle time [s]	3
Total number of measured profiles	4158

Table 9.64 Description of the position and distance to the bottom for each transducer

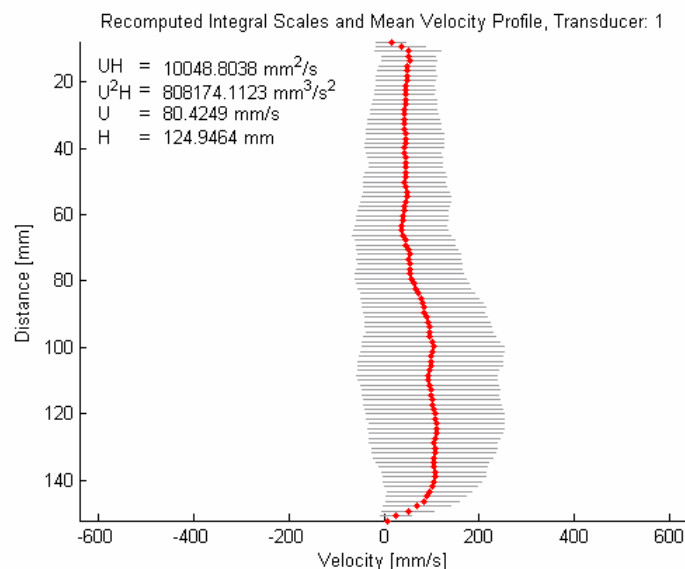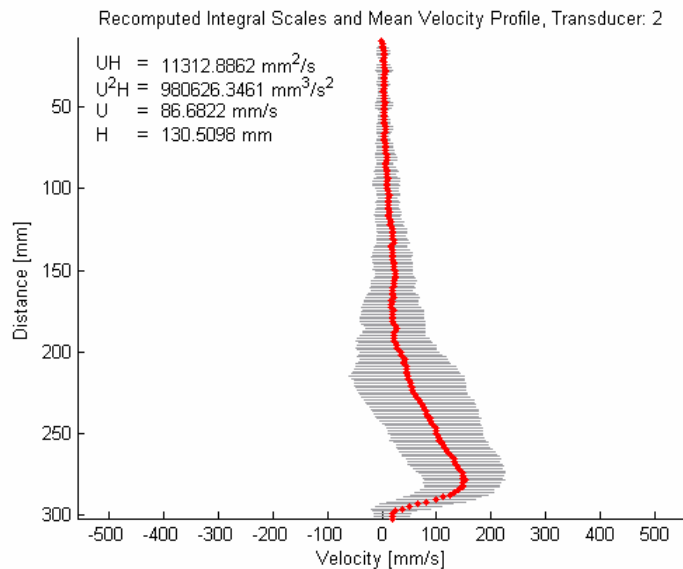| Transducer n°	1	2	3	4	5	6	7
Longitudinal location [m]	8.4	8.0	7.0	6.0	5.0	3.0	1.0
Transducer angle [°]	10	10	20	20	20	20	20
Bottom distance [mm]	152	308	389	398	416	430	452
Projected bottom distance [mm]	150	303	366	374	391	404	425

9.9.1 *Velocity measurements transducer 1*

Figure 9.65 Mean velocity profile for transducer 1 after noise and aliasing filtering

Table 9.65 Resume of the values used in the data processing for transducer 1

Channel number of the bottom	99
Registered distance for bottom channel	152.222 mm
First profile considered	12 originally 84 at 12.045 s
Last profile considered	593 originally 4139 at 593.383 s
Percentage of the maximum velocity for aliasing filtering	90%
Maximum grade for mean profile adjustment	7
Threshold number for polynomial coefficients (*S*)	4
Total number of profiles considered	432
Initial time selected to recompute the mean profile [s]	250
Upper channel defining positive mean velocity region	0

9.9.2 *Velocity measurements transducer 2*

Recomputed Integral Scales and Mean Velocity Profile, Transducer: 2

UH = 11312.8862 mm^2/s
U^{2}H = 980626.3461 mm^3/s^2
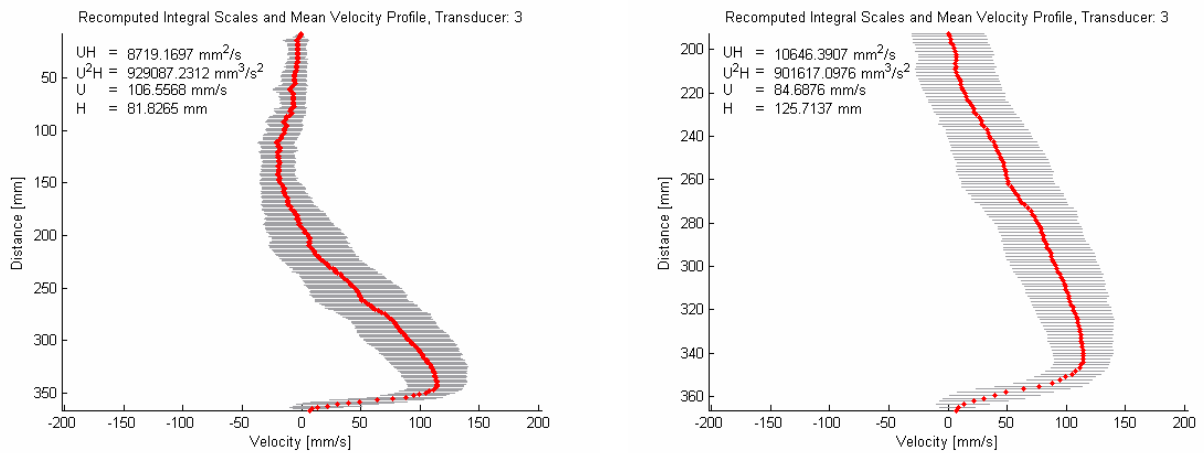U = 86.6822 mm/s
H = 130.5098 mm

Figure 9.66 Mean velocity profile for transducer 2 after noise and aliasing filtering

Table 9.66 Resume of the values used in the data processing for transducer 2

Channel number of the bottom	202
Registered distance for bottom channel	302.346 mm
First profile considered	21 originally 150 at 21.51 s
Last profile considered	520 originally 3637 at 521.471 s
Percentage of the maximum velocity for aliasing filtering	90%
Maximum grade for mean profile adjustment	7
Threshold number for polynomial coefficients (*S*)	4
Total number of profiles considered	357
Initial time selected to recompute the mean profile [s]	250
Upper channel defining positive mean velocity region	0

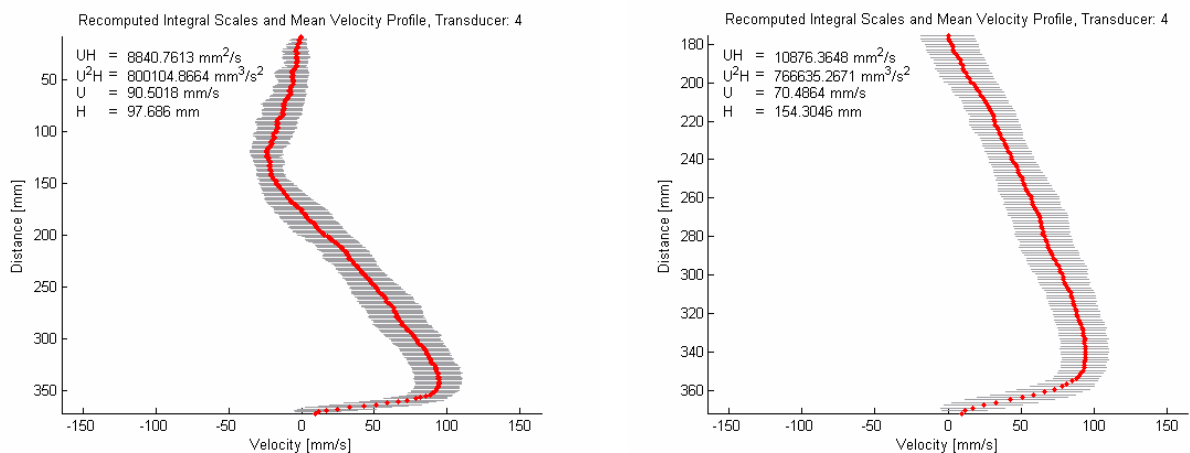### 9.9.3 *Velocity measurements transducer 3*

Figure 9.67 Mean velocity profile for transducer 3 after noise and aliasing filtering

Table 9.67 Resume of the values used in the data processing for transducer 3

Channel number of the bottom	258
Registered distance for bottom channel	366.377 mm
First profile considered	33 originally 237 at 33.986 s
Last profile considered	471 originally 3303 at 473.65 s
Percentage of the maximum velocity for aliasing filtering	90%
Maximum grade for mean profile adjustment	7
Threshold number for polynomial coefficients (*S*)	4
Total number of profiles considered	285
Initial time selected to recompute the mean profile [s]	200
Upper channel defining positive mean velocity region	133

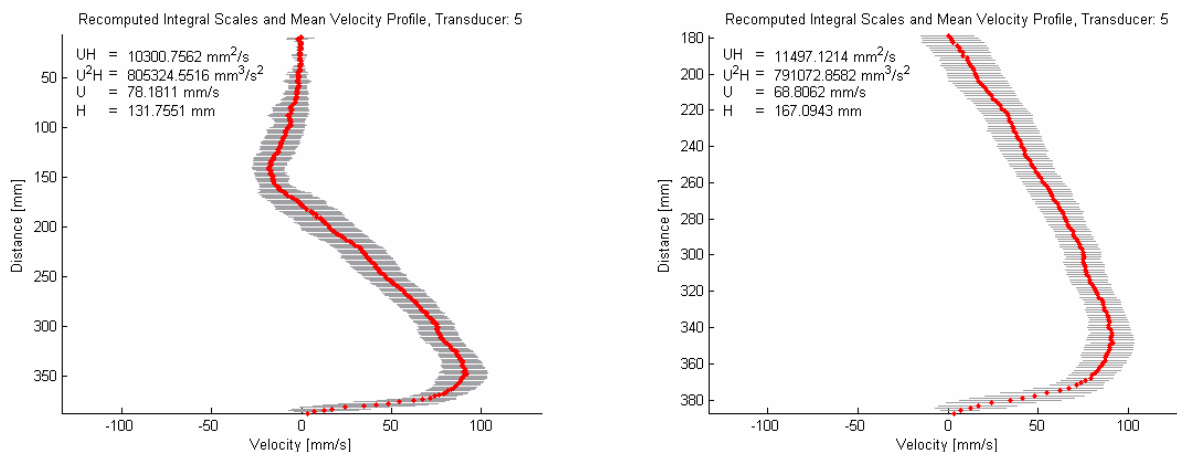### 9.9.4 *Velocity measurements transducer 4*

Figure 9.68 Mean velocity profile for transducer 4 after noise and aliasing filtering

Table 9.68 Resume of the values used in the data processing for transducer 4

Channel number of the bottom	262
Registered distance for bottom channel	371.940 mm
First profile considered	51 originally 366 at 52.484 s
Last profile considered	445 originally 3118 at 447.046 s
Percentage of the maximum velocity for aliasing filtering	90%
Maximum grade for mean profile adjustment	7
Threshold number for polynomial coefficients (*S*)	4
Total number of profiles considered	290
Initial time selected to recompute the mean profile [s]	180
Upper channel defining positive mean velocity region	121

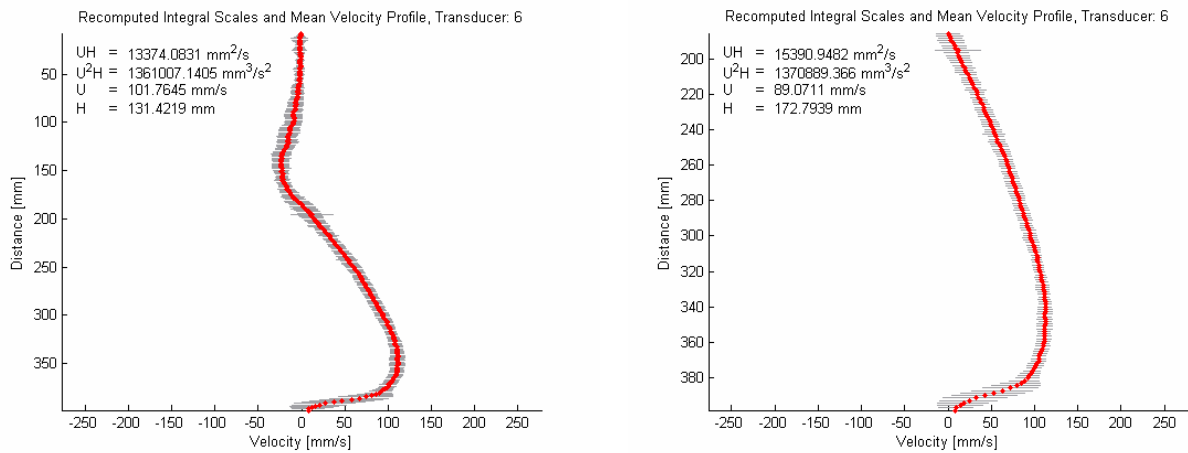## 9.9.5   *Velocity measurements transducer 5*

Figure 9.69 Mean velocity profile for transducer 5 after noise and aliasing filtering

Table 9.69 Resume of the values used in the data processing for transducer 5

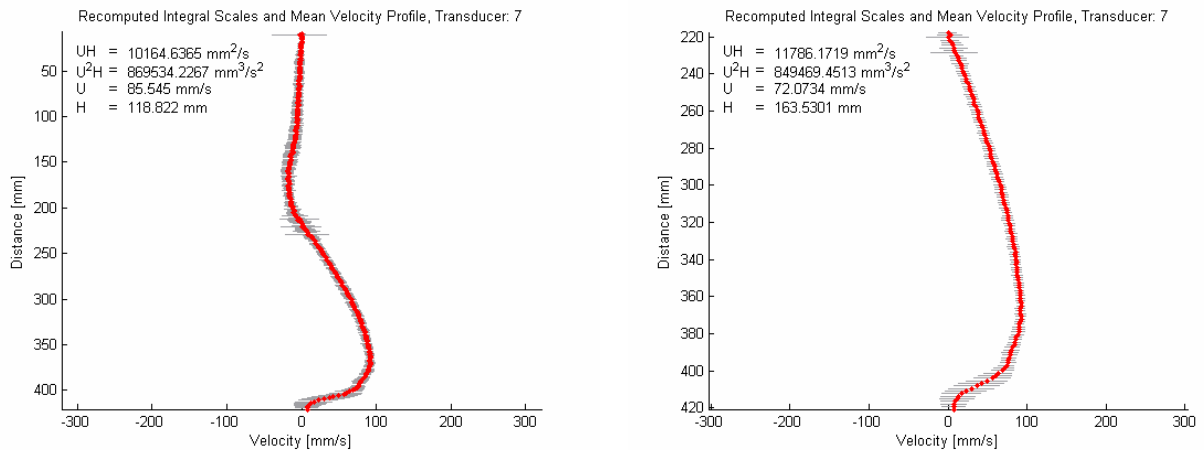| Channel number of the bottom	273
Registered distance for bottom channel	387.238 mm
First profile considered	71 originally 497 at 71.12 s
Last profile considered	416 originally 2912 at 417.431 s
Percentage of the maximum velocity for aliasing filtering	90%
Maximum grade for mean profile adjustment	7
Threshold number for polynomial coefficients (*S*)	4
Total number of profiles considered	258
Initial time selected to recompute the mean profile [s]	200
Upper channel defining positive mean velocity region	123

9.9.6 Velocity measurements transducer 6

Figure 9.70 Mean velocity profile for transducer 6 after noise and aliasing filtering

Table 9.70 Resume of the values used in the data processing for transducer 6

Channel number of the bottom	281
Registered distance for bottom channel	398.364 mm
First profile considered	102 originally 729 at 104.538 s
Last profile considered	373 originally 2620 at 375.633 s
Percentage of the maximum velocity for aliasing filtering	90%
Maximum grade for mean profile adjustment	7
Threshold number for polynomial coefficients (S)	4
Total number of profiles considered	230
Initial time selected to recompute the mean profile [s]	230
Upper channel defining positive mean velocity region	128

9.9.7 Velocity measurements transducer 7

Figure 9.71 Mean velocity profile for transducer 7 after noise and aliasing filtering

Table 9.71 Resume of the values used in the data processing for transducer 7

Channel number of the bottom	297
Registered distance for bottom channel	420.616 mm
First profile considered	129 originally 921 at 132.071 s
Last profile considered	328 originally 2308 at 330.892 s
Percentage of the maximum velocity for aliasing filtering	90%
Maximum grade for mean profile adjustment	7
Threshold number for polynomial coefficients (S)	4
Total number of profiles considered	166
Initial time selected to recompute the mean profile [s]	200
Upper channel defining positive mean velocity region	151

9.10 Experiment 2007.03.15

Discharge [%]	26.7
Discharge [l/s]	1.04
Volumetric fine sediment concentration [%]	0.3
Number of transducers	7
Maximum Depth	549.82 mm
Total number of channels	360
Profiles measured in each transducer per cycle	3
Estimated total cycle time [s]	3
Total number of measured profiles	4158

Table 9.72 Description of the position and distance to the bottom for each transducer

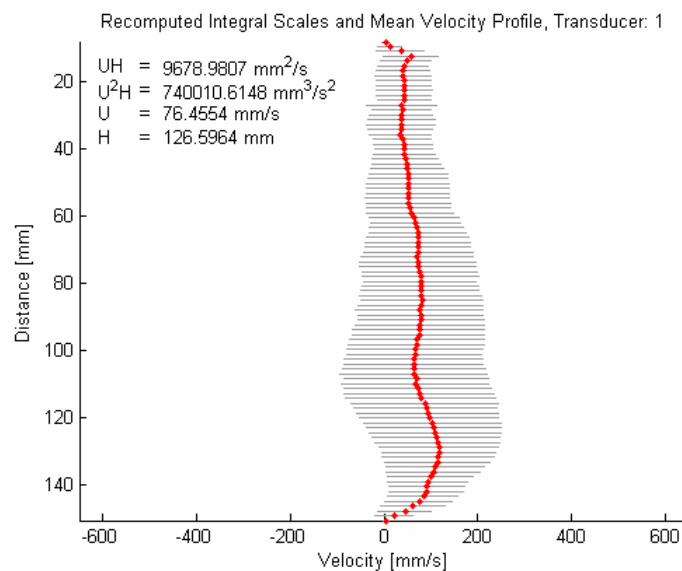| Transducer nº	1	2	3	4	5	6	7
Longitudinal location [m]	8.4	8.0	7.0	6.0	5.0	3.0	1.0
Transducer angle [º]	10	10	20	20	20	20	20
Bottom distance [mm]	151	315	383	400	416	431	447
Projected bottom distance [mm]	149	310	360	376	391	405	420

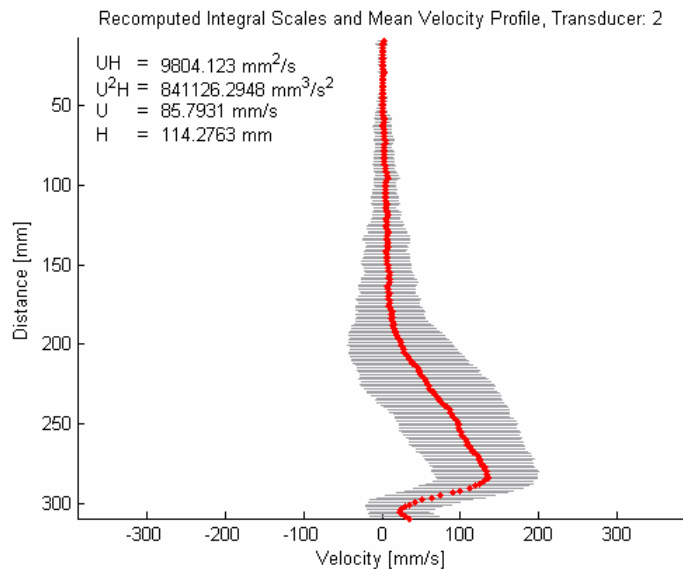## 9.10.1 *Velocity measurements transducer 1*

Figure 9.72 Mean velocity profile for transducer 1 after noise and aliasing filtering

Table 9.73 Resume of the values used in the data processing for transducer 1

Channel number of the bottom	98
Registered distance for bottom channel	150.764 mm
First profile considered	18 originally 126 at 18.068 s
Last profile considered	593 originally 4139 at 593.384 s
Percentage of the maximum velocity for aliasing filtering	90%
Maximum grade for mean profile adjustment	7
Threshold number for polynomial coefficients (*S*)	4
Total number of profiles considered	426
Initial time selected to recompute the mean profile [s]	250
Upper channel defining positive mean velocity region	0

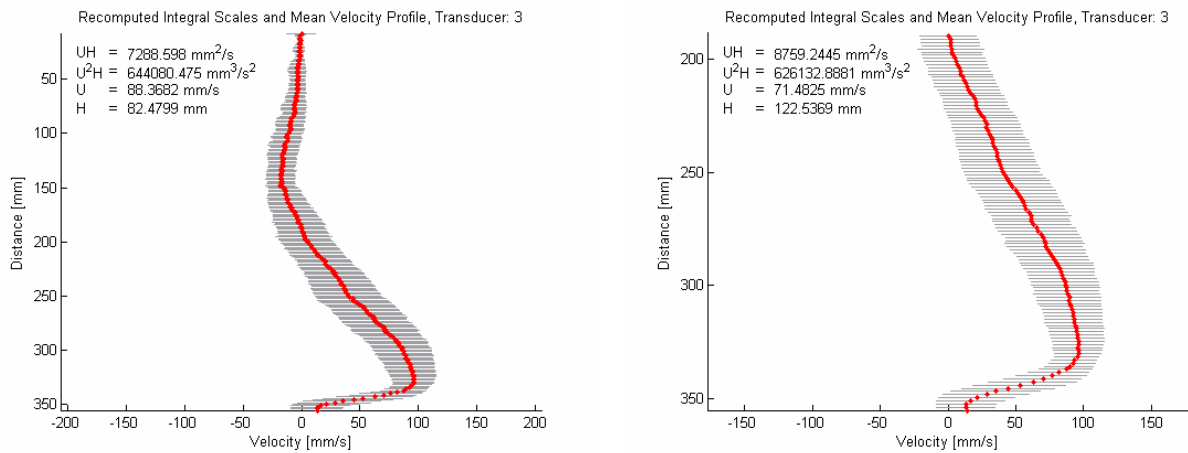## 9.10.2 *Velocity measurements transducer 2*

Figure 9.73 Mean velocity profile for transducer 2 after noise and aliasing filtering

Table 9.74 Resume of the values used in the data processing for transducer 2

Channel number of the bottom	207
Registered distance for bottom channel	309.633 mm
First profile considered	30 originally 213 at 30.544 s
Last profile considered	593 originally 4142 at 593.814 s
Percentage of the maximum velocity for aliasing filtering	90%
Maximum grade for mean profile adjustment	7
Threshold number for polynomial coefficients (*S*)	4
Total number of profiles considered	402
Initial time selected to recompute the mean profile [s]	200
Upper channel defining positive mean velocity region	0

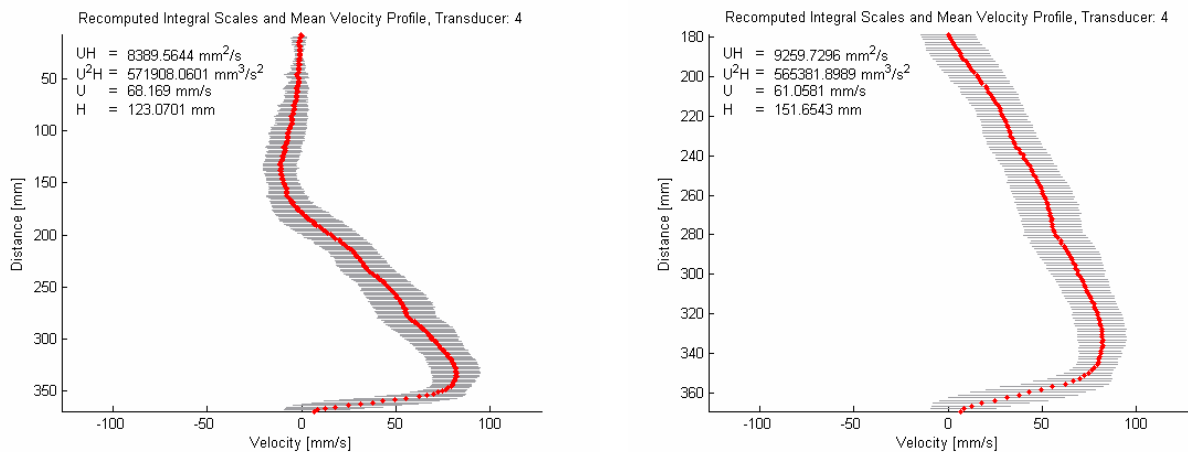### 9.10.3 _Velocity measurements transducer 3_

Figure 9.74 Mean velocity profile for transducer 3 after noise and aliasing filtering

Table 9.75 Resume of the values used in the data processing for transducer 3

Channel number of the bottom	250
Registered distance for bottom channel	355.251 mm
First profile considered	45 originally 321 at 46.031 s
Last profile considered	593 originally 4145 at 594.295 s
Percentage of the maximum velocity for aliasing filtering	90%
Maximum grade for mean profile adjustment	7
Threshold number for polynomial coefficients (S)	4
Total number of profiles considered	220
Initial time selected to recompute the mean profile [s]	383
Upper channel defining positive mean velocity region	130

9.10.4 _Velocity measurements transducer 4_

Figure 9.75 Mean velocity profile for transducer 4 after noise and aliasing filtering

Table 9.76 Resume of the values used in the data processing for transducer 4

Channel number of the bottom	260
Registered distance for bottom channel	369.158 mm
First profile considered	63 originally 450 at 64.53 s
Last profile considered	557 originally 3896 at 558.538 s
Percentage of the maximum velocity for aliasing filtering	90%
Maximum grade for mean profile adjustment	7
Threshold number for polynomial coefficients (S)	4
Total number of profiles considered	365
Initial time selected to recompute the mean profile [s]	200
Upper channel defining positive mean velocity region	123

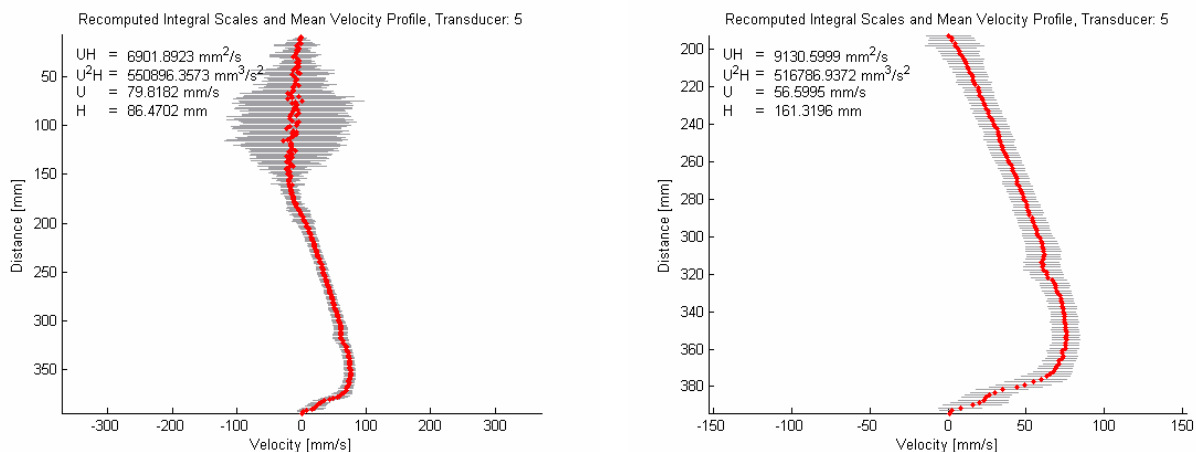## 9.10.5 *Velocity measurements transducer 5*

Figure 9.76 Mean velocity profile for transducer 5 after noise and aliasing filtering

Table 9.77 Resume of the values used in the data processing for transducer 5

Channel number of the bottom	278
Registered distance for bottom channel	394.192 mm
First profile considered	80 originally 560 at 80.154s
Last profile considered	522 originally 3666 at 525.706 s
Percentage of the maximum velocity for aliasing filtering	90%
Maximum grade for mean profile adjustment	7
Threshold number for polynomial coefficients (S)	4
Total number of profiles considered	318
Initial time selected to recompute the mean profile [s]	250
Upper channel defining positive mean velocity region	133

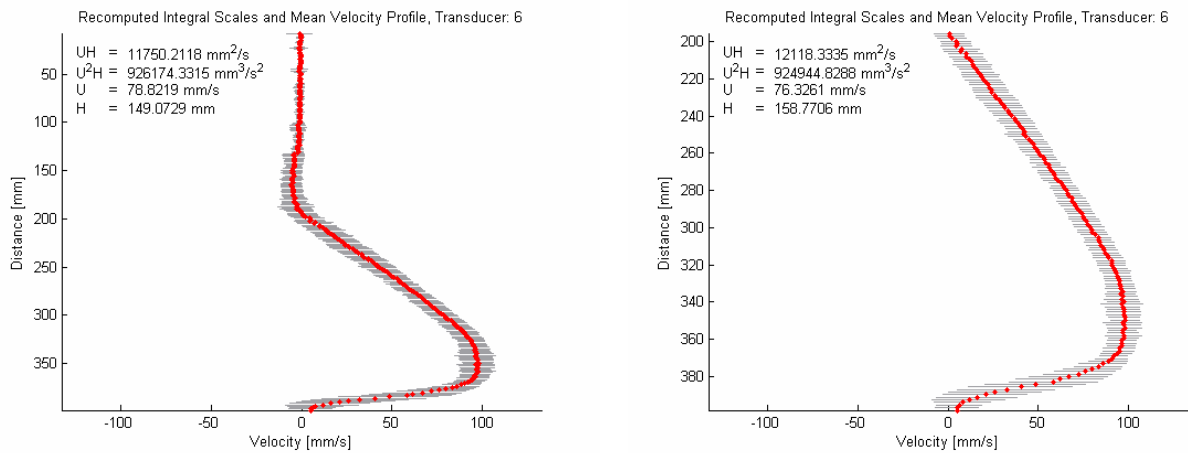### 9.10.6 *Velocity measurements transducer 6*

Figure 9.77 Mean velocity profile for transducer 6 after noise and aliasing filtering

Table 9.78 Resume of the values used in the data processing for transducer 6

Channel number of the bottom	281
Registered distance for bottom channel	398.364 mm
First profile considered	123 originally 876 at 125.619 s
Last profile considered	472 originally 3313 at 475.01 s
Percentage of the maximum velocity for aliasing filtering	90%
Maximum grade for mean profile adjustment	7
Threshold number for polynomial coefficients (*S*)	4
Total number of profiles considered	265
Initial time selected to recompute the mean profile [s]	300
Upper channel defining positive mean velocity region	135

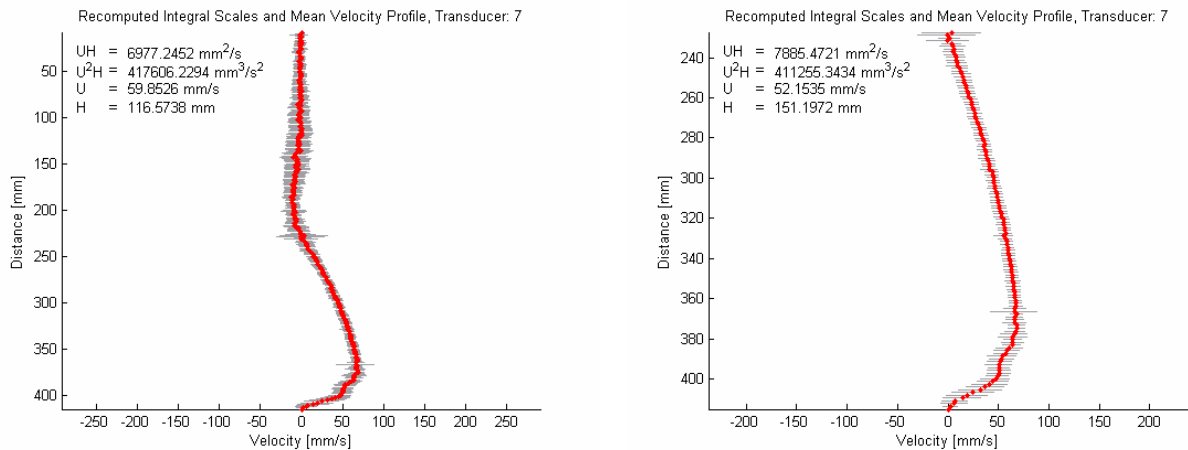### 9.10.7 *Velocity measurements transducer 7*

Figure 9.78 Mean velocity profile for transducer 7 after noise and aliasing filtering

Table 9.79 Resume of the values used in the data processing for transducer 7

Channel number of the bottom	293
Registered distance for bottom channel	415.053 mm
First profile considered	162 originally 1152 at 165.197 s
Last profile considered	409 originally 2875 at 412.201 s
Percentage of the maximum velocity for aliasing filtering	90%
Maximum grade for mean profile adjustment	7
Threshold number for polynomial coefficients (S)	4
Total number of profiles considered	227
Initial time selected to recompute the mean profile [s]	300
Upper channel defining positive mean velocity region	158

9.11   Experiment 2007.03.16

Discharge [%]	38
Discharge [l/s]	1.48
Volumetric fine sediment concentration [%]	0.55
Number of transducers	7
Maximum Depth	549.82 mm
Total number of channels	360
Profiles measured in each transducer per cycle	3
Estimated total cycle time [s]	3
Total number of measured profiles	3738

Table 9.80 Description of the position and distance to the bottom for each transducer

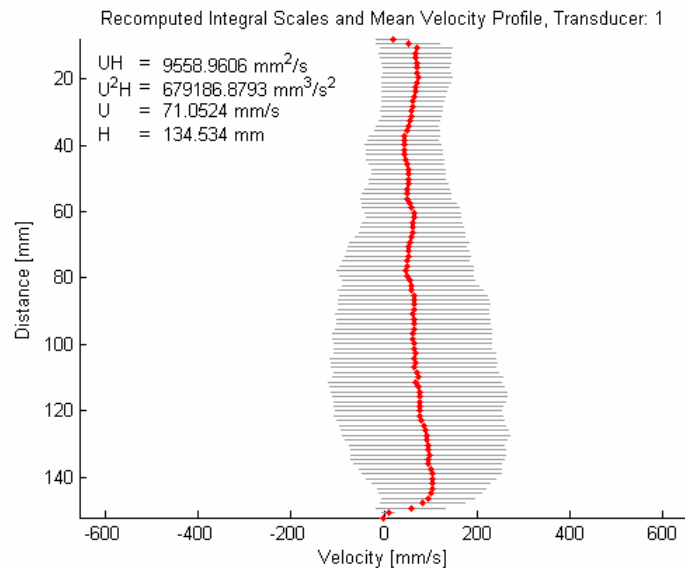| Transducer nº	1	2	3	4	5	6	7
Longitudinal location [m]	8.4	8.0	7.0	6.0	5.0	3.0	1.0
Transducer angle [º]	10	10	20	20	20	20	20
Bottom distance [mm]	152	306	390	397	406	438	460
Projected bottom distance [mm]	150	301	366	373	382	412	432

9.11.1 *Velocity measurements transducer 1*

Figure 9.79 Mean velocity profile for transducer 1 after noise and aliasing filtering

Table 9.81 Resume of the values used in the data processing for transducer 1

Channel number of the bottom	99
Registered distance for bottom channel	152.222 mm
First profile considered	15 originally 105 at 15.057 s
Last profile considered	533 originally 3719 at 533.155 s
Percentage of the maximum velocity for aliasing filtering	90%
Maximum grade for mean profile adjustment	7
Threshold number for polynomial coefficients (*S*)	4
Total number of profiles considered	369
Initial time selected to recompute the mean profile [s]	250
Upper channel defining positive mean velocity region	0

9.11.2 *Velocity measurements transducer 2*

Recomputed Integral Scales and Mean Velocity Profile, Transducer: 2

$UH = 15622.251$ mm^2/s
$U^2H = 1221391.3237$ mm^3/s^2
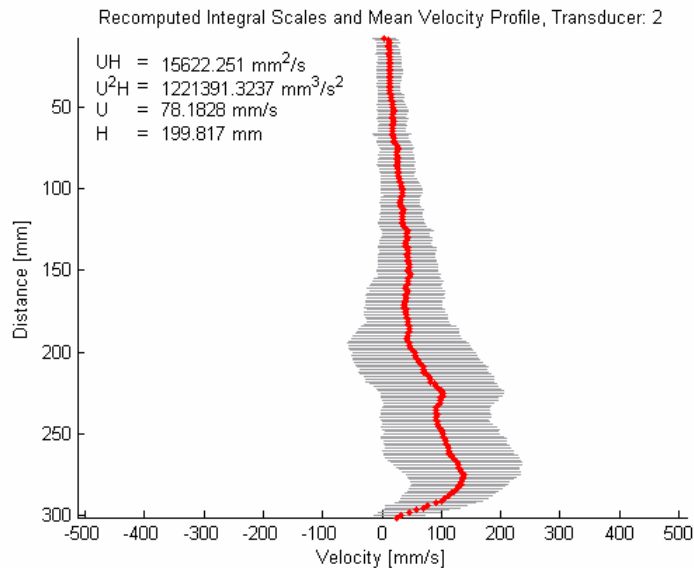$U = 78.1828$ mm/s
$H = 199.817$ mm

Figure 9.80 Mean velocity profile for transducer 2 after noise and aliasing filtering

Table 9.82 Resume of the values used in the data processing for transducer 2

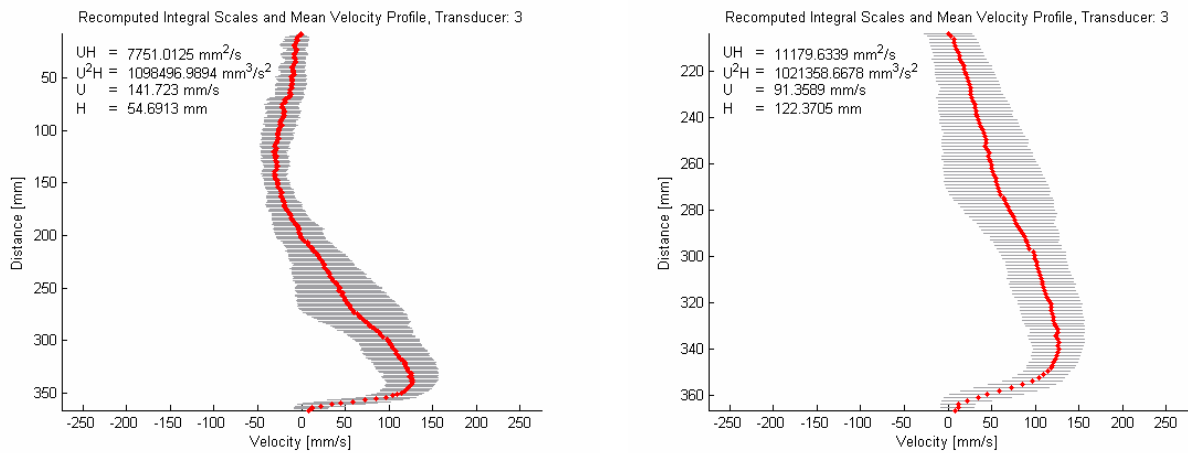|	
Channel number of the bottom	201
Registered distance for bottom channel	300.888 mm
First profile considered	24 originally 171 at 24.521 s
Last profile considered	533 originally 3722 at 533.586 s
Percentage of the maximum velocity for aliasing filtering	90%
Maximum grade for mean profile adjustment	7
Threshold number for polynomial coefficients (*S*)	4
Total number of profiles considered	339
Initial time selected to recompute the mean profile [s]	220
Upper channel defining positive mean velocity region	0

9.11.3 Velocity measurements transducer 3

Figure 9.81 Mean velocity profile for transducer 3 after noise and aliasing filtering

Table 9.83 Resume of the values used in the data processing for transducer 3

Channel number of the bottom	258
Registered distance for bottom channel	366.377 mm
First profile considered	33 originally 237 at 33.985 s
Last profile considered	415 originally 2905 at 416.502 s
Percentage of the maximum velocity for aliasing filtering	90%
Maximum grade for mean profile adjustment	7
Threshold number for polynomial coefficients (*S*)	4
Total number of profiles considered	266
Initial time selected to recompute the mean profile [s]	250
Upper channel defining positive mean velocity region	141

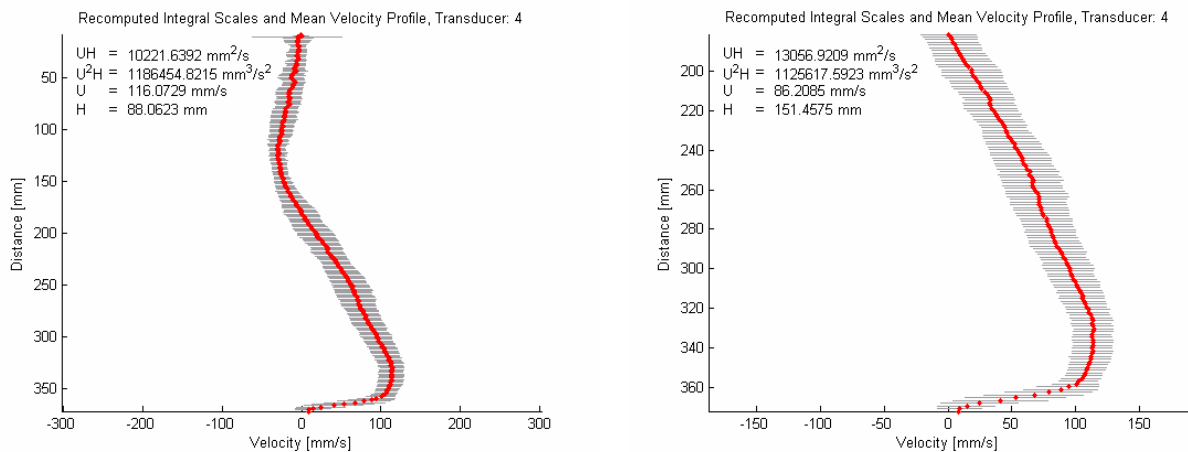## 9.11.4 Velocity measurements transducer 4

Figure 9.82 Mean velocity profile for transducer 4 after noise and aliasing filtering

Table 9.84 Resume of the values used in the data processing for transducer 4

Channel number of the bottom	262
Registered distance for bottom channel	371.940 mm
First profile considered	48 originally 345 at 49.473 s
Last profile considered	398 originally 2783 at 398.933 s
Percentage of the maximum velocity for aliasing filtering	90%
Maximum grade for mean profile adjustment	7
Threshold number for polynomial coefficients (*S*)	4
Total number of profiles considered	243
Initial time selected to recompute the mean profile [s]	200
Upper channel defining positive mean velocity region	125

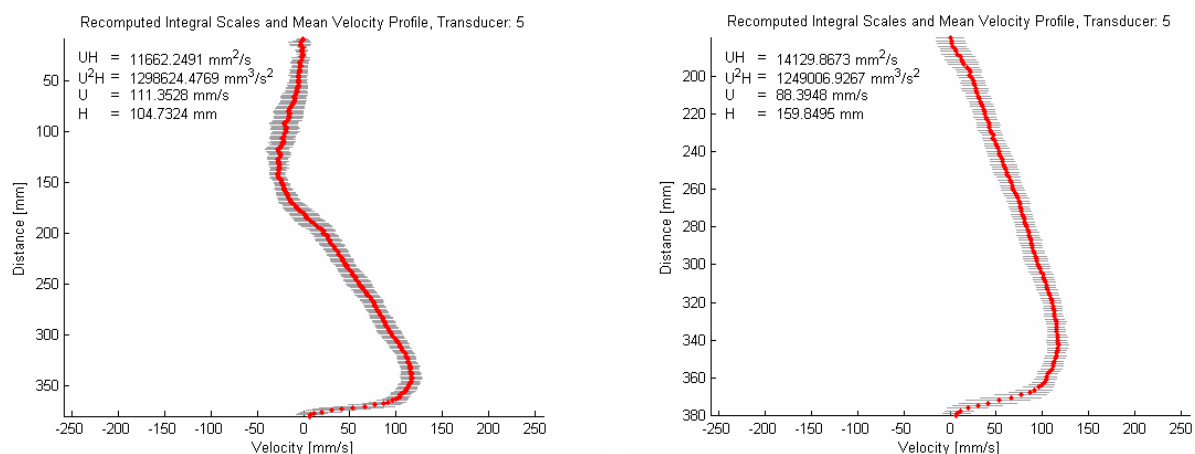## 9.11.5 *Velocity measurements transducer 5*

Figure 9.83 Mean velocity profile for transducer 5 after noise and aliasing filtering

Table 9.85 Resume of the values used in the data processing for transducer 5

Channel number of the bottom	268
Registered distance for bottom channel	380.284 mm
First profile considered	60 originally 432 at 61.949 s
Last profile considered	374 originally 2618 at 375.272 s
Percentage of the maximum velocity for aliasing filtering	90%
Maximum grade for mean profile adjustment	7
Threshold number for polynomial coefficients (*S*)	4
Total number of profiles considered	223
Initial time selected to recompute the mean profile [s]	200
Upper channel defining positive mean velocity region	124

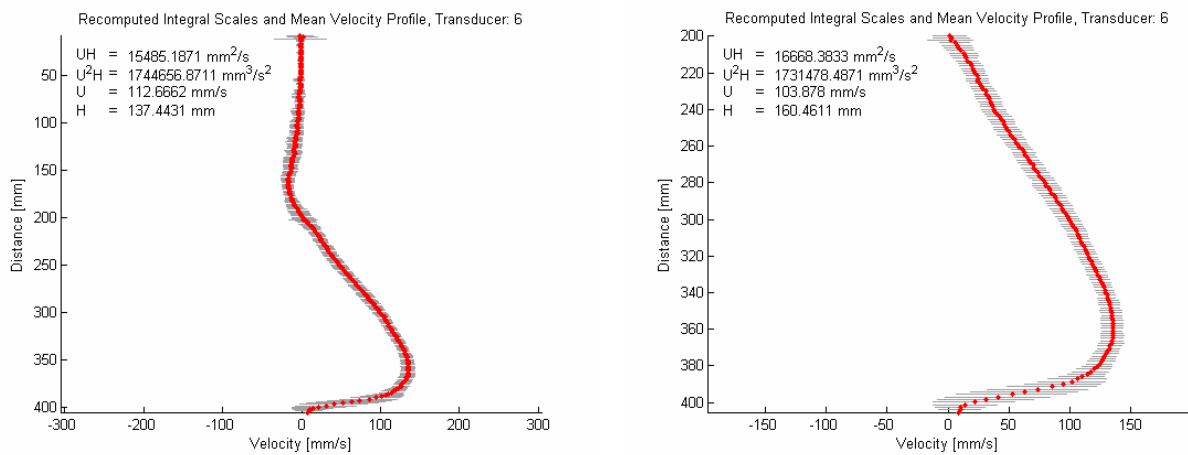### 9.11.6 *Velocity measurements transducer 6*

Figure 9.84 Mean velocity profile for transducer 6 after noise and aliasing filtering

Table 9.86 Resume of the values used in the data processing for transducer 6

Channel number of the bottom	286
Registered distance for bottom channel	405.317 mm
First profile considered	87 originally 624 at 89.481 s
Last profile considered	336 originally 2367 at 339.428 s
Percentage of the maximum velocity for aliasing filtering	90%
Maximum grade for mean profile adjustment	7
Threshold number for polynomial coefficients (S)	4
Total number of profiles considered	191
Initial time selected to recompute the mean profile [s]	190
Upper channel defining positive mean velocity region	138

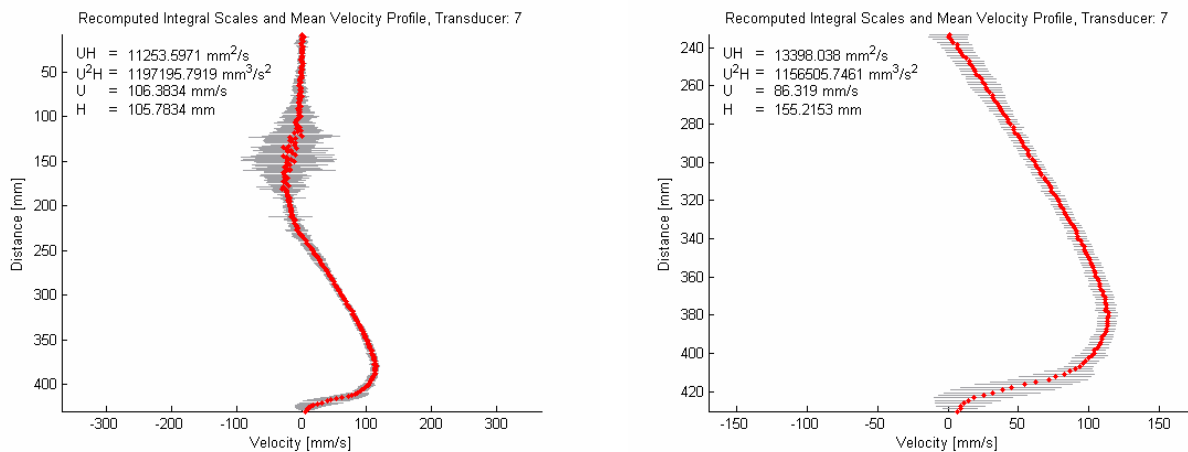### 9.11.7 *Velocity measurements transducer 7*

Figure 9.85 Mean velocity profile for transducer 7 after noise and aliasing filtering

Table 9.87 Resume of the values used in the data processing for transducer 7

Channel number of the bottom	304
Registered distance for bottom channel	430.651 mm
First profile considered	114 originally 816 at 117.014 s
Last profile considered	292 originally 2056 at 294.756 s
Percentage of the maximum velocity for aliasing filtering	90%
Maximum grade for mean profile adjustment	7
Threshold number for polynomial coefficients (*S*)	4
Total number of profiles considered	125
Initial time selected to recompute the mean profile [s]	190
Upper channel defining positive mean velocity region	162